

**Anti-inflammatory effects of methyl fumarate-derived  
iron carbonyl complexes (FumET-CORMs) and  
reactive oxygen species on dendritic cell differentiation**

**Dissertation**

der Mathematisch-Naturwissenschaftlichen Fakultät

der Eberhard Karls Universität Tübingen

zur Erlangung des Grades eines

Doktors der Naturwissenschaften

(Dr. rer. nat.)

vorgelegt von

**M.Sc. Britta Juliana Bauer**

aus Stuttgart

Tübingen

2021

Gedruckt mit Genehmigung der Mathematisch-Naturwissenschaftlichen Fakultät der  
Eberhard Karls Universität Tübingen.

Tag der mündlichen Qualifikation: 19.10.2021

Dekan: Prof. Dr. Thilo Stehle

1. Berichterstatter Prof. Dr. med. Martin Röcken

2. Berichterstatter Prof. Dr. Robert Feil

# TABLE OF CONTENTS

<b>TABLE OF CONTENTS</b>	<b>III</b>
<b>LIST OF FIGURES</b>	<b>VII</b>
<b>LIST OF TABLES</b>	<b>IX</b>
<b>ZUSAMMENFASSUNG</b>	<b>XI</b>
<b>ABSTRACT</b>	<b>XIII</b>
<b>1. INTRODUCTION</b>	<b>1</b>
<b>1.1. THE IMMUNE SYSTEM</b>	<b>1</b>
1.1.1. INNATE IMMUNE SYSTEM	1
1.1.2. ADAPTIVE IMMUNE SYSTEM	3
<b>1.2. DENDRITIC CELLS</b>	<b>5</b>
1.2.1. DENDRITIC CELL SUBSETS	5
1.2.2. DENDRITIC CELL MATURATION AND ANTIGEN PRESENTATION	6
1.2.3. STIMULATION OF T CELLS BY DENDRITIC CELLS	9
<b>1.3. AUTOIMMUNE DISEASES</b>	<b>10</b>
1.3.1. MULTIPLE SCLEROSIS	11
1.3.2. PSORIASIS	13
1.3.3. FUMARIC ACID ESTERS	14
1.3.4. CARBON MONOXIDE-RELEASING MOLECULES	16
<b>1.4. REACTIVE OXYGEN SPECIES</b>	<b>21</b>
1.4.1. ROS GENERATION AND ITS BIOLOGICAL ROLE	21
1.4.2. CELLULAR ANTIOXIDANT DEFENSES	24
<b>1.5. AIM OF THE THESIS</b>	<b>26</b>
<b>2. MATERIALS</b>	<b>27</b>

<b>2.1. LABORATORY EQUIPMENT</b>	<b>27</b>
<b>2.2. LABORATORY MATERIALS</b>	<b>28</b>
<b>2.3. CHEMICALS</b>	<b>29</b>
<b>2.4. BUFFERS AND SOLUTIONS</b>	<b>30</b>
<b>2.5. ANTIBODIES</b>	<b>32</b>
<b>2.6. KITS</b>	<b>33</b>
<b>2.7. OLIGONUCLEOTIDES</b>	<b>34</b>
<b>2.8. FUMET-CORMs</b>	<b>35</b>
<b>2.9. SOFTWARE</b>	<b>36</b>
<b>2.10. LABORATORY ANIMALS</b>	<b>36</b>
<b>3. METHODS</b>	<b>37</b>
<hr/>	
<b>3.1. ISOLATION OF BMDC</b>	<b>37</b>
<b>3.2. MEASUREMENT OF INTRACELLULAR GSH/GSSG</b>	<b>38</b>
3.2.1. BMDC HARVEST AND GSH SAMPLE PREPARATION	38
3.2.2. SAMPLE PREPARATION FOR GSSG MEASUREMENT	39
3.2.3. SPECTROMETRIC MEASUREMENT OF SAMPLES	39
<b>3.3. ENZYME-LINKED IMMUNOSORBENT ASSAY (ELISA)</b>	<b>39</b>
<b>3.4. WESTERN BLOT</b>	<b>40</b>
3.4.1. PREPARATION OF WHOLE CELL LYSATES	40
3.4.2. PREPARATION NUCLEAR AND CYTOPLASMIC LYSATES	40
3.4.3. MEASUREMENT OF PROTEIN CONCENTRATION	41
3.4.4. GEL ELECTROPHORESIS	41
3.4.5. WESTERN BLOTTING	41
<b>3.5. MEASUREMENT OF CELL VIABILITY</b>	<b>42</b>
3.5.1. TRYPAN BLUE EXCLUSION ASSAY	42
3.5.2. XTT ASSAY	42
3.5.3. LDH ASSAY	42
<b>3.6. ANALYSIS OF GENE EXPRESSION</b>	<b>43</b>
3.6.1. SAMPLE PREPARATION	43
3.6.2. RNA ISOLATION	43
3.6.3. SYNTHESIS OF CDNA	44

3.6.4. CONTROL PCR WITH HOUSEKEEPING GENE	44
3.6.5. QUANTITATIVE REAL-TIME PCR	45
3.6.6. PCR ARRAY	45
<b>3.7. FLUORESCENCE ACTIVATED CELL SORTING (FACS)</b>	<b>46</b>
<b>3.8. DETECTION OF ROS</b>	<b>47</b>
<b>3.9. ANALYSIS OF THIOREDOXIN REDUCTASE ACTIVITY</b>	<b>47</b>
<b>3.10. STATISTICAL ANALYSIS</b>	<b>47</b>
<b><u>4. RESULTS</u></b>	<b><u>49</u></b>
<b>4.1. DMF-MEDIATED ANTI-INFLAMMATORY EFFECTS IN WILDTYPE BMDCs</b>	<b>49</b>
<b>4.2. FUMET-CORMs AS POWERFUL ANTI-INFLAMMATORY AGENTS</b>	<b>53</b>
4.2.1. INDUCTION OF TYPE II DENDRITIC CELLS BY FUMET-CORMs	54
4.2.2. MODULATION OF REDOX HOMEOSTASIS BY FUMET-CORMs	61
<b>4.3. EFFECTS OF ENDOGENOUS ROS STRESS ON DENDRITIC CELL DIFFERENTIATION</b>	<b>64</b>
4.3.1. CHARACTERIZATION OF CYSTINE/GLUTAMATE ANTIporter KNOCKOUT CELLS	64
4.3.2. DIFFERENTIAL REGULATION OF REDOX HOMEOSTASIS AFTER XCT KNOCKOUT	68
4.3.3. EFFECTS OF XCT KNOCKOUT ON DENDRITIC CELL DIFFERENTIATION	71
4.3.4. POSSIBLE OVERCOMPENSATION AFTER XCT KNOCKOUT BY OTHER REDOX PATHWAYS	77
4.3.5. EFFECTS OF THIOREDOXIN PATHWAY INHIBITION ON BMDC DIFFERENTIATION	82
4.3.6. EFFECTS OF NADPH OXIDASE KNOCKOUT ON DMF TREATMENT	88
<b><u>5. DISCUSSION</u></b>	<b><u>92</u></b>
<b>5.1. FUMET-CORMs AS POWERFUL ANTI-INFLAMMATORY AGENTS</b>	<b>92</b>
<b>5.2. ASSESSMENT OF XCT KNOCKOUT MICE AS MODEL SYSTEM FOR ENDOGENOUS ROS STRESS</b>	<b>96</b>
<b>5.3. THE RELEVANCE OF REDOX HOMEOSTASIS FOR EFFECTIVE DMF TREATMENT</b>	<b>98</b>
<b>5.4. POSSIBLE COMPENSATORY MECHANISMS UNDER ENDOGENOUS ROS STRESS</b>	<b>102</b>
<b>5.5. FURTHER CELLULAR IMPLICATIONS ASSOCIATED WITH FUMARATE TREATMENT</b>	<b>105</b>
<b>5.6. CONCLUSIONS AND PERSPECTIVES</b>	<b>107</b>
<b><u>6. ABBREVIATIONS</u></b>	<b><u>109</u></b>

<b><u>7.</u></b>	<b><u>ACKNOWLEDGMENTS</u></b>	<b><u>113</u></b>
<b><u>8.</u></b>	<b><u>LITERATURE</u></b>	<b><u>115</u></b>
<b><u>9.</u></b>	<b><u>PUBLICATIONS</u></b>	<b><u>132</u></b>
<b><u>10.</u></b>	<b><u>ERKLÄRUNG ZUM EIGENANTEIL</u></b>	<b><u>133</u></b>
<b><u>11.</u></b>	<b><u>EIDESSTATTLICHE ERKLÄRUNG</u></b>	<b><u>134</u></b>

# LIST OF FIGURES

FIGURE 1: DIFFERENTIATION OF NAIVE T CELLS INTO DEFINED SUBPOPULATIONS. ....	4
FIGURE 2: DEVELOPMENT OF DIFFERENT DENDRITIC CELL SUBSETS AND INVOLVED TRANSCRIPTION FACTORS.....	8
FIGURE 3: POSSIBLE EFFECTS OF DIMETHYL FUMARATE IN THE TREATMENT OF MULTIPLE SCLEROSIS. ....	12
FIGURE 4: DMF TREATMENT IMPACTS SEVERAL SIGNALING PATHWAYS TO MODULATE IMMUNITY. ....	16
FIGURE 5: MODULATION OF INTRACELLULAR SIGNALING CASCADES BY CARBON MONOXIDE.....	18
FIGURE 6: OVERVIEW OF CO-RELEASING MOLECULES.....	20
FIGURE 7: CELLULAR MAINTENANCE OF REDOX HOMEOSTASIS. ....	23
FIGURE 8: ISOLATION OF DCs FROM BONE MARROW OF MICE.....	50
FIGURE 9: DMF TREATMENT INDUCES OXIDATIVE STRESS IN WILDTYPE BMDCs. ....	51
FIGURE 10: DMF MODULATES THE HO-1 AND STAT1 SIGNALING PATHWAY. ....	52
FIGURE 11: ANALYSIS OF CORM TOXICITY ON BMDCs.....	54
FIGURE 12: INHIBITION OF INFLAMMATORY CYTOKINE SECRETION BY FUMET-CORMs.....	56
FIGURE 13: FUMET-CORM TREATMENT INDUCES HO-1. ....	57
FIGURE 14: INHIBITION OF STAT1 PHOSPHORYLATION BY FUMET-CORMs.....	58
FIGURE 15: EFFECTS OF CORMs AND ANTI-OXIDANT TREATMENT ON SIGNALING PATHWAYS.....	59
FIGURE 16: NAC TREATMENT REVERSES INFLAMMATORY CYTOKINE INHIBITION BY FUMET-CORMs. ....	60
FIGURE 17: CORM TREATMENT DOESN'T DIMINISH INTRA-CELLULAR GSH LEVEL. ....	61
FIGURE 18: STRONG INDUCTION OF REACTIVE OXYGEN SPECIES IN FUMET-CORM-TREATED DCs. ....	63
FIGURE 19: POSTULATED EFFECTS OF CYSTINE/GLUTAMATE ANTIporter KNOCKOUT ON INTRACELLULAR GSH LEVELS. ....	65
FIGURE 20: GENERATION OF BMDCs FROM XCT KNOCKOUT MICE REQUIRES B-MERCAPTOETHANOL. ....	66
FIGURE 21: VERIFICATION OF XCT KNOCKOUT IN BMDCs.....	67
FIGURE 22: NO MODULATION OF GSH LEVELS BY XCT KNOCKOUT <i>EX VIVO</i> . ....	69
FIGURE 23: MODULATION OF REDOX HOMEOSTASIS IN XCT KNOCKOUT CELLS.....	70
FIGURE 24: TREATMENT REGIMEN OF WILDTYPE AND XCT KNOCKOUT BMDCs.....	72
FIGURE 25: EFFECTS OF XCT KNOCKOUT ON HO-1 AND STAT1 SIGNALING PATHWAYS. ....	73
FIGURE 26: HO-1 INDUCTION IS NOT INFLUENCED BY GENETIC LOSS OF XCT ANTIporter ALONE. ....	74
FIGURE 27: STAT1 PHOSPHORYLATION IS NOT INFLUENCED BY GENETIC LOSS OF XCT ANTIporter ALONE.....	76
FIGURE 28: KNOCKOUT OF XCT ANTIporter IS NOT SUFFICIENT TO INHIBIT INFLAMMATORY CYTOKINE SECRETION. ....	77
FIGURE 29: DIFFERENTIAL EXPRESSION OF GENES RELATED TO OXIDATIVE STRESS RESPONSE. ....	79
FIGURE 30: <i>EX VIVO</i> ANALYSIS OF OXIDATIVE STRESS RESPONSE IN WILDTYPE AND XCT KNOCKOUT CELLS. ....	80
FIGURE 31: EFFECTS OF DMF TREATMENT AND XCT KNOCKOUT ON MRNA EXPRESSION. ....	81
FIGURE 32: TOXICITY OF AURANOFIN ON WILDTYPE AND XCT KNOCKOUT BMDCs.....	83
FIGURE 33: INHIBITION OF THIOREDOXIN REDUCTASE. ....	84
FIGURE 34: AURANOFIN INDUCES HO-1 IN XCT KNOCKOUT BUT NOT IN WILDTYPE CELLS. ....	85

## VIII

FIGURE 35: AURANOFIN TREATMENT HAS NO INFLUENCE ON INFLAMMATORY CYTOKINE RELEASE. ....	86
FIGURE 36: NO INCREASED TRANSLOCATION OF HO-1 INTO THE NUCLEUS AFTER AURANOFIN TREATMENT. ....	87
FIGURE 37: NO DETECTABLE MODULATION OF ROS LEVELS AFTER AURANOFIN TREATMENT. ....	89
FIGURE 38: MODULATION OF HO-1 AND STAT1 SIGNALING PATHWAYS IN NADPH OXIDASE KNOCKOUT CELLS. ....	90
FIGURE 39: INHIBITION OF INFLAMMATORY CYTOKINES IN WILDTYPE AND NADPH OXIDASE KNOCKOUT CELLS. ....	90
FIGURE 40: NADPH OXIDASE KNOCKOUT CELLS STILL SHOW ROS INDUCTION AFTER DMF TREATMENT. ....	91



# LIST OF TABLES

TABLE 1: LABORATORY EQUIPMENT .....	27
TABLE 2: LABORATORY MATERIALS.....	28
TABLE 3: CHEMICALS .....	29
TABLE 4: COMMERCIAL BUFFERS AND SOLUTIONS .....	30
TABLE 5: SELF-MADE BUFFERS AND SOLUTIONS. ....	31
TABLE 6: ANTIBODIES.....	32
TABLE 7: COMMERCIAL KITS .....	33
TABLE 8: OLIGONUCLEOTIDES .....	34
TABLE 9: FUMET-CORMs .....	35
TABLE 10: SOFTWARE .....	36
TABLE 11: LABORATORY ANIMALS .....	36
TABLE 12: REVERSE TRANSCRIPTION CYCLING CONDITIONS. ....	44
TABLE 13: GAPDH TEST PCR CYCLING CONDITIONS. ....	44
TABLE 14: QRT-PCR CYCLING CONDITIONS. ....	45
TABLE 15: PCR ARRAY CYCLING CONDITIONS. ....	46



## ZUSAMMENFASSUNG

Einer der grundlegenden Schritte einer erfolgreichen Therapie von  $T_h1/T_h17$ -vermittelten Autoimmunerkrankungen ist die Induktion von Typ II dendritischen Zellen (DCs), welche im Folgenden zu einer Immundeviation hin zu einer anti-inflammatorischen  $T_h2$  Antwort führen. Im ersten Teil der Arbeit erfolgte deshalb die Charakterisierung neuer Substanzen, welche sowohl Kohlenstoffmonoxid als auch Fumarsäureester freisetzen. Die Behandlung mit diesen FumET-CORMs zeigte sich als sehr effektiv, da es zu einer robusten Induktion von Typ II DCs kam. Die dabei charakteristische Verminderung der STAT1 Phosphorylierung, Induktion von HO-1 und die daraus resultierende Inhibition der Zytokine IL-12p70 und IL-23 erfolgte sogar stärker und bei deutlich niedrigeren Konzentrationen als bei der Kontrollbehandlung mit Dimethylfumarat (DMF). Für eine detaillierte mechanistische Aufklärung der Therapie mit DMF wurde im zweiten Teil der Arbeit ein Cystin/Glutamat Antiporter Knockout Mausmodell herangezogen. In DCs dieser Mäuse wurde damit der Verlust des Radikalfängers Glutathion (GSH) und eine einhergehende Induktion von reaktiven Sauerstoffspezies auf genetischer Ebene erreicht, ohne Nebeneffekte einer pharmakologischen Behandlung. Entgegen der zuvor aufgestellten Hypothese resultierten diese Änderungen der Redox Homöostase nicht in der Differenzierung der DCs hin zu einem Typ II Phänotyp. Stattdessen führte die zusätzliche Behandlung dieser bereits GSH-depletierten Zellen trotzdem zur Modulation des HO-1 und STAT1 Signalweges, sowie der Inhibition der nachgeschalteten Zytokine IL-12p70 und IL-23. Dies zeigt, dass weitere Modifikationen durch das Fumarat für die Vermittlung der Effekte verantwortlich zu machen sind. Des Weiteren konnte auch eine Überkompensation des Antiporterverlustes über den Thioredoxin Signalweg durch den Einsatz von Auranofin ausgeschlossen werden. Die Modulation der Redox Homöostase allein war nicht ausreichend, um DCs in einen anti-inflammatorischen Typ II Phänotyp zu überführen, stattdessen spielen dabei wahrscheinlich noch weitere intrazelluläre Ziele der DMF Behandlung eine entscheidende Rolle.



## ABSTRACT

One of the fundamental steps in a successful therapy of  $T_h1/T_h17$ -mediated autoimmune diseases is the induction of type II dendritic cells (DCs), which subsequently cause an immune deviation towards an anti-inflammatory  $T_h2$  response. In the first part of the work, the characterization of new substances, which release carbon monoxide as well as fumaric acid esters, was carried out. The treatment with these FumET-CORMs proved to be highly effective, as a robust induction of type II DCs was achieved. The characteristic reduction of STAT1 phosphorylation, induction of HO-1 and the resulting inhibition of the cytokines IL-12p70 and IL-23 occurred even more pronounced and at significantly lower concentrations than in the control treatment with dimethyl fumarate (DMF).

For a detailed mechanistic analysis of the DMF therapy, a cystine/glutamate antiporter knockout mouse model was employed in the second part of the study. In DCs of these mice, the loss of the scavenger of reactive oxygen species, glutathione (GSH), and an associated induction of said chemical entities was achieved on the genetic level without additional effects of pharmacological treatment. In contrast to the previously proposed hypothesis, these changes in redox homeostasis did not result in the differentiation of the DCs into a type II phenotype. Instead, the additional treatment of these already GSH-depleted cells still resulted in the HO-1 and STAT1 signaling pathway's modulation and the inhibition of downstream cytokines IL-12p70 and IL-23, indicating that additional targets of the fumarate are responsible for the mediation of these effects. In further experiments, an overcompensation of the antiporter loss via the thioredoxin signaling pathway could be excluded by using the inhibitor auranofin. Accordingly, the modulation of redox homeostasis alone is not sufficient to transform DCs into an anti-inflammatory type II phenotype. Instead, further intracellular targets of DMF treatment probably also play a decisive role in this process.



# 1. INTRODUCTION

## 1.1. THE IMMUNE SYSTEM

Every day we encounter a vast number of disease-causing pathogens. To combat this threat, our body is equipped with the immune system. It is composed of a complex interplay of different cell types and molecules that interact to protect the organism from invading pathogens or toxins, as well as to eliminate cancer cells. At the same time, disorders of the immune systems can lead to serious consequences, such as severe infections, immunodeficiency, or overactivities resulting in allergies and autoimmune diseases. In vertebrates, this complex network can be divided into two sections based on the kinetics and the specificity of its activation. These sections are referred to as the innate and the adaptive immune system and the interactions between these two systems are very diverse.

### 1.1.1 *INNATE IMMUNE SYSTEM*

The innate immune system uses several barriers to defend itself against invading pathogens. The first line of defense is represented by anatomic barriers such as skin, oral mucosa, or gastric acid. The second barrier in this system are soluble proteins and small bioactive molecules represented by the complement system, but also defensins, cytokines and chemokines. Finally, it is completed by innate immune cells. They comprise different cell types, including macrophages, granulocytes and dendritic cells, all of which originate from a common pluripotent hematopoietic stem cell [1].

The innate immune response is a fast, initial reaction that is able to eliminate a wide range of microorganisms and toxins but does not confer lasting immunity. If pathogens succeed in breaking through the anatomical barriers of the body, an inflammatory program is initiated that can be divided into a cell-mediated response of the previously mentioned innate immune cells and the humoral response conducted by the complement system.

The first step of the cell-mediated immune response is the recognition of microorganisms by phagocytes. One type of phagocytes are macrophages, which can eliminate both pathogens and infected cells, especially when attacked by the adaptive immune system. The second group are granulocytes consisting of neutrophils, eosinophils and basophils. One main function of neutrophils, for example, is phagocytosis and destruction of pathogens at the site of infection, where they are recruited in large numbers. The third group of phagocytes is represented by dendritic cells (DCs). These cells are also capable of eliminating pathogens, but their main function is the processing of captured microorganisms and the subsequent presentation of antigens to T cells [2]. Thus, they act as a mediator between the innate and the adaptive immune systems by triggering T cell reactions as well as producing cytokines that can activate other immune cells.

Essential components in pathogen detection by the innate immune system are the so-called pattern recognition receptors (PRRs). These sensors are germline-encoded and capable of detecting a limited spectrum of pathogen-associated molecular patterns (PAMPs). PAMPs are structural motifs that are conserved in bacteria or fungi, for instance but are not expressed on endogenous cells [3]. A well-established group of PRRs, the toll-like receptors (TLRs), can transform innate immune cells like macrophages and dendritic cells to produce high amounts of proinflammatory cytokines and chemokines [4, 5]. Different TLRs respond to their specific ligands such as lipoteichoic acid, peptidoglycan and viral DNA or RNA. This allows them to induce a variety of signaling cascades, also depending on which intracellular adapter molecule is involved.

As an example, TLR4 is implicated in recognition of lipopolysaccharide (LPS) from Gram-negative bacteria [6]. After the binding of ligands, oligomerization and interaction with intracellular adapter molecules such as myeloid differentiation primary response gene 88 (MyD88), TIR domain-containing adaptor protein (TIRAP), TIR domain-containing adaptor inducing IFN- $\beta$  (TRIF) or TRIF-related adaptor molecule (TRAM) occurs [7-10]. This, in turn, leads to the stimulation of different signaling cascades, depending on which adapter molecule was involved. Important pathways induced by LPS recognition are NF $\kappa$ B and mitogen-activated protein kinase (MAPK), which lead to the production of proinflammatory cytokines and type I interferons [11].



This is of great importance both for the enhancement of the immune reaction as well as for the initiation of an adaptive immune response.

### 1.1.2 ADAPTIVE IMMUNE SYSTEM

The adaptive or acquired immune response has evolved as a second major defense strategy and can specifically react to a vast spectrum of pathogens. Similar to the innate immune system, it consists of humoral and cell-based components. The latter is mediated by lymphocytes like T and B cells, which in turn induce the antibody-based humoral response. One of the main differences to the innate immune system is that it can react highly specifically to a particular pathogen. This is possible as antigen-specific receptors are not germline-encoded, but are instead acquired through somatic rearrangement during the entire lifespan of an organism [12, 13].

T and B lymphocytes normally circulate in the blood, lymph and secondary lymphoid organs. When T cells recognize their specific antigen, which is presented via a major histocompatibility complex (MHC) molecule on the surface of host cells, they are activated and mature to effector cells. There are two main groups of T lymphocytes. First,  $CD8^+$  cytotoxic T cells that specialize in directly killing infected host cells. Secondly,  $CD4^+$  T-helper ( $T_h$ ) cells, whose primary function is the activation of other immune cells such as macrophages by the secretion of different cytokines [2].  $T_h$  cells can differentiate into several subpopulations that perform distinct biological functions depending on the predominant cytokine milieu at the site of activation (Figure 1). The three major classes of  $CD4^+$  T lymphocytes being important for this work are the  $T_h1$ ,  $T_h2$  and  $T_h17$  cells.

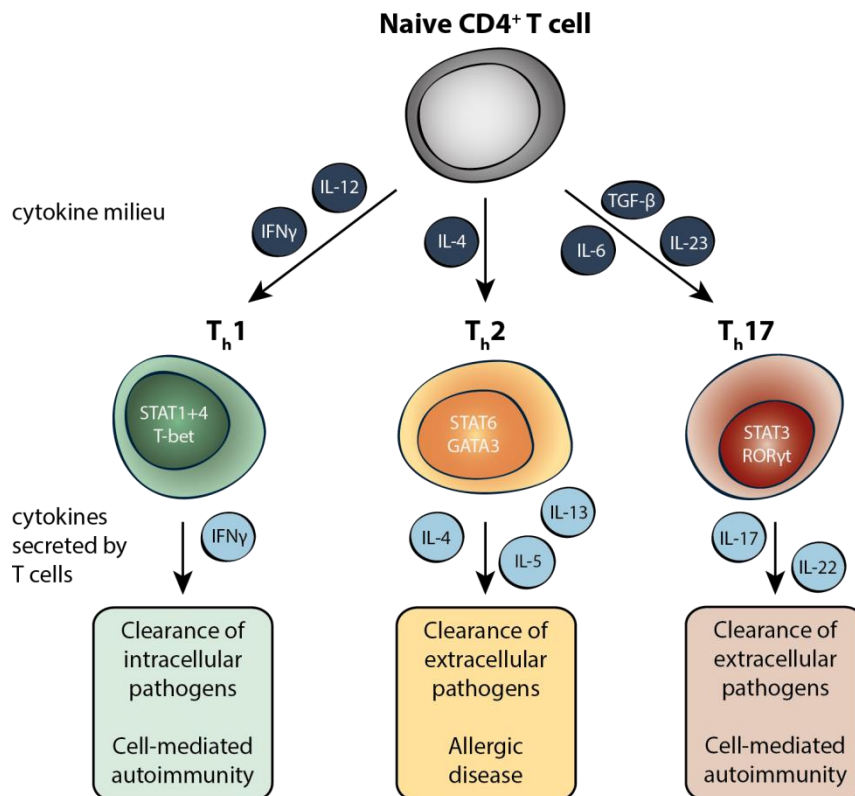


**Figure 1: Differentiation of naive T cells into defined subpopulations.**

Cytokines secreted by e.g. DCs and other APCs (dark blue circles) determine the maturation of naive T lymphocytes into effector cells with specialized functions within the immune response. During this process of activation, each cell expresses specific transcription factors that further promote the cytokine-induced differentiation. The T helper cells shown here are composed of  $T_h1$ ,  $T_h2$  and  $T_h17$  cells, with each subpopulation expressing a defined set of cytokines (light blue circles) necessary for the mediation of effector functions. DC, dendritic cell; APC, antigen-presenting cell;  $T_h$ , T helper cell; IL, interleukin; IFN, interferon; TGF- $\beta$ , transforming growth factor beta; STAT, signal transducer and activator of transcription; T-bet, T-box expressed in T cells; ROR $\gamma$ t, receptor-related orphan receptor  $\gamma$ -T. Figure adapted from [14].

$T_h1$  cells play an essential role in the clearance of intracellular pathogens by e.g., secreting interferon (IFN)- $\gamma$  and thereby enhancing the anti-microbial activity of infected macrophages [15]. The important cytokine leading to  $T_h1$  differentiation is interleukin (IL)-12 secreted by antigen-presenting cells. IFN- $\gamma$  and IL-12 activate signal transducer and activator of transcription (STAT) 1 and STAT4 signaling cascades, respectively [16-19]. Induction of these pathways leads to the expression of T-box expressed in T cells (T-bet) transcription factor, which causes an increased IFN- $\gamma$  production of the activated T cells, creating a positive feedback loop that further strengthens  $T_h1$  differentiation [20-22].

The second main group of T-helper lymphocytes is represented by  $T_h2$  cells. This subpopulation has an important function in the elimination of extracellular pathogens. Differentiation to the  $T_h2$  subset is achieved through T cell receptor binding

in the presence of IL-4 [23, 24]. In the presence of this cytokine, STAT6 is phosphorylated and GATA3 is induced [25]. The expression of this transcription factor is crucial for the maintenance of the T<sub>h</sub>2 phenotype, as GATA3 knockout leads to impaired secretion of the T<sub>h</sub>2 cytokines IL-4, IL-5 and IL-13 [26].

The third T lymphocyte subpopulation discussed in this thesis consists of T<sub>h</sub>17 cells. The purpose of this cell type is to eliminate extracellular pathogens. The main targets are bacteria and fungi whose elimination by T<sub>h</sub>1 or T<sub>h</sub>2 cells is not sufficient and requires a robust inflammatory response [27, 28]. The initial factors required for differentiation into T<sub>h</sub>17 lymphocytes are transforming growth factor beta (TGF- $\beta$ ) and IL-6. Both cytokines trigger a complex signaling cascade leading to the expression of the transcription factors STAT3 and receptor-related orphan receptor  $\gamma$ -T (ROR $\gamma$ T), which subsequently induce the cytokine IL-17 [29-32]. In this context, the induction of the IL-23 receptor and subsequent responsiveness to the cytokine seems to play an essential role for the successful and sustained differentiation, since without IL-23 a non-inflammatory phenotype of T<sub>h</sub>17 lymphocytes occurs [33-36].

## 1.2 DENDRITIC CELLS

Dendritic cells are professional antigen-presenting cells (APCs), with their main function of capturing foreign antigens, followed by the presentation of said antigen-derived peptides to T cells. Thus, they represent a crucial link between the innate and adaptive immune system, whose important role becomes even more apparent, as the lack of dendritic cells can lead to severe immune-deficient phenotypes and abrogated T cell priming in specific knockout mouse models [37, 38].

### 1.2.1 DENDRITIC CELL SUBSETS

Dendritic cells can be divided into different phenotypic subpopulations that represent their diversity and ability to adapt to their specific microenvironment. The two main classes of DCs are the plasmacytoid DCs (pDCs) and the conventional DCs (cDCs). They are both part of the mononuclear-phagocyte system and originate from a

common hematopoietic stem cell (HSC) in the bone marrow. The exact mechanisms and expression of transcription factors during the differentiation of dendritic cells are very complex and are not yet fully understood. However, a basic overview is presented in Figure 2.

For differentiation into the different DC subsets, HSC gives rise to a myeloid precursor (MP), macrophage and DC precursor (MDP) and finally a common DC precursor (CDP). Besides fms-related tyrosine kinase 3 (Flt3), the transcription factor interferon regulatory factor (Irf) 8 is strongly expressed in the early stages of DC development [39-41]. Plasmacytoid dendritic cells and pre-classical dendritic cells (pre-cDCs) are then formed from CDPs, whereby the availability of E-protein transcription factor 4 (E2-2) or E-protein inhibitor of DNA binding 2 (Id2) determines the development in the respective direction [42-44]. Subsequently, these pre-cDCs can further differentiate into either cDC1 in the presence of basic leucine zipper transcription factor ATF-like 3 (Batf3), or cDC2, if the transcription factor Irf 4 is available [41, 45-48]. Finally, cDC2 can be divided into two further subsets. The first subset depends on Irf4 and Kruppel-like factor 4 (Klf4), which plays a crucial role in the efficient induction of T<sub>h</sub>2 immunity in response to extracellular pathogens or allergens. And secondly, a neurogenic locus notch homolog protein 2 (Notch-2)-dependent subset of cDCs that secrete high amounts of IL-23 and subsequently induce T<sub>h</sub>17 cell differentiation [49-51]. In contrast, the primary function of cDC1 is the activation of CD8<sup>+</sup> cytotoxic T lymphocytes by MHC class I cross-presentation and the induction of a T<sub>h</sub>1 immune response by secretion of IL-12 [45, 52]. Finally, pDCs are specialized in the secretion of high levels of type 1 interferons in response to viral infections [53, 54].

### 1.2.2 DENDRITIC CELL MATURATION AND ANTIGEN PRESENTATION

After their formation in the bone marrow, DC precursors circulate in the blood and eventually accumulate in peripheral tissue. Here they reside as immature DCs with a high degree of phagocytic activity. Upon exposure to an antigen, e.g. at the site of a tissue injury, it is efficiently absorbed and processed in the cell. This is followed by migration of the DCs to secondary lymphoid tissues, where the matured DCs present peptide fragments of these antigens via MHC class I or II complexes to the antigen-specific T cells of the adaptive immune response encountered there.

The uptake of antigens primarily occurs through three different pathways: the non-specific uptake of large amounts of soluble molecules and antigens in the DC microenvironment, known as micropinocytosis, as well as the receptor-mediated endocytosis and finally phagocytosis of pathogens or apoptotic and necrotic bodies [55-60]. Exogenous and endogenous peptides are then proteolyzed in the cell to obtain short peptides that can be presented via MHCs. Endogenous antigens are mainly presented via MHC I. Therefore, peptides degraded through proteasomes in the cytosol are transported into the ER. There, the MHC I molecules are loaded with the peptides and the complex is transported to the cell surface via the Golgi apparatus [61]. On the other hand, exogenous proteins are mainly degraded by lysosomal proteolysis and presented via MHC II. These MHC II are formed in the ER and then transported into the late endosomes. At these sites, binding to antigenic peptides and subsequent transport to the cell surface takes place [61].

As DCs now encounter an antigen or a pathogen, several additional functional changes in the cells are triggered. This process of maturation leads to a shift from efficient antigen-capturing cells to professional antigen-presenting cells (APCs). Not only pathogen-associated molecules such as LPS can activate DCs but also many other substances, including bacterial DNA, pro- and anti-inflammatory cytokines, or signals from T cells [62, 63]. An important step in DC maturation is the upregulation of costimulatory signals like the surface molecules CD80 and CD86, which are required for successful activation of T cells [64]. Furthermore, the maturation leads to morphological changes of the cells. Adhesive structures are expressed only to a reduced extent and the dendrites that give the cells their name are formed [65]. This, together with the expression of CC-chemokine receptor 7 (CCR7) and the resulting sensitivity to its ligands CC-chemokine ligand 19 (CCL19) and CCL21, enables the subsequent migration of the cells to the secondary lymphoid organs [66, 67]. Here, the mature DCs can present their processed antigens on MHC molecules to the T cells and induce an adaptive immune response.

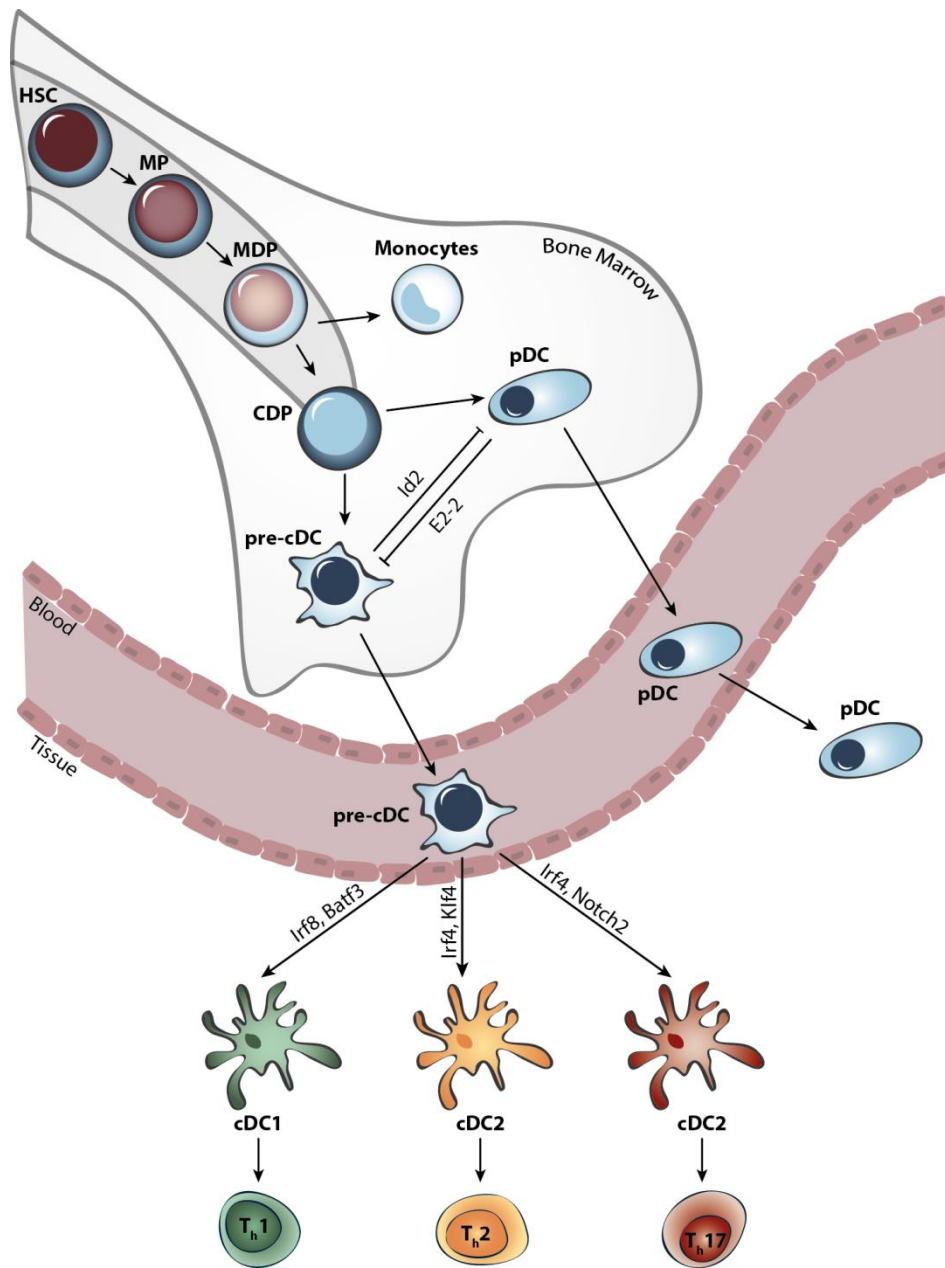


**Figure 2: Development of different dendritic cell subsets and involved transcription factors.**

In the bone marrow HSCs give rise to a variety of precursor cells until pre-cDCs and pDCs are formed. These cells then migrate through the blood into the different tissues where pre-cDCs can further evolve into cDC1 and cDC2. These differentiation processes are controlled by the expression of several transcription factors. After successful activation and maturation of DCs, they can induce distinct T helper subsets and thereby mediate adaptive immunity against invading pathogens. HSC, hematopoietic stem cell; MP, myeloid precursor; MDP, macrophage-DC precursor; CDP, common DC precursor; pre-cDC, pre-classical dendritic cell; pDC, plasmacytoid dendritic cell; cDC, conventional dendritic cell; Th, T helper cell; Id2, E-protein inhibitor of DNA binding 2; E2-2, E-protein transcription factor 4; Irf, interferon regulatory factor; Batf3, basic leucine zipper transcription factor ATF-like 3; Klf4, Kruppel-like factor 4; Notch2, neurogenic locus notch homolog protein 2. Figure adapted from [68] and [69].

### 1.2.3 STIMULATION OF T CELLS BY DENDRITIC CELLS

An essential step for a functional adaptive immune response is the activation of naive T lymphocytes by APCs. This interaction and the subsequent differentiation into T effector cells is called priming. In the lymph nodes, naive T cells continually bind APCs by means of adhesion molecules. When their specific peptide:MHC complex, which is presented by dendritic cells, is recognized, the affinity of these adhesion molecules is increased by conformational changes to enable a stronger binding of the T cell to the APC [70, 71]. However, the interaction between the T cell receptor (TCR) and its peptide:MHC complex alone is not sufficient to induce rapid proliferation and differentiation of naive T cells. Successful priming requires several additional signals.

The second important factor besides the recognition of the presented antigen is the binding of costimulatory molecules. Well-characterized examples are the molecules CD80 and CD86, which are present on the surface of dendritic cells. These can be bound by CD28 on the surface of T cells [72, 73]. After activation of T lymphocytes, a strong proliferation of the cells and an increased expression of IL-2 occurs, which can be further enhanced by co-stimulation with CD28 signals, by promoting the transcription of the cytokine, but also by increasing the stability of the produced mRNA [74, 75]. The IL-2 signaling facilitated by CD28 now enables the cell to increase proliferation and also supports differentiation into effector cells. In addition to CD80/86, dendritic cells also possess various other costimulatory molecules with their dedicated T cell ligands, examples are CD40/CD40L or OX40L/OX40 [76, 77].

In contrast to CD8<sup>+</sup> T cells, CD4<sup>+</sup> lymphocytes can differentiate into several different subpopulations. Decisive for this is the third factor required for successful T cell priming, the cytokine milieu prevailing in the microenvironment. Different cytokines lead to differentiation into specialized classes of T helper cells. Accordingly, T<sub>h</sub>1 cells are formed in the presence of IL-12, whereas lymphocytes differentiate into T<sub>h</sub>2 cells when IL-4 is present during the time of stimulation. The different T helper subpopulations and the underlying factors and mechanisms have already been discussed in chapter 1.1.2 (Figure 1)

After the strong proliferation and differentiation into their specific effector cells, the T helper subpopulations can perform their distinct functions within the immune response. In contrast to naïve T cells, a direct immune response occurs when the

effector cells are exposed to their specific antigen a second time without the need for further costimulatory molecules.

### 1.3 AUTOIMMUNE DISEASES

As described in the previous chapters, the immune system is able to react specifically to invading pathogens and to eliminate them. However, if disturbances in this highly complex system occur, serious immunodeficiencies, allergies or autoimmune diseases can result. In the case of autoimmunity, there is an undesired reaction of T or B cells against the body's own antigens, which results in damage to the affected tissue.

The body has multiple control mechanisms to prevent the reaction to the body's own antigens, whereby the maintenance of self-tolerance plays a central role. As a first step, central tolerance is developed by the expression of autoantigens on epithelial cells in the thymus. If the TCR of a T cell has a high affinity to these self-antigens, cell death occurs and consequently negative selection of these autoreactive lymphocytes [78, 79]. However, some of the cells escape this central tolerance mechanism and must therefore be killed or inactivated in the periphery. If an antigen is recognized by such a T cell in the absence of costimulatory molecules, either deletion or anergy of the cell or induction of regulatory T lymphocytes, which can modulate the activity of other T cells, occurs [80].

In autoimmune diseases, various causes can lead to pathogenesis. On the one hand, the autoantibodies formed can directly lead to tissue damage. This is the case, amongst others, with pemphigus vulgaris, where autoantibodies against the cell surface molecule desmoglein play a predominant role in the development of the disease [81]. On the other hand, the effector T cells can also damage the respective tissue. This type of disease is often based on an aberrant induction of  $T_H1$  and  $T_H17$  cells. Examples of T cell-mediated autoimmune diseases are multiple sclerosis (MS) and psoriasis [82].



### 1.3.1 MULTIPLE SCLEROSIS

Multiple sclerosis is one of the most common neurological autoimmune diseases in young adults. The exact causes of the disease's development are not yet known, although a number of risk factors such as UVB radiation, obesity, vitamin D metabolism and smoking appear to be involved [83-87]. Tissue damage in this autoimmune disease is mainly due to an immune response of autoreactive T<sub>h</sub>1 and T<sub>h</sub>17 cells against myelin antigens from the central nervous system (CNS), such as myelin basic protein (MBP), myelin proteolipid protein (PLP) or myelin oligodendrocyte glycoprotein (MOG) [88-91]. In addition, further cells of the adaptive and innate immune system are recruited to the initial site of inflammation, which enhances the immune response even more. Recruited T and B cells now produce autoantibodies, which lead to demyelination. The disintegration of myelin, that normally surrounds the axons of the nerves, leads to the formation of the name-giving sclerotic lesions in the white matter. Since these inflammatory reactions can occur throughout the entire CNS, the neurological symptoms observed in multiple sclerosis are also very diverse. Typical conditions can include but are not limited to visual disturbances, incontinence or muscle weakness up to paralysis [92]. There are also variations in the course of the disease. It is distinguished between relapsing-remitting MS (RRMS), secondary progressive MS (SPMS) and primary progressive MS (PPMS) [93]. RRMS is the most common form of MS [94]. It is accompanied by the development of so-called relapses, which are characterized by the appearance of new symptoms or the flare-up of already known symptoms. Once the relapse has subsided, complete or partial remission occurs. Between the relapses, the clinical course of MS remains fairly stable, but over time, most of the patients develop SPMS [95]. This type is defined by a progressive deterioration of the symptoms, whereby occasional relapses can also occur. The last remaining form of multiple sclerosis is PPMS. In contrary to the two previously mentioned courses, there is no occurrence of relapses in PPMS, but rather a gradual progression of the disease [93].

Many medications are approved for the treatment of MS. It is differentiated among other things between short-term relapse therapy, which is primarily carried out by treatment with high-dose corticosteroids, and long-term, disease-modifying therapy. The choice of drugs for the basic therapy of MS is guided by the disease's level of gravity, with the aim of achieving a long-term reduction in the severity and frequency of

the relapses that occur. For example, in the treatment of RRMS with a mild to moderate course, interferon- $\beta$ , glatiramer acetate, dimethyl fumarate (DMF) or teriflunomide are used for therapy. These drugs are characterized by their immunomodulatory properties, which result in a decreased relapse rate and improved remission compared to placebo-treated patients, with only mild adverse effects [96-99]. However, should a highly active MS progression occur under this basic therapy, the change to the so-called escalation therapy can be implemented. For this purpose, drugs that show a higher efficacy are used, but at the same time, the risk for serious side effects is elevated. Examples of such first-line drugs of an escalation therapy are the monoclonal antibodies alemtuzumab and natalizumab, as well as cladribine or fingolimod [100-103]. There are several other approved drugs for the treatment of MS, but this thesis will focus on the use and cellular mechanisms of treatment with fumaric acid. Therefore, the effects of DMF are further described in chapter 1.3.3.

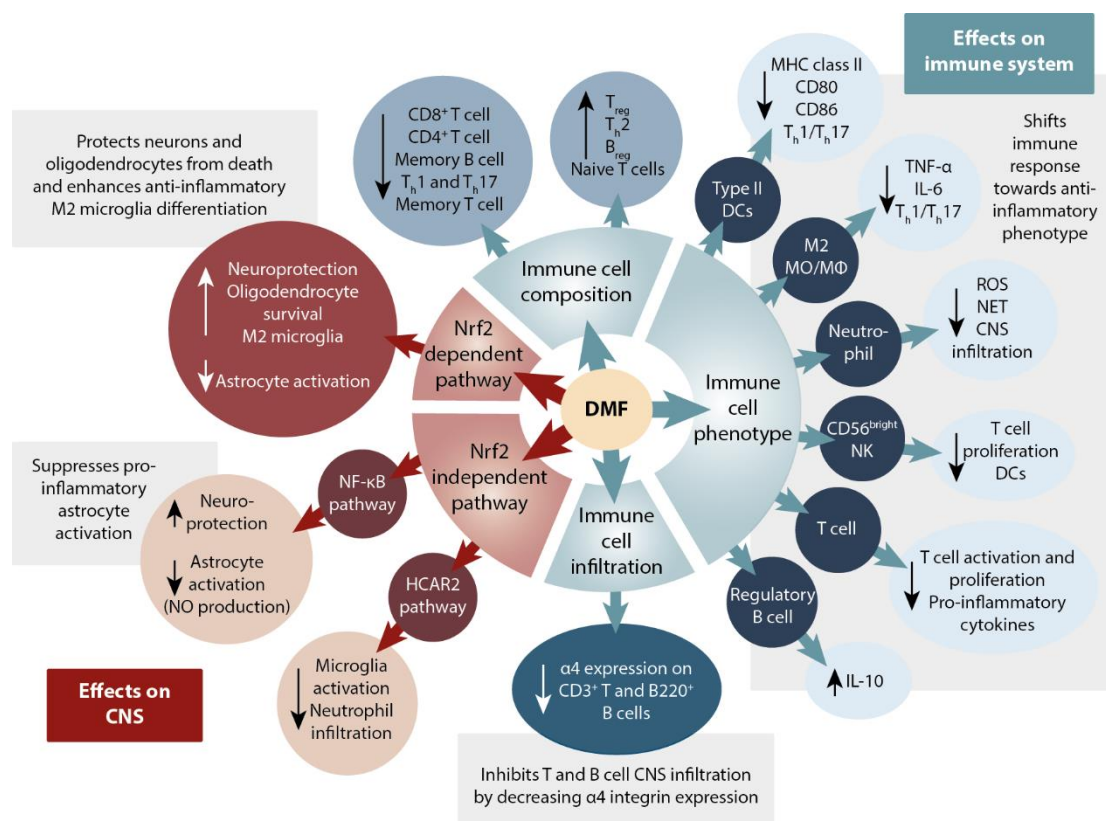


**Figure 3: Possible effects of dimethyl fumarate in the treatment of multiple sclerosis.**

DMF therapy has numerous effects on a variety of cell types of the immune system and the central nervous system (CNS). Treatment with the fumaric acid ester leads to changes in the infiltration of immune cells into the CNS and to an altered polarization of said immune cells. Nrf2, nuclear factor erythroid 2-related factor 2; NF- $\kappa$ B, nuclear factor kappa-light-chain-enhancer of activated B cells; NO, nitric oxide; HCAR2, hydroxycarboxylic acid receptor 2; CD, cluster of differentiation; IL, interleukin; ROS, reactive oxygen species; NET, neutrophil extracellular traps; TNF, tumor necrosis factor; MHC, major histocompatibility complex; M $\phi$ , macrophage; DC, dendritic cell; NK, natural killer cell. Figure adapted from [104]

### 1.3.2 PSORIASIS

Like MS, psoriasis belongs to the T cell-mediated autoimmune diseases. It is an inflammatory skin disease with various occurring forms, the most common being *psoriasis vulgaris* [105]. It is characterized by clearly defined, inflamed plaques of the skin, which are covered by silvery scales. The name plaque-like psoriasis is derived from these clearly defined plaques that can appear all over the body in varying degrees, typically on the extensor areas of the extremities such as the elbows and knees, but also on the back or scalp [106]. The plaques of the skin are mainly due to an increased proliferation and also incomplete maturation of the epidermis. The cells thereupon form the silvery lamellar scales, whereby the underlying skin layer has a strong blood circulation due to the increased growth rate and therefore appears red [105].

Both genetic and immunological factors are causes of psoriasis. A familial clustering can be observed in psoriasis, and the risk of an identical twin also developing the disease is 65-72%, which indicates a genetic disposition [107]. At the same time, the role of the immune system in the pathogenesis of psoriasis is widely accepted and there are studies in which the analysis of psoriasis-associated genes has primarily identified genes of the immune system [108, 109]. The immunological pathogenesis involves a complex interaction between the innate and adaptive immune systems as well as with the resident epithelial cells.

The proinflammatory cytokine milieu plays a decisive role in this cross-talk, with the involvement of TNF- $\alpha$ , IL-12, IL-23 and later IFN- $\gamma$ . Hence, pDCs are activated by an initial trigger such as the release of antimicrobial peptides through an injury. These cells now secrete type 1 interferons, which triggers the activation of cDCs and stimulates them to express IL-23. The resulting activation of T cells leads to differentiation into a T<sub>h</sub>1/T<sub>h</sub>17-dominated lymphocyte population [110-112].

The therapy of psoriasis often requires treatment over a long period of time. Thereby, the choice of medication depends on the severity of the disease. For most patients with a mild course, topical treatment of the lesions is sufficient [113]. Vitamin D derivatives with or without corticosteroids belong to the basic topical therapy [114-116]. For more severe courses of disease, the use of phototherapy or systemic treatments is indicated. One established therapy is the use of fumaric acid esters, which are described in detail in chapter 1.3.3. Further substances used in this context are the

calcineurin inhibitor ciclosporin, methotrexate and retinoids [117-119]. In addition, numerous so-called biologicals have been developed and approved for use in psoriasis in recent years. With these substances, a distinction is made between TNF blockers and those that inhibit IL-17 or IL-23. The first group includes the monoclonal antibody adalimumab and etanercept [120, 121]. The latter are represented by the IL-12/23 blocker ustekinumab and the IL-17A blocking monoclonal antibody secukinumab [122-124].

### 1.3.3 FUMARIC ACID ESTERS

The fumaric acid ester (FAE) DMF is the methyl ester derivative of fumaric acid and is used in the treatment of both psoriasis and multiple sclerosis. For the treatment of severe forms of psoriasis, the drug Fumaderm® has been approved since 1994 and for moderate forms since 2008 [125, 126]. It is a preparation of four different FAEs, namely dimethyl fumarate and the three Ca/Mg/Zn salts of ethyl hydrogen fumarate. Due to its immunomodulatory properties, the use of FAE was also considered for the treatment of multiple sclerosis and consequently, the pure DMF preparation BG-12 was developed and clinically tested [98, 127]. Promising results with a decreased relapse rate and slower progression of the disease finally led to the approval of Tecfidera® for the treatment of RRMS in Germany in 2014.

Compared to other available therapies, treatment with FAE has only mild adverse effects, which primarily occur at high doses. Among the most frequently observed side effects are usually gastrointestinal complaints and the occurrence of cutaneous flushes. In rare cases, a reduction in the number of lymphocytes, eosinophilia or an increase in transaminase may occur [126, 128]. Due to its good benefit-risk profile, the use of DMF is suitable for long-term therapy.

As described in the previous chapters, multiple sclerosis and psoriasis are  $T_h1/T_h17$ -mediated autoimmune diseases. Formerly, it was assumed that elimination of these autoreactive T cells by, for example, monoclonal antibodies, was required to achieve therapeutic success [129-132]. However, early on it was shown that  $CD4^+$  T cells can differentiate into  $T_h1$ -like cells secreting IFN- $\gamma$  and IL-2 as well as polarize into IL-4, IL-5 and IL-10 secreting  $T_h2$  cells. Thereby, both *in vitro* and *in vivo*, IL-4

plays a crucial role [23, 133, 134]. In 1994 it was first demonstrated that the administration of IL-4 resulted in a transformation of the proinflammatory immune response to a  $T_h2$  response in an *in vivo* model of EAE and subsequently to an amelioration of the disease [91]. Furthermore, in patients with psoriasis, therapy with IL-4 and the resulting  $T_h2$  differentiation has also been shown to exhibit promising results [135]. However, therapy with IL-4 requires frequent injection of the cytokine. This proves to be difficult to be implemented over long time periods, which is why other therapeutic options that induce  $T_h2$  induction or blockade of effector cytokines are pursued. An example of this is the treatment with DMF. The administration of the fumarate results in immune deviation towards an anti-inflammatory  $T_h2$  phenotype. The induced  $T_h2$  cells can then locally produce IL-4 at the site of action, leading to inhibition of the effector cytokines IL-17 and IL-23 [136, 137].

Thereby the exact mechanism of action of FAE treatment is still uncertain. For instance, treatment with DMF produces various effects in different cell types, all of which can lead to an improvement in the clinical course of the disease. An overview of how DMF-treatment can impact different cell types to improve MS progression is shown in Figure 3. The modulation of immune cell differentiation is discussed as the primary effector mechanism of FAE therapy. Treatment with DMF results in a shift from IL-12 and IL-23-producing type I DCs to type II DCs with low levels of IL-12/23 and increased secretion of IL-10. Subsequently, these DCs can induce an anti-inflammatory  $T_h2$  response. This immune deviation away from an aberrant  $T_h1/T_h17$  response, which is the underlying cause of psoriasis or MS, leads to an improvement and prevents the disease progression [136, 137]. Again, several mechanisms can lead to a change in polarization and they presumably interact with one another. An exemplary mechanism is depicted in Figure 4. For instance, after the uptake of DMF, there is a decrease in the intracellular reduced form of glutathione (GSH), probably through direct conjugation of the two molecules, which results in an increase in reactive oxygen species (ROS) [137-140]. This induction of oxidative stress induces a number of signaling cascades. For example, DMF is regarded as an activator of nuclear factor erythroid 2-related factor 2 (Nrf2), a master regulator of various antioxidative pathways [141, 142]. However, there are also contradictory publications suggesting a Nrf2-independent mechanism of DMF treatment [143]. Other signaling pathways that are influenced by DMF treatment are the heme oxygenase 1 (HO-1) or STAT1 signaling pathways [137]. The inhibition of NF- $\kappa$ B activity is also considered [144-147]. All these

mechanisms of action lead to 1) a reduced production and secretion of proinflammatory cytokines and 2) cause a shift away from a T<sub>h</sub>1/T<sub>h</sub>17 phenotype towards a T<sub>h</sub>2-mediated immune response.

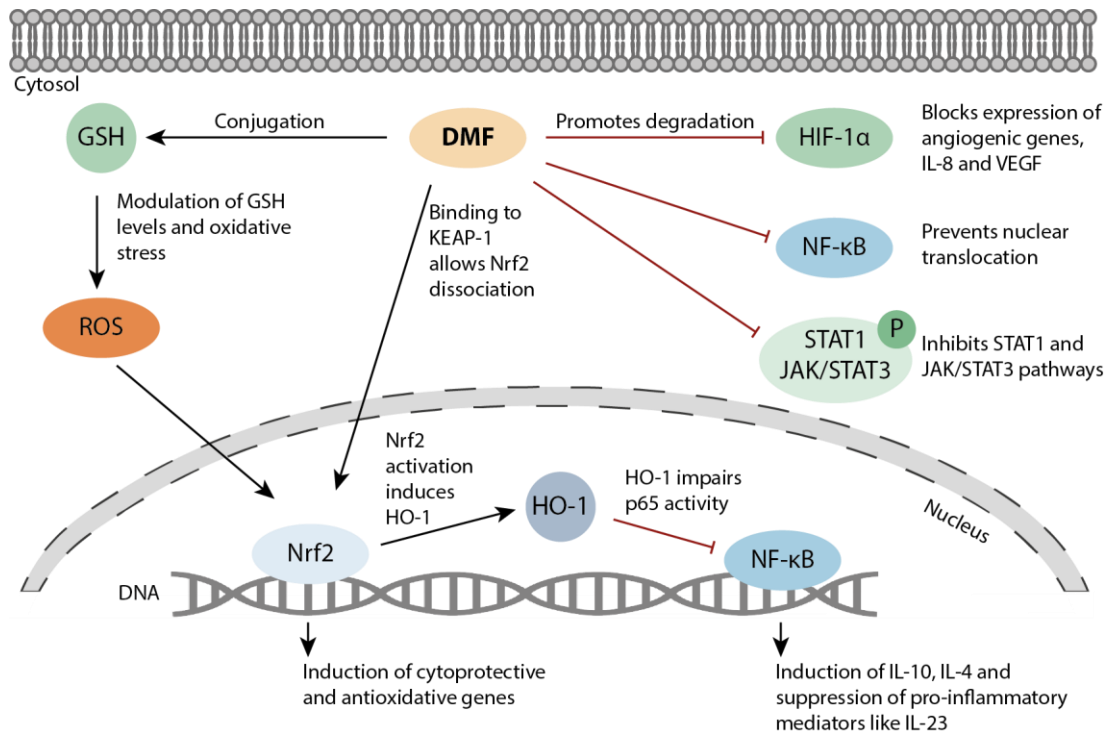


**Figure 4: DMF treatment impacts several signaling pathways to modulate immunity.**

DMF treatment results in various effects on different pathways in the immune cell. It can decrease intracellular GSH levels, thereby inducing oxidative stress and Nrf2 signaling cascades. But at the same time it can also inhibit NF-κB activity, with the downstream effect of decreased inflammatory cytokine production. DNA, deoxyribonucleic acid; DMF, dimethyl fumarate; GSH, reduced form of glutathione; ROS, reactive oxygen species; Nrf2, nuclear factor erythroid 2-related factor 2; HO-1, heme oxygenase 1; NF-κB, nuclear factor kappa-light-chain-enhancer of activated B cells; HIF-1α, hypoxia-inducible factor 1-alpha; STAT, signal transducer and activator of transcription; JAK, janus kinase; KEAP1, kelch-like ECH-associated protein 1; IL, interleukin. Figure adapted from [148].

#### 1.3.4 CARBON MONOXIDE-RELEASING MOLECULES

For a long time, carbon monoxide (CO) was only studied as a toxic gas, but in recent years there has been a growing acceptance of the therapeutic potential of the molecule with its cytoprotective and anti-inflammatory properties [149-151]. CO is a compound composed of carbon and oxygen, which manifests itself as a colorless and odorless gas and has a high affinity for hemoglobin. Because of these properties, it also has the reputation of being a "silent killer", as it can rise unnoticed to high

concentrations and then lead to symptoms ranging from headaches, dizziness or fainting up to death [152]. In the body, CO is mainly produced by the heme oxygenase-mediated cleavage of heme. During this process, the products CO, iron and biliverdin are formed, which is then further transformed into bilirubin [153, 154].

The fact that small amounts of the gas are continuously produced in the body, and that in some disease conditions elevated CO levels can be observed, focused the attention on the therapeutic potential of the gas and its role as a signaling molecule [154-157]. Thereby, the route of CO delivery seems to play a major role in the efficiency but also the toxicity of the therapy. In a study with dogs, no CO toxicity was observed after the transfusion of erythrocytes with 80% carboxyhemoglobin (COHb), whereas inhalation of CO led to rapid lethality after only 15 minutes [158]. To overcome these challenges of CO administration by inhalation, CO-releasing molecules (CORMs) were developed, which are often provided in the form of metal carbonyl compounds. In the ideal case, these molecules are stable in circulation and release CO only after transport to the corresponding target tissue in order to prevent binding to hemoglobin and thus its transport to the lungs and exhalation.

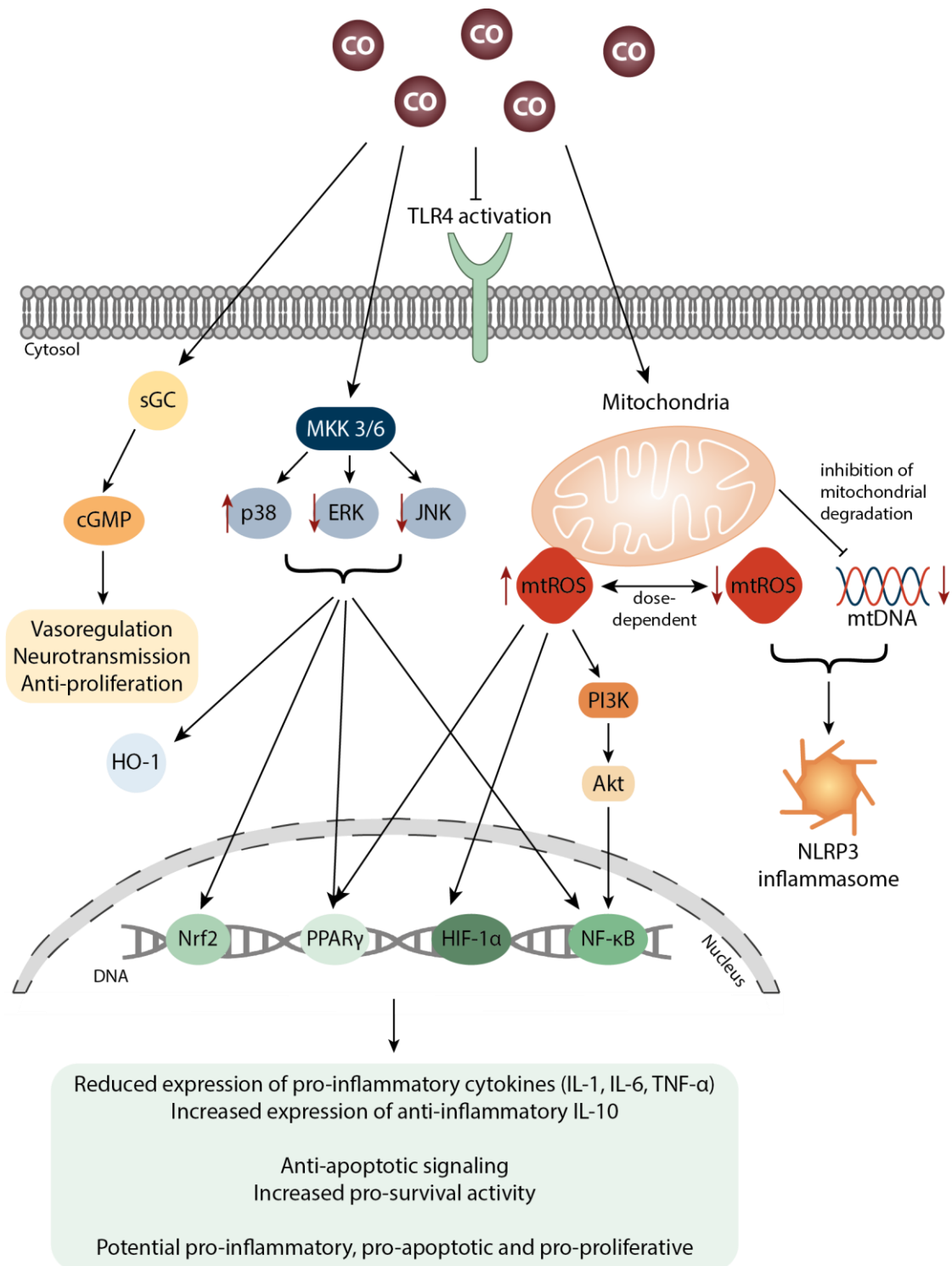


**Figure 5: Modulation of intracellular signaling cascades by carbon monoxide.**

Schematic overview of signaling pathways affected by CO. Endogenous CO or treatment with CO-releasing molecules can lead to anti-inflammatory, anti-apoptotic, or anti-proliferative effects through modulation of sGC activity, MAPK signaling pathways, or mitochondrial function. CO, carbon monoxide; TLR4, toll-like receptor; sGC, soluble guanylyl cyclase; cGMP, cyclic guanosine monophosphate; MKK, mitogen-activated protein kinase kinase; ERK, extracellular signal-regulated kinase; JNK, c-Jun N-terminal kinase; mtROS, mitochondrial reactive oxygen species; mtDNA, mitochondrial deoxyribonucleic acid; PI3K, phosphoinositide 3-kinase; Akt, serine/threonine-protein kinase; Nrf2, nuclear factor erythroid 2-related factor 2; PPAR $\gamma$ , peroxisome proliferator-activated receptor gamma; HIF-1 $\alpha$ , hypoxia-inducible factor 1-alpha; NF- $\kappa$ B, nuclear factor kappa-light-chain-enhancer of activated B cells. Figure adapted from [159-161]



Since CO can act as a signaling molecule, it has modulating properties on different pathways. The various signaling mechanisms of carbon monoxide are illustrated in Figure 5. One possibility for the gasotransmitter CO to unfold its signaling regime is through the activation of the enzymatic activity of soluble guanylyl cyclase (sGC). This occurs through conformational changes as a result of direct binding of CO to the heme iron of sGC and ultimately results in increased production of cyclic guanosine monophosphate (cGMP). This upregulation occurs in a cell type-specific manner and can result in effects, for example, on vasoregulation, neurotransmission, or even anti-proliferative effects [161-163].

The second mechanism of action is the inhibition of TLR4 activation. It was demonstrated that CO decreases the expression of TLR4/myeloid differentiation factor-2 (MD-2) of dendritic cells and is also able to inhibit the maturation of these cells [164, 165]. Thus, the gasotransmitter also has wide-ranging effects on innate and adaptive immune responses.

Furthermore, the production of endogenous CO by HO-1 or the administration of exogenous CO by e.g. CORMs leads to an inhibition of the expression of inflammatory cytokines such as IL-1, IL-6 or TNF- $\alpha$ , as well as to an increase of anti-inflammatory IL-10. This can be accomplished through a variety of molecular mechanisms. In LPS-stimulated macrophages, activation of p38 MAPK, as well as inhibition of extracellular signal-regulated kinase (ERK) and c-Jun N-terminal kinase (JNK), were shown to be responsible for the modulation of cytokine levels [166-168]. Also, mitochondrial ROS (mtROS) induction and subsequent stimulation of the peroxisome proliferator-activated receptor gamma (PPAR $\gamma$ ) and hypoxia-inducible factor 1-alpha (HIF-1a) signaling pathways have been shown to be responsible for the anti-inflammatory effects [169, 170]. Another consequence of increased mtROS production by endogenous CO is the activation of NF- $\kappa$ B via the phosphoinositide 3-kinase (PI3K)/serine/threonine-protein kinase (AKT) signaling pathway, resulting in decreased apoptosis [171]. However, the effects of carbon monoxide on mitochondrial ROS production appear to be concentration- as well as context-dependent. In this regard, inhibition of mtROS could also be demonstrated after the administration of CO. In macrophages stimulated with LPS and adenosine triphosphate (ATP), treatment with the gasotransmitter stabilized mitochondrial function, resulting in low mtROS levels,

reduced translocation of mitochondrial DNA (mtDNA) into the cytoplasm of the cell and consequently inhibition of inflammasome activation [172].

Out of the various signaling mechanisms mentioned above a promising characteristic for its therapeutic use are the anti-inflammatory effects induced by CO. For instance, in macrophages, inflammatory cytokines are inhibited after CO treatment, with a simultaneous increase in the expression of anti-inflammatory IL-10 [166, 167, 173]. Furthermore, a positive effect of treatment with CO gas or CORMs has already been demonstrated in various models of inflammatory diseases, such as autoimmune neuroinflammation, sepsis or vascular inflammation [174-177].

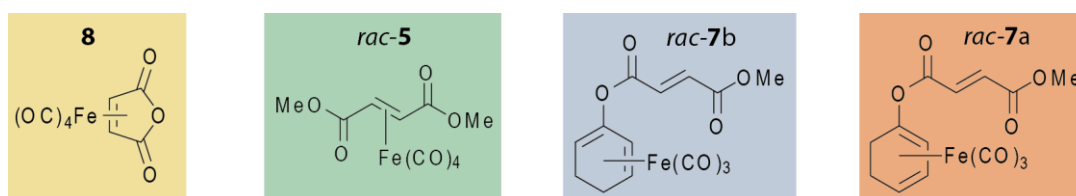


**Figure 6: Overview of CO-releasing molecules.**

Various carbon monoxide (CO)-releasing molecules (CORMs), which are simultaneously coupled to fumaric acid derivatives, were synthesized by the Department of Chemistry at the University of Cologne [178]. Thereby **8** and *rac-5* release CO and fumaric acid or dimethyl fumarate already in aqueous solution. The molecules *rac-7a* and *rac-7b* are enzyme-triggered CORMs (ET-CORMs). These must first be cleaved by esterases, after which they release CO, monomethyl fumarate, cyclohexenone and iron into the cell.

As already mentioned, the heme oxygenase signaling pathway plays a central role in the formation of CO. Also, the gas can stimulate the mitochondrial production of ROS [179]. Due to these properties, being very similar to those of fumaric acid, various CO-releasing molecules were synthesized in a cooperative project with the Department of Chemistry in Cologne [178]. These methyl fumarate-derived iron carbonyl complexes (FumET-CORMs) are simultaneously releasing fumaric acid and CO, in order to supplement or even enhance their anti-inflammatory effects. An overview of the structural formulas of the CO-releasing molecules is shown in Figure 6. Two molecules spontaneously release CO in aqueous solution, i.e., in the cell culture medium. The molecule *rac-5* releases dimethyl fumarate, iron and CO, while molecule **8** releases fumaric acid, iron and higher amounts of CO. In contrast, the substances *rac-7a* and *rac-7b* are so-called enzyme-triggered CO-releasing molecules (ET-CORMs). In a first step they must be transported into the cell, where they release monomethyl fumarate (MMF), iron, cyclohexenone and CO into the cytoplasm after

cleavage by esterases. Again, different kinetics of CO release can be observed. In the case of *rac-7a*, a linear detection of low amounts of CO after esterase addition occurs, whereas *rac-7b* shows a rapid increase of CO in higher concentrations. The two molecules *rac-8* and *rac-12*, which are not coupled to MMF and, therefore, only form CO, iron and cyclohexenone after esterase addition, served as control substances.

## 1.4 REACTIVE OXYGEN SPECIES

Reactive oxygen species (ROS) are generally classified as highly reactive, oxygen-containing chemical entities [180]. In this context, a distinction between oxygen radicals and their non-radical derivatives can be made. Examples of these chemical species include the superoxide radical ( $O_2^{\cdot-}$ ) or the highly reactive hydroxyl radical ( $HO^{\cdot}$ ). As a non-radical representative, hydrogen peroxide ( $H_2O_2$ ) is to be mentioned [181]. Excessive production of ROS or a disturbance in its degradation can lead to elevated concentrations in the cell. This condition, termed oxidative stress, can result in damage to various cellular structures as well as cell death [180].

### 1.4.1 ROS GENERATION AND ITS BIOLOGICAL ROLE

There are several well-established sites for reactive oxygen species production in the cell (Figure 7). One of the primary sources of endogenous ROS are the mitochondria. In various sources it is reported that between 0.1% and up to 5% of the oxygen consumed is processed into these highly reactive molecules [182-184]. In these organelles, the process of oxidative phosphorylation is responsible for the generation of ATP. During this conversion, a leakage of electrons can occur along the electron transport chain, subsequently reducing molecular oxygen to superoxide [184-186].

Another source of endogenous ROS is the endoplasmic reticulum (ER). In the lumen of the ER, the protein folding and posttranslational modification of proteins take place. Here, an oxidizing environment is advantageous, as it facilitates the formation of disulfide bonds and protein folding [187-189]. Thus, the ratio of reduced glutathione (GSH) to its oxidized form (GSSG) in the ER is as low as 5:1 as opposed to 100:1 in the

cytoplasm [190]. One of the main causes of ROS is the ER oxidoreductin (Ero1 $\alpha$ ) - protein disulfide isomerase (PDI) protein folding pathway, which is involved in the formation of disulfide bridges. During this process, the enzyme Ero1 has to maintain its oxidized form, which it achieves by primarily reducing molecular oxygen to H<sub>2</sub>O<sub>2</sub> [187, 191].

As a third source of reactive oxygen species, NADPH oxidase (NOX) should be mentioned. This enzyme is mainly responsible for the production of superoxide radicals, but also hydrogen peroxide. Thereby NOXs are responsible for the transport of electrons across the plasma membrane. Depending on the particular isoform and cell type, they can also be located at other membranes of cell organelles such as the ER, nucleus or mitochondria [192-196]. In phagocytes, such as macrophages and neutrophils, but also in dendritic cells, the generation of ROS plays a role in the so-called 'respiratory burst'. Here, the catalytic subunit NOX2 enables electron transfer from NADPH via FAD and heme cofactors to O<sub>2</sub>, which results in the formation of O<sub>2</sub><sup>-</sup> [197, 198]. Furthermore, the isoform NOX4, which is localized in some cell types at the ER membrane, can lead to the production of H<sub>2</sub>O<sub>2</sub> [199, 200].

As shown in the preceding sections, one of the most frequently formed oxidants is the superoxide radical. After its formation, it can spontaneously undergo dismutation to hydrogen peroxide. This process is further accelerated by the activity of sodium dismutase (SOD), an enzyme capable of catalyzing the conversion of O<sub>2</sub><sup>-</sup> into H<sub>2</sub>O<sub>2</sub> [201, 202]. The hydrogen peroxide formed through these various processes can then be eliminated by several antioxidant signaling pathways, which will be described in more detail in the following chapter 1.4.2. Alternatively, hydrogen peroxide can also be converted into the highly reactive hydroxyl radical. This is implemented by the so-called Fenton reaction, involving the oxidation of Fe<sup>2+</sup> to Fe<sup>3+</sup> in the course of which HO $\cdot$  is formed [203, 204].

If reactive oxygen species are present at basal concentrations, they play an important role as signaling molecules. H<sub>2</sub>O<sub>2</sub>, in particular, is considered to play an important role as a second messenger due to its higher stability compared to the hydroxyl or superoxide free radicals and thus its ability to diffuse over a comparatively long distance of 1  $\mu$ m [205]. For example, hydrogen peroxide is able to induce the transcription factor NF- $\kappa$ B in T cells [206]. A discussed mechanism of action in the modulation of signaling pathways is the modification of reactive cysteine residues of,

e.g., phosphatases and thus their regulation of activity [207-209]. Further examples of redox-mediated signaling are the regulation of HIF-1 $\alpha$  levels, the formation of the inflammasome and autophagy-related protein 4 (Atg4) -mediated autophagy [210-214].

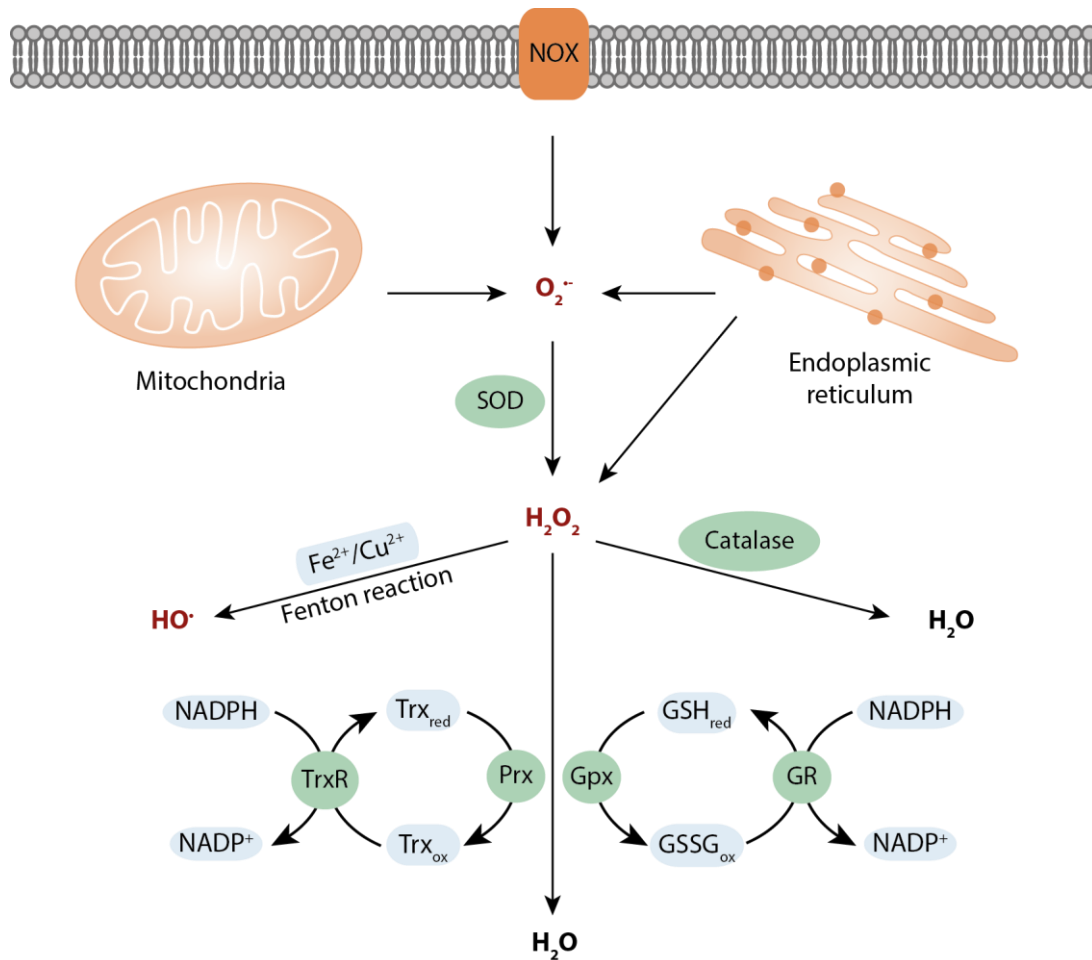


**Figure 7: Cellular maintenance of redox homeostasis.**

Different sources within a cell can form reactive oxygen species. These include but are not limited to mitochondria, the endoplasmic reticulum and NADPH oxidases (NOX). The superoxide radical ( $O_2^{\cdot-}$ ), which is formed by the different pathways, can be rapidly converted to hydrogen peroxide ( $H_2O_2$ ) through sodium dismutase (SOD) activity. The hydrogen peroxide eventually either proceeds to the highly reactive hydroxyl radical ( $HO^{\cdot}$ ) via the so-called Fenton reaction or is scavenged by various antioxidative systems. The conversion of  $H_2O_2$  to water ( $H_2O$ ) and oxygen can be performed by the glutathione or thioredoxin systems or it can be catalyzed by the enzyme catalase. Trx, thioredoxin; TrxR, thioredoxin reductase; Prx, peroxiredoxins; Gpx, glutathione peroxidase; GSH, reduced glutathione; GSSG, oxidized glutathione; GR, glutathione reductase. Figure adapted from [231] and [232].

However, if an aberrant induction of ROS and thus persistent oxidative stress occurs, severe negative consequences for the cell can be observed. This might be caused by damage to the nuclear or mitochondrial DNA, whereby the base guanine is most frequently affected by oxidative mutagenesis [215, 216]. Moreover, if excessively high

concentrations of, e.g., hydrogen peroxide are obtained, further, sometimes irreversible modifications of proteins and lipids may be induced, leading to the induction of senescence or even apoptosis [180, 217-222]. Accordingly, despite their beneficial role as a signaling molecule, ROS are often associated with numerous diseases. For instance, they have been linked to the development of cancer, diabetes mellitus, cardiovascular diseases and many more [223-230].

### 1.4.2 CELLULAR ANTIOXIDANT DEFENSES

Due to the concentration-dependent, opposing effects of ROS as important signaling molecules on the one hand and inducers of oxidative stress and its negative consequences on the other hand, close control of these reactive molecules is indispensable. Thus, the elimination of reactive oxygen species is regulated by several complementary antioxidant mechanisms (Figure 7).

The most frequently occurring ROS scavenger in the cell is the tripeptide glutathione (GSH). It can be found with intracellular concentrations ranging up to 10 mM, but only a very small percentage of the molecule is found in its oxidized form as glutathione disulfide (GSSG) [233]. In the presence of H<sub>2</sub>O<sub>2</sub> and glutathione peroxidase, GSH is oxidized to its disulfide GSSG, converting the hydrogen peroxide to H<sub>2</sub>O and O<sub>2</sub>. The redox cycle is finally completed by glutathione reductase activity in an NADPH-dependent reaction, allowing the process to repeat [234]. If a state of oxidative stress is reached, an increased abundance of oxidized glutathione is generated. In this context, the GSH:GSSG ratio can be used as an indication of the cellular redox status. Besides its function as a ROS scavenger, glutathione also has additional functions. For instance, it prevents the oxidation of thiol groups in proteins or reduces the disulfide groups already formed during oxidative stress [235, 236]. Furthermore, it plays a role in the detoxification of electrophiles, through mercapturic acid formation, or in cellular processes such as DNA synthesis [237, 238].

A second important antioxidant system in the cell is represented by thioredoxin (Trx). Similar to glutathione, it forms a redox cycle at the beginning of which it serves as a hydrogen donor for oxidized proteins, resulting in the formation of oxidized thioredoxin. The pool of the reduced form of thioredoxin is subsequently restored by

thioredoxin reductase (TrxR) activity utilizing NADPH [231, 239]. Molecules that are often restored to their reduced state by the activity of the thioredoxin system are peroxiredoxins. These enzymes are another important catalyst in the conversion of  $H_2O_2$  to water and oxygen [240].

In addition to the previously mentioned sodium dismutase, the protein catalase represents an enzymatic antioxidant significantly involved in ROS's detoxification. After the conversion of the superoxide radical by SOD to  $H_2O_2$ , catalase plays a major role in its further degradation [231]. Catalyzed by the enzyme, the disproportionation of hydrogen peroxide takes place rapidly [241, 242]. Initially, oxidation of the heme protein occurs and  $H_2O$  and compound I are formed. This intermediate is then rapidly reduced once again by a second  $H_2O_2$  molecule, resulting in the generation of  $H_2O$  and  $O_2$  [243]. Accordingly, two hydrogen peroxide molecules are dismutated over the entire course of the reaction.

Besides the endogenous redox systems and enzymatic antioxidants mentioned above, there are many other potential ways to contribute to cellular redox homeostasis. To conclude, vitamin A, coenzyme Q10, vitamin C, dietary antioxidants such as zinc and the metabolite uric acid should be mentioned exemplarily [244-248].

## 1.5 AIM OF THE THESIS

Many autoimmune diseases, such as multiple sclerosis or psoriasis, are caused by an aberrant induction of inflammatory  $T_h1/T_h17$  cells. As an effective therapeutic approach, the deviation of  $T_h1/T_h17$  cells into an anti-inflammatory  $T_h2$  immune response by e.g., dimethyl fumarate has been established [91, 135, 137]. The basis for this is the induction of type II dendritic cells, which in turn cause the differentiation of a  $T_h2$  response [137]. This is where the work for this thesis steps in.

In general, the experiments for this dissertation can be divided into two subprojects. In order to guarantee optimal treatment and minimize possible side effects, the continuous improvement of existing therapies and the development of new therapeutic approaches are essential. Therefore, the first part should include the biological characterization of newly synthesized substances. These so-called FumET-CORMs release both CO and fumaric acid into the cells. The aim was to combine the anti-inflammatory properties of CO and DMF in order to improve therapeutic efficiency even further.

The second part of the project focused on a more detailed clarification of the mechanistic background of dimethyl fumarate treatment. The induction of oxidative stress was previously associated with DMF therapy, but now the causal involvement of ROS in this treatment should be investigated in detail. For this purpose, cystine-glutamate antiporter knockout mice were used, which are not capable of producing intracellular glutathione. Thus, oxidative stress is induced in cells of these mice. This genetic disruption in redox homeostasis allowed the analysis of a possible role of ROS induction in DMF treatment without the occurrence of drug-mediated off-target effects, as in the case of pharmacological inhibition.



## 2 MATERIALS

### 2.1 LABORATORY EQUIPMENT

**Table 1: Laboratory equipment**

<b>Name</b>	<b>Vendor</b>
Airflow Controller AC2	Waldner
Axiovert 25	Zeiss
BD™ LSR II	BD Biosciences
Biofuge fresco	Thermo Fisher Scientific
Biofuge pico	Thermo Fisher Scientific
BioPhotometer 6131	Eppendorf AG
Gel documentation E.A.S.Y 442 K	Herolab
Gelco 102B	biostep GmbH
HB-LS2	VLM
Hera Cell 240	Heraeus
HeraSafe KS 18	Heraeus
Kühlschrank Liebherr Premium no-frost	Liebherr
Laborwaage EW 1500-2M	Kern
Laborwaage Kern 770	Kern
LightCycle 480 II	Roche
Mastercycler gradient	Eppendorf AG
Microwave oven	Samsung
MilliQ Synthesis A10	Millipore
Mini-Protean System Glass Plates	Bio-Rad Laboratories, Inc
Mini-Protean Tetra	Bio-Rad Laboratories, Inc
Model Reference	Eppendorf AG
Model Research	Eppendorf AG
Modell CG842	Schott
Multifuge 3 S-R	Thermo Fisher Scientific
Multiskan EX	Thermo Fisher Scientific
Nalgene™ Cryo 1°C Freezing Container	Nalgene
Neubauer improved counting chamber	Hecht-Assistent
Odyssey Sa Infrared Imaging System	LI-COR, Inc
Pipette boy	Hirschmann
PowerPac 300	Bio-Rad Laboratories, Inc
PowerPac Basic	Bio-Rad Laboratories, Inc
Präzisionswaage CP224SOCE	Sartorius
Primus 96 advanced	Peqlab
Primus 96 plus	Biotech
Reax Top	Heidolph
Sky Line DRS-12	ELMI

STR Rocking Platform	Stuart Scientific
Sub-Cell GT	Bio-Rad Laboratories, Inc
Thermomixer Comfort	Eppendorf AG
Tiefkühlschrank -20 Liebherr Premium no-frost	Liebherr
Tiefkühlschrank -80 Hera freeze	Heraeus
Trans-Blot Turbo	Bio-Rad Laboratories, Inc
VC-10	Caso
Waterbath Type 1003	GFL

## 2.2 LABORATORY MATERIALS

**Table 2: Laboratory materials**

<b>Name</b>	<b>Vendor</b>	<b>Cat #</b>
PCR 8er-SoftStrips, 0.2 ml	Biozym Scientific GmbH	711038
10 ml Stripette®	Corning Incorporated	4101
10 µl TipOne® pipette tips	Starlab International GmbH	S1111-3000
1000 µl TipOne® pipette tips	Starlab International GmbH	S1111-6001
12 Well Cell Culture Plate	Corning Incorporated	3512
200 µl TipOne® pipette tips	Starlab International GmbH	S1111-1006
24 Well Cell Culture Plate	Greiner Bio-One	662160
5 ml Stripette®	Corning Incorporated	4051
6 Well Cell Culture Plate	Greiner Bio-One	657160
96 Well Cell Culture Plate	TPP Techno Plastic Products AG	92096
Biosphere® FilterTips, 0.1-20 µl	Sarstedt AG & Co. KG	70.1114.210
Biosphere® FilterTips, 1250 µl extra long	Sarstedt AG & Co. KG	70.1186.210
Biosphere® FilterTips, 2-100 µl	Sarstedt AG & Co. KG	70.760.212
Cell lifter	Corning Incorporated	3008
Cellstar® tube 15 ml	Greiner Bio-One	188271
Cellstar® tube 50 ml	Greiner Bio-One	227 261
Cryo S™	Greiner Bio-One	126 263
Immobilon-FL Transfer Membrane	Merck KGaA	IPFL00010
Injekt® 20 ml syringe	B. Braun Melsungen AG	4606205V
Needle 30G ½" 0,3x13 mm	BD Biosciences	304000
Petri dishes 94/16 mm	Greiner Bio-One	633161
Safelock 0.5 ml tube	Eppendorf AG	0030 121.023
Safelock 1.5 ml tube	Eppendorf AG	0030 120.086
Safelock 2.0 ml tube	Eppendorf AG	0030 120.094
UV transparent disposable cuvettes	Sarstedt AG & Co. KG	67.759
Whatman Paper	GE Healthcare Life Science	I3017-915

## 2.3 CHEMICALS

Table 3: Chemicals

Name	Vendor	Cat #
2-Vinylpyridine (2VP)	Merck KGaA	132292
5,5'-dithiobis-2-nitrobenzoic acid (DTNB)	Merck KGaA	D8130
Agarose NEEO Ultra quality	Carl Roth GmbH + Co. KG	2267.4
Ammoniumpersulfat (APS)	Merck KGaA	A3678-100G
Ampuwa	Fresenius Kabi AG	B23067A
Auranofin	Merck KGaA	A6733
Bovine serum albumin (BSA)	Carl Roth GmbH + Co. KG	8076.4
Bromophenol blue	Thermo Fisher Scientific	18047
CM-H <sub>2</sub> DCFDA	Thermo Fisher Scientific	C6827
cComplete Tablets, Mini, EDTA-free, EASYpack	Roche	4693159001
Descosept AF	Dr. Schumacher GmbH	00-311-005
Dimethyl sulfoxide (DMSO)	Carl Roth GmbH + Co. KG	A994.1
di-Potassium hydrogen phosphate (K <sub>2</sub> HPO <sub>4</sub> )	Carl Roth GmbH + Co. KG	479.1
Ethanol	VWR International	20.821.330
Ethylenediamine tetraacetic acid (EDTA)	Carl Roth GmbH + Co. KG	8043.1
Fetal Bovine Serum (FCS)	Merck KGaA	F7524
Formaldehyde	Merck KGaA	252549
Glutathione disulfide (GSSG)	Merck KGaA	G4376
Glutathione reductase (GR)	Merck KGaA	G3664
Glycerol	Carl Roth GmbH + Co. KG	3783.1
Glycin	Carl Roth GmbH + Co. KG	3908.2
HEPES 50x	Biochrom	FG0435
Hydrochloric acid (HCl), fuming 37 %	Carl Roth GmbH + Co. KG	4625.1
Isopropanol	Honeywell International Inc	33539
Lipopolysaccharide (LPS)	Merck KGaA	L4524
MEM non-essential amino acids 50x	Merck KGaA	M5550-100ml
Methanol	Carl Roth GmbH + Co. KG	0082.2
Non-fat dry milk	Cell Signaling Technology, Inc	9999
Nonidet™ P 40 Substitute (NP-40)	Merck KGaA	74385
PhosSTOP EASYpack	Roche	4906837001
Potassium chloride (KCl)	Carl Roth GmbH + Co. KG	6781.3
Potassium dihydrogen phosphate (KH <sub>2</sub> PO <sub>4</sub> )	Merck KGaA	1.048.731.000
recombinant GM-CSF	PeproTech, Inc	AF-315-03
Sodium chloride (NaCl)	Carl Roth GmbH + Co. KG	3957.1
Sodium deoxycholate	Merck KGaA	D6750

Sodium dodecyl sulfate (SDS)	Carl Roth GmbH + Co. KG	5136.1
Sodium hydroxide (NaOH)	Merck KGaA	31.05.14
Sodium pyruvate 100mM	Biochrom	L0473
Sulfosalicylic acid (SSA)	Merck KGaA	S2130
Taq DNA-Polymerase	Genaxxon bioscience GmbH	M3001.5000 B
TEMED	Merck KGaA	T9281
Triethanolamine (TEA)	Merck KGaA	T58300
Tris ultrapure	AppliChem GmbH	A1086
Triton X-100	Carl Roth GmbH + Co. KG	3051.2
Tween®20	Carl Roth GmbH + Co. KG	9127.1
β-mercaptoethanol	Merck KGaA	M3148
β-Nicotinamide adenine dinucleotide 2'-phosphate (β-NADPH)	Merck KGaA	N7505

## 2.4 BUFFERS AND SOLUTIONS

**Table 4: Commercial buffers and solutions**

Name	Vendor	Cat #
10x PCR Buffer S complete	Genaxxon bioscience GmbH	M3454.0015
2-log DNA ladder (0.1-10.0 kb)	New England Biolabs GmbH	N3200L
ACK Lysing Buffer	Lonza	10-548E
DMEM	Biochrom	FG0435
dNTP Mix	Genaxxon bioscience GmbH	M3016.1010
GelRed® Nucleic Acid Gel Stain	Biotium, Inc	41003
KAPA SYBR FAST for LightCycler® 480	Merck KGaA	KK4610
MEM non-essential amino acids 50x	Merck KGaA	M5550- 100ml
Odyssey Blocking Buffer	LI-COR, Inc	927-40000
PageRuler™ Plus Prestained Protein Ladder, 10 to 250 kDa	Thermo Fisher Scientific	26619
PBS	Merck KGaA	D8537- 500ml
Penicillin/Streptomycin 10000µg/ml	Biochrom	A2212
Trypan Blue stain 0.4%	Thermo Fisher Scientific	15250-061

Table 5: Self-made buffers and solutions.

Name	Composition	
10 % Acrylamide resolving gel for SDS-PAGE	3.95 ml	H <sub>2</sub> O
	3.33 ml	Acrylamide (30 %)
	2.5 ml	Tris lower (ph 8.8)
	100 µl	SDS (10 %)
	100 µl	APS (10 %)
7.5 % Acrylamide resolving gel for SDS-PAGE	4 µl	TEMED
	5.75 ml	H <sub>2</sub> O
	3 ml	Acrylamide (30 %)
	3 ml	Tris lower (ph 8.8)
	120 µl	SDS (10 %)
5 % Acrylamide stacking gel for SDS-PAGE	120 µl	APS (10 %)
	12 µl	TEMED
	3.4 ml	H <sub>2</sub> O
	850 µl	Acrylamide (30 %)
	625 µl	Tris upper (ph 6.8)
Culture Medium	50 µl	SDS (10 %)
	50 µl	APS (10 %)
	5 µl	TEMED
	solvent	DMEM
	10 % (v/v)	FCS
FACS buffer	1 % (v/v)	Penicillin/Streptomycin
	1 % (v/v)	MEM non-essential amino acids
	1 % (v/v)	HEPES
	1 % (v/v)	Sodium pyruvate
	25 mM	β-mercaptoethanol
GSH buffer	solvent	PBS
	0.1 %	BSA
GSH solution A	16 % (v/v)	GSH solution A
	84 % (v/v)	GSH solution B
GSH solution B	adjust pH to 7.5	
	8.8 mM	EDTA
2x Laemmli buffer	100 mM	KH <sub>2</sub> PO <sub>4</sub>
RIPA buffer	100 mM	K <sub>2</sub> HPO <sub>4</sub>
	4 % (w/v)	SDS
	10 % /v/v)	β-mercaptoethanol
	20 % (v/v)	glycerol
	0.004 % (v/v)	bromophenol blue
RIPA buffer	125 mM	Tris-HCl
	adjust pH to 6.8	
	50 mM	Tris-HCl
	150 mM	NaCl
	1 % (v/v)	NP-40
	0.5 % (w/v)	Sodium deoxycholate

	0.1 % (w/v)	SDS
10x Running buffer	248 mM	Tris-Base
	1.92 M	Glycine
	1 % (w/v)	SDS
Semi-Dry buffer	48 mM	Tris
	29 mM	Glycine
	13 mM	SDS
	20 % (v/v)	MeOH
10x TBS	200 mM	Tris-Base
	1.5 M	NaCl
	adjust pH to 7.6	
1x TBST	solvent	1x TBS
	0.05 % (v/v)	Tween-20
Tris lower	1.5 M	Tris-Base
	0.4 % (w/v)	SDS
	adjust pH to 8.8	
Tris upper	0.5 M	Tris-Base
	0.4 % (w/v)	SDS
	adjust pH to 6.8	

## 2.5 ANTIBODIES

**Table 6: Antibodies**

Target	Vendor	Cat #	Working Dilution
APC/Cy7 Armenian Hamster IgG	BioLegend, Inc	400927	1:25-
Isotype Control			1:50
APC/Cyanine7 anti-mouse CD11c	BioLegend, Inc	117324	1:25-
			1:50
FITC anti-mouse CD86	BioLegend, Inc	105005	1:25-
			1:50
FITC anti-rat IgG2a Isotype Control	BioLegend, Inc	407505	1:25-
			1:50
HO-1	Enzo Life Sciences, Inc	ADI-SPA-896	1:1000
IRDye 680RD Goat (polyclonal) anti-rabbit IgG	LI-COR, Inc	926-68071	1:20000
IRDye 680RD Goat (polyclonal) anti-mouse IgG	LI-COR, Inc	926-68070	1:20000
IRDye 800CW Goat (polyclonal) anti-mouse IgG	LI-COR, Inc	926-32210	1:15000
IRDye 800CW Goat (polyclonal) anti-rabbit IgG	LI-COR, Inc	926-32211	1:15000
Lamin A/C	Cell Signaling Technology, Inc	4777S	1:1000
Nrf2	Santa Cruz	sc-722	1:500

PE anti-mouse CD80	Biotechnology, Inc BioLegend, Inc	104707	1:25- 1:50
PE Armenian Hamster IgG Isotype Control	BioLegend, Inc	400908	1:25- 1:50
pSTAT1 (pY701)	BD Biosciences	612232	1:1000
STAT1	BD Biosciences	610119	1:1000
xCT/SLC7A11	Cell Signaling Technology, Inc	98051	1:1000
$\alpha$ -Tubulin	Novus Biologicals	NB100-690	1:5000
$\beta$ -Actin	Merck KGaA	MAB1501R	1:1000
$\beta$ -Actin	Cell Signaling Technology, Inc	4970S	1:1000

## 2.6 KITS

**Table 7: Commercial kits**

<b>Name</b>	<b>Vendor</b>	<b>Cat #</b>
Cell Proliferation Kit II (XTT)	Merck KGaA	11465015001
DCFDA Cellular ROS Detection Assay Kit	Abcam	ab113851
DuoSet Ancillary Reagent Kit 2	R&D Systems, Inc	DY008
DuoSet ELISA Mouse IL-12p70	R&D Systems, Inc	DY419-05
DuoSet ELISA Mouse IL-23	R&D Systems, Inc	DY1887-05
iScript™ cDNA Synthesis Kit	Bio-Rad Laboratories, Inc	1708890
NE-PER Nuclear and Cytoplasmic Extraction Reagents	Thermo Fisher Scientific	78835
NucleoSpin RNA Plus Kit	MACHEREY-NAGEL GmbH & Co. KG	740984
Pierce BCA Protein Assay Kit	Thermo Fisher Scientific	23225
Pierce LDH Cytotoxicity Assay Kit	Thermo Fisher Scientific	88954
PrimePCR™ Panel, Oxidative Stress Tier 1 M96	Bio-Rad Laboratories, Inc	10029234
Thioredoxin Reductase (TrxR) Assay Kit	Abcam	ab83463

## 2.7 OLIGONUCLEOTIDES

Table 8: Oligonucleotides

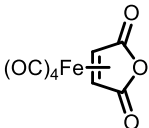
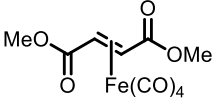
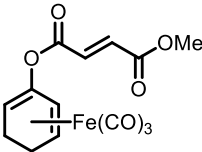
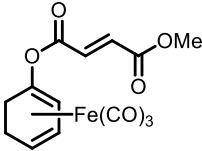
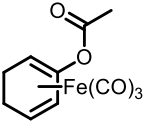
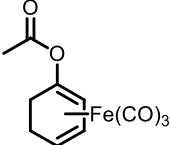
Name	Sequence (5' to 3')
ACTB_LC_as	ACCAGAGGCATACAGGGACA
ACTB_LC_s	CTAAGGCCAACCGTGAAAAG
Eef1a1_LC_as	AGGAGCCCTTTCCCATCTC
Eef1a1_LC_s	ACACGTAGATTCCGGCAAGT
GAPDH forward	CTCACTCAAGATTGTCAGCAATG
GAPDH reverse	GAGGGAGATGCTCAGTGTTGG
GAPDH_as_LC_1	GTTGAAGTCGCAGGAGACAAC
GAPDH_s_LC_1	TGGAGAAACCTGCCAAGTATG
Hmox1_as	CTTCCAGGGCCGTGTAGATA
Hmox1_s	AGGGTCAGGTGTCCAGAGAA
HPRT_LC_as	CCTGGTTCATCATCGCTAATC
HPRT_LC_s	TCCTCCTCAGACCGATTTT
Nrf2_1_as	GCTTGTTTTCGGTATTAAGACACTG
Nrf2_1_s	GAGCAGGACATGGAGCAAGT
Nrf2_2_as	CATGTCCTGCTCTATGCTGCT
Nrf2_2_s	CCCATTTGTAGATGACCATGAG
Slc7a11_as	GAGCATCACCATCGTCAGAG
Slc7a11_s	GATTCATGTCCACAAGCACAC
Sod2_as	GTAGTAAGCGTGCTCCCACAC
Sod2_s	TGCTCTAATCAGGACCCATTG
Txn1_1_as	GAAGTCCACCACGACAAGC
Txn1_1_s	TGAAGCTGATCGAGAGCAAG
Txn1_2_as	TTCAGAGCATGATTAGGCATATTCAG
Txn1_2_s	TGCAGACTGTGAAGTCAAATGCA
Txnrd1_as	TTCCAATGGCCAAAAGAAAC
Txnrd1_s	TCTGAAGAAAAAGCCGTAGAGAA



## 2.8 FUMET-CORMs

FumET-CORMs were kindly provided by Prof. Dr. Schmalz from the Department of Chemistry at the University of Cologne. Substances were synthesized as published in Bauer et al [178]. An overview of utilized substances, structural formulas, cleavage mechanism and released molecules is shown in Table 9.

**Table 9: FumET-CORMs**

Name	Structural Formula	Cleavage	Released Molecules
<b>8</b>		spontaneous	dimethyl fumarate, CO, iron
<i>rac-5</i>		spontaneous	fumaric acid, CO, iron
<i>rac-7a</i>		enzymatic	monomethyl fumarate, CO, iron, cyclohexenone
<i>rac-7b</i>		enzymatic	monomethyl fumarate, CO, iron, cyclohexenone
<i>rac-8</i>		enzymatic	CO, iron, cyclohexenone
<i>rac-12</i>		enzymatic	CO, iron, cyclohexenone

## 2.9 SOFTWARE

**Table 10: Software**

<b>Name</b>	<b>Vendor</b>
Adobe Illustrator CS6	Adobe
BD FACSDiva Software v 6.1.3	BD Biosciences
Bio-Rad PrimePCR Analysis V1.0.03001023	Bio-Rad Laboratories, Inc
Ascent Software Version 2.6	Thermo Fisher Scientific
FlowJo V10	FlowJo LLC
GNU Image Manipulation Program 2.10.8	The GIMP Team
GraphPad Prism 8	GraphPad Software
Image Studio Lite V3.1.4	LI-COR, Inc
Light Cycler 480 SW 1.5.1	Roche
Endote X9.2	Alfasoft GmbH
Odyssey Sa Application Software V1.1.7	LI-COR, Inc
Office 2010	Microsoft Corporation
qBase +	Biogazelle

## 2.10 LABORATORY ANIMALS

Mice used for this study were bred and held in the animal facilities of the Eberhard Karls University Tübingen under specific pathogen-free conditions. Mice were handled in accordance with the „Einrichtung für Tierschutz, Tierärztlichen Dienst und Labortierkunde“ and the „Regierungspräsidium Tübingen“ (Mitteilung §4 vom 10.08.16). For isolation of bone marrow-derived dendritic cells mice aged 8 weeks and older were used. All mouse strains and their laboratory names are listed in Table 11.

**Table 11: Laboratory animals**

<b>Name</b>	<b>Laboratory name</b>
C57BL/6J	WT
B6- <i>Slc7a11</i> <sup>tm</sup>	xCT.KO
B6.129S- <i>Cybb</i> <sup>tm1Din/J</sup>	GP91.KO

## 3 METHODS

### 3.1 ISOLATION OF BMDC

Protocol for isolation of bone marrow-derived dendritic cells was modified from [249]. On day 0 mice were euthanized by CO<sub>2</sub> suffocation. The following steps for isolation of cells were performed under sterile conditions. The following experimental steps were performed in a laminar air flow. Incisions were made to expose the muscles of the hind legs. Afterwards both hind legs were cut off just above the hip joint and transferred to a sterile petri dish with 1x PBS. The remaining skin and paws were removed and the bones were freed from muscle tissue by rubbing the muscle off the bone with a tissue previously sprayed with Descosept. Isolated bones were collected in a sterile petri dish with 1x PBS. For harvesting of bone marrow bones were put in 80 % EtOH for a few seconds and afterwards both ends of femurs and tibias were cut off with a scissor. Bones were then flushed with 1x PBS using a syringe until they appeared white. The bone marrow suspension was collected in a 50 ml tube and occurring clusters were resolved by extensive pipetting. Afterwards cells were purified using a cell strainer and flow through was collected in a fresh 50 ml tube. The cell suspension was then centrifuged at 480 rcf for 5 min. For lysis of red blood cells the supernatant was removed and cells were resuspended in 500 µl ACK lysing buffer. Incubation took place for 2.5-3 min with occasional gentle shaking of the tube. Lysis of red blood cells was stopped by adding 10 ml of 1x PBS, followed by centrifugation of the cell suspension at 480 rcf for 5 min. Total number of cells was determined using a hemocytometer. Finally cells were seeded in 10 cm bacterial petri dishes with a density of  $\sim 1.5\text{-}2 \times 10^6$  cells/plate in 7 ml DMEM culture medium supplemented with 20 ng/ml recombinant GM-CSF. Cells were incubated at 37 °C, 7.5 % CO<sub>2</sub> for 3 days.

On day 3 after isolation of bone marrow-derived stem cells a replenishment with fresh culture medium was performed. Therefore 7 ml of fresh DMEM culture medium with 20 µg/ml recombinant GM-CSF were added to the cells. Cells were then incubated at 37 °C, 7.5 % CO<sub>2</sub> for another 3 days.

On day 6 after isolation of bone marrow-derived stem cells 7 ml of medium was removed from each petri dish and collected in a 50 ml tube. The pooled cell culture medium from all plates was centrifuged at 480 rcf for 5 min and the supernatant was discarded. Cells were then resuspended in 7 ml per plate of fresh DMEM culture medium with 20 µg/ml recombinant GM-CSF and distributed on the original petri dishes. Cells were then incubated at 37 °C, 7.5 % CO<sub>2</sub> for another 1-2 days.

On day 7 or 8 after isolation of cells immature dendritic cells could be harvested. This was done by gently collecting the non-adherent cells from each petri dish in a 50 ml tube. BMDCs are only lightly-adherent, while macrophages are adherent and can't be easily detached from the plate. Cell suspension was then centrifuged at 480 rcf for 5 min and supernatant was discarded. For determination of total cell number cells were counted in a hemocytometer. For following biological assays cell density was adjusted as needed with DMEM. For most assays a cell density of 1x10<sup>6</sup> cells/ml was used.

## 3.2 MEASUREMENT OF INTRACELLULAR GSH/GSSG

Subchapters of 3.2 comprise all necessary steps for the detection of intracellular levels of GSH and GSSG. The protocol was adapted from [250].

### 3.2.1 *BMDC HARVEST AND GSH SAMPLE PREPARATION*

For harvesting BMDC after treatment the cells were washed with ice-cold 1x PBS. Non-adherent cells were collected and washed as well. Non-adherent cells were then resuspended in 500 µl 1 % SSA and the cell suspension was added to the corresponding wells with the adherent cells. This cell mixture was then incubated on ice for 30-45 min for cell lysis and protein precipitation. Cells were then detached with a cell scraper and the suspension was collected in a 1.5 ml tube. For better lysis of cells subsequently two freeze/thaw were performed. This cell suspension was then centrifuged at 13 000 rcf for 5 min at 4 °C. Supernatants were transferred to a new 1.5 ml tube and could either be directly used for GSH measurement or they were stored at -80 °C.

### 3.2.2 SAMPLE PREPARATION FOR GSSG MEASUREMENT

Cell pellets from chapter 3.2.1 were resuspended in 500  $\mu$ l 0.5 M NaOH, vigorously vortexed and incubated for 30 min at room temperature (RT). Samples could now be measured directly or stored at 4 °C. To prevent GSH oxidation to GSSG 5  $\mu$ l 2VP diluted 1:10 in GSH buffer were added to 250  $\mu$ l cell extract under the hood. After 1 h incubation at RT 15  $\mu$ l TEA diluted 1:6 in GSH buffer were added and then incubated for another 15 min. Samples were now ready for GSSG measurement.

### 3.2.3 SPECTROMETRIC MEASUREMENT OF SAMPLES

A GSH standard was prepared by diluting GSSG in 1 % SSA. For GSSG measurement a separate standard and blank sample should be used that was treated with 2VP and TEA as well. Importantly all samples should be kept on ice and DTNB, GR and  $\beta$ -NADPH solution should additionally be covered in aluminum foil to protect from light. Spectrometric analysis of samples was performed in a 96 well plate. First, 20  $\mu$ l of GSH buffer (blank), standard or sample were pipetted per well. Thereby the measurements were performed in duplets. Equal volumes of 1.68  $\mu$ M DTNB in GSH buffer and 3.33 U/ml GR in GSH buffer were mixed. To allow conversion of GSSG to GSH 120  $\mu$ l of this solution was added into each well and incubated for ~30 sec. Finally 60  $\mu$ l of 800  $\mu$ M  $\beta$ -NADPH in GSH buffer was added to each well and absorbance was measured immediately at 412 nm for ten times every 30 seconds.

## 3.3 ENZYME-LINKED IMMUNOSORBENT ASSAY (ELISA)

For the analysis of secreted inflammatory cytokines IL-12p70 and IL-23 cell culture supernatants were harvested. Therefore supernatants were collected in a 1.5 ml tube and centrifuged at 480 rcf for 5 min. Cell-free supernatants were then transferred to a new 1.5 ml tube and were stored at -80 °C until analysis. Detection of cytokines was performed with commercial kits DuoSet ELISA Mouse IL-12p70, DuoSet ELISA Mouse IL-23 and DuoSet Ancillary Reagent Kit 2 according to manufacturer's instructions. In short, 96 well plates were coated with the respective capture antibody overnight. Subsequently the plates were washed with wash buffer and blocked with reagent diluent for 1 h. After another washing step the wells were incubated in duplets with the undiluted cell culture supernatants for 2 h at RT. After this the plates were washed again and incubated with the respective detection antibody for 2 h. After

removal of excess detection antibody, Streptavidin-HRP was added, which binds to the detection antibody and allows subsequent analysis of cytokine concentrations.

### 3.4 WESTERN BLOT

#### 3.4.1 *PREPARATION OF WHOLE CELL LYSATES*

For the preparation of protein lysates from whole cells the treated cell culture plates were put on ice. The medium was removed and collected in a 15 ml tube to collect the non-adherent cells as well. The plates were then washed with 1x PBS, which was collected in the respective 15 ml tubes as well. To harvest the adherent cells ice-cold the required amount of RIPA buffer with 1x PhosStop and 1x cOmplete protease inhibitor was added to the plate and cells were scraped with a cell scraper or a sterile 100 µl pipette tip. This lysate was then transferred to a 1.5 ml tube and stored on ice. Simultaneously to the harvest of adherent cells the suspension containing the non-adherent cells was centrifuged at 480 rcf for 5 min. The cell pellet was washed with 1x PBS and spun down at 480 rcf for 5 min one more time. Finally these cells were resuspended in RIPA buffer with 1x PhosStop and 1x cOmplete protease inhibitor and pooled with the respective suspension containing the adherent cells. Samples could then be stored at -80 °C or the protein concentration was measured directly.

#### 3.4.2 *PREPARATION NUCLEAR AND CYTOPLASMIC LYSATES*

For separation of nuclear and cytoplasmic fractions the “NE-PER Nuclear and Cytoplasmic Extraction Reagents” kit was used, following manufacturer’s instructions. Briefly, the treated cells were collected in CER I buffer and vortexed vigorously. After addition of CER II and repeated vortexing, the sample was centrifuged at 13 000 rcf for 5 min at 4 °C. The supernatant contained the cytoplasmic fraction, and was therefore transferred to a fresh tube. In order to isolate the nuclear fraction the pellet was resuspended in ice-cold NER, vortexed several times over a time period of 40 min and centrifuged at 13 000 rcf for 10 min at 4°C. Once again the supernatant was transferred to a fresh tube. The cytoplasmic and nuclear lysates were both stored at -80 °C.

### 3.4.3 MEASUREMENT OF PROTEIN CONCENTRATION

Isolated samples from step 3.4.1 or 3.4.2 were centrifuged at 13 000 rcf for 5 min and subsequently stored on ice. Measurement of protein concentrations was performed with the commercially available “Pierce BCA Protein Assay Kit” from Thermo Fisher Scientific according to manufacturer’s instructions. In short, samples were diluted with lysis buffer if necessary and 10 µl of sample, blank or standard were pipetted per well in a 96 well plate. Then BCA working reagent was added to the samples and incubated at 37 °C for 30 min to allow color formation with BCA. Colorimetric detection was performed with a Multiskan EX at 540 nm.

### 3.4.4 GEL ELECTROPHORESIS

Samples were prepared by adding the appropriate amount of Laemmli buffer to achieve a final concentration of 1x and subsequently heated for 5 min at 95 °C. To assemble the Mini-Protean Tetra electrophoresis cell handcast 7.5 % or 10 % polyacrylamide gels were placed into the chamber and filled with 1x running buffer. Then the required amount of samples and PageRuler™ Plus Prestained Protein Ladder were loaded onto the gel. Finally SDS-PAGE was performed at 80 V to 120 V until the dye-front had reached the end of the gel.

### 3.4.5 WESTERN BLOTTING

Gels were transferred onto an Immobilon-FL Transfer membrane using a Gelco 102B system filled with Semi-Dry buffer. Membranes were first activated for a few seconds in 100 % MeOH and then stacked between two Whatman papers soaked in Semi-Dry buffer together with the gel. Transfer was then performed at 100 V, 300 mA for 2 h. After the transfer membranes were either blocked with Odyssey blocking buffer for 1 h at RT or with 5 % non-fat dry milk in TBST for 30 min at RT depending on the antibody. After incubation with primary antibodies (Table 6) over night at 4 °C membranes were washed three times with 1x TBST, incubated with IRDye secondary antibodies for 1 h at RT in the dark and washed again three times with TBST. Membranes were scanned using the Odyssey Sa Infrared Imaging System. Band intensities were analyzed using Odyssey Sa Application Software.

## 3.5 MEASUREMENT OF CELL VIABILITY

### 3.5.1 *TRYPAN BLUE EXCLUSION ASSAY*

Harvesting of treated BMDCs was performed by carefully scraping the cells of the plate with a cell scraper. The cell suspension was then transferred to a 15 ml tube and centrifuged at 480 rcf for 5 min. Subsequently the cells were resuspended in an appropriate amount of cell culture medium. For determination of cell numbers harvested BMDCs were diluted 1:10 in 1:2 trypan blue/1x PBS solution and living and dead cells were counted using a hemocytometer. Viable cells are not stained by trypan blue, but dead or dying cells appear blue due to a loss of membrane integrity. Cell viability was determined by calculation of stained/unstained cell ratios.

### 3.5.2 *XTT ASSAY*

This assay was performed with the commercially available “Cell Proliferation Kit II (XTT)” according to manufacturer’s instructions. BMDCs were plated and treated in a 96 well plate in triplets. After 24 h to 48 h of treatment 50  $\mu$ l XTT labeling reagent and 1  $\mu$ l electron coupling reagent were added per well and incubated for 2.5 h at 37 °C, 7.5 % CO<sub>2</sub>. In viable cells the orange formazan dye is formed by cleavage of the tetrazolium salt XTT which was directly measured at 492 nm in a Multiskan EX ELISA Reader.

### 3.5.3 *LDH ASSAY*

Lactate dehydrogenase (LDH) is released into the cell culture media as a consequence of membrane damage induced by cytotoxicity. To determine the cell viability the amount of released LDH was measured with the “Pierce LDH Cytotoxicity Assay Kit”, following manufacturer’s instructions. Briefly, extracellular LDH released by treated BMDCs was measured by transferring 50  $\mu$ l of cell culture supernatants onto a new 96 well plate and adding 50  $\mu$ l Reaction Mix. After incubation for 30 min at RT in the dark the chemical reaction catalyzed by LDH was interrupted by adding 50  $\mu$ l of Stop Solution. The formazan formed by this reaction was then directly measured at 492 nm in a Multiskan EX ELISA Reader.



## 3.6 ANALYSIS OF GENE EXPRESSION

Changes in gene expression can be measured by analyzing RNA transcription. Therefore RNA was isolated from BMDCs and the corresponding cDNA was synthesized. Through the utilization of specific primers the desired gene sequences can be amplified and analyzed via quantitative real-time polymerase chain reaction (qRT-PCR). The workflow applied for this analysis is described in the following subchapters.

### 3.6.1 SAMPLE PREPARATION

For the preparation of RNA samples the treated cell culture plates were put on ice. BMDCs were gently scraped off the plates using a cell scraper, then cell suspension was collected in a 15 ml tube and centrifuged at 480 rcf for 5 min. The cell pellet was then resuspended with 1x PBS, transferred to a 1.5 ml tube and centrifuged once more. After washing of the cells the supernatant was removed leaving the pellet as dry as possible. In the end the sample was directly frozen in liquid nitrogen and stored at -80 °C.

### 3.6.2 RNA ISOLATION

When working with RNA it is of utmost importance to avoid the introduction of ribonucleases (RNases) into the sample. Therefore all surfaces were decontaminated prior to proceeding with the RNA isolation. For this procedure the “NucleoSpin RNA Plus Kit” was used, following the manufacturer’s protocol. RNA was eluted twice with 40 µl RNase-free H<sub>2</sub>O. The concentration of isolated RNA was measured diluted 1:16 in RNase-free H<sub>2</sub>O in a cuvette using a BioPhotometer 6131. Quality of isolated RNA was checked by calculating the 260 nm/280 nm and 260 nm/230 nm ratios. Thereby the 260/280 ratio should be around ~2.0 and 260/230 ratios should be around 2.0-2.2, indicating RNA purity. Deviations from these values show the presence of contaminants in the RNA sample. Next 200 ng of RNA was separated on a 1 % agarose gel using gel electrophoresis. Here RNA integrity was further assessed by inspecting bands for 28S and 18S ribosomal RNA, which should be clearly visible.

### 3.6.3 SYNTHESIS OF CDNA

In this next step a reverse transcription of isolated RNA to cDNA was performed using the commercially available “iScript™ cDNA Synthesis Kit”. For that purpose kit components were thawed on ice and the incubation mix was prepared by adding 4 µl of 5x iScript Reaction Mix and 1 µl iScript Reverse Transcriptase to 16 µl isolated RNA in RNase-free H<sub>2</sub>O from step 3.6.2 containing 1 µg of RNA. Reverse transcription was conducted in a PCR cycler using the program shown in Table 12.

**Table 12: Reverse transcription cycling conditions.**

Step	Temperature [°C]	Time
1	25	5 min
2	42	45 min
3	85	5 min
4	4	hold

### 3.6.4 CONTROL PCR WITH HOUSEKEEPING GENE

To allow quality control of synthesized cDNA from step 3.6.3, a test PCR was conducted. In order to amplify glyceraldehyde 3-phosphate dehydrogenase (GAPDH) DNA fragments 1 µl cDNA from step 3.6.3, 2 µl 10x PCR Buffer, 1 µl forward primer (10 µM), 1 µl reverse primer (10 µM), 0.4 µl dNTPs (10 mM each) and 0.2 µl Taq DNA polymerase were added and filled up to 20 µl with nuclease-free H<sub>2</sub>O. Amplification was performed in a PCR cycler using the conditions listed in Table 13 and afterwards a 1 % agarose gel electrophoresis was carried out. For this, 5 µl of loading dye was added to the previously synthesized DNA sample and 10 µl of this mixture were loaded onto the gel. Electrophoresis was performed at 120 V until the dye-front had reached the end of the gel and visualization was performed under UV-light using gel documentation E.A.S.Y 442 K and Herolab software.

**Table 13: GAPDH test PCR cycling conditions.**

Step	Temperature [°C]	Time	Repetitions
1	95	1 min	} 25 cycles
2	56	1 min	
3	72	1 min	
4	72	5 min	
5	4	hold	

### 3.6.5 QUANTITATIVE REAL-TIME PCR

One difference of RT-PCR in contrast to PCR is that the amplification of specific targets can be monitored during the PCR run and not only at the end. To enable this fluorescent dyes are added to the sample that can intercalate with the synthesized DNA. Moreover, if a standard is included in the RT-PCR the amplification of the respective template can be quantified. To determine the copy number of various target genes 1  $\mu$ l of cDNA from step 3.6.3 diluted 1:5 in nuclease-free H<sub>2</sub>O was added to 5  $\mu$ l KAPA SYBR FAST qPCR mix, 1  $\mu$ l forward primer (10  $\mu$ M), 1  $\mu$ l reverse primer (10  $\mu$ M) and 2  $\mu$ l nuclease-free water. As a first step a pre-amplification was performed, to allow the preparation of a DNA standard and a first quality control of used samples and primers. For this, a cDNA pool, RNA pool of all samples and a H<sub>2</sub>O control were deployed for each primer pair used in the assay. After the RT-PCR was completed following the protocol seen in Table 14, the cDNA pool was collected and used for the preparation of a 10<sup>-2</sup> to 10<sup>-9</sup> standard in nuclease-free H<sub>2</sub>O. The RNA pool and H<sub>2</sub>O sample give information about primer and sample quality. After successful pre-amplification of controls the RT-PCR with respective cDNA samples was conducted in duplets. For quantification the 10<sup>-3</sup>, 10<sup>-5</sup>, 10<sup>-7</sup> and 10<sup>-9</sup> standard was used for each primer pair. Additionally a negative control (H<sub>2</sub>O) and a RNA control were carried out to ensure PCR specificity. The amplification was conducted following the conditions listed in Table 14 in a LightCyle 480 II.

**Table 14: qRT-PCR cycling conditions.**

Step	Temperature [°C]	Time	Repetitions
1	95	5 min	} 45 cycles
2	95	10 sec	
3	60	10 sec	
4	72	10 sec	
5	95	10 sec	
6	65	1 min	
7	95	0.06 °C/sec starting at 65 °C	
8	40	hold	

### 3.6.6 PCR ARRAY

In order to screen a large amount of different genes involved in oxidative stress response a PCR array was performed. Here, the commercially available “PrimePCR™ Panel, Oxidative Stress Tier 1 M96” was used, according to manufacturer’s protocol. In

short, cDNA samples were prepared as described in steps 3.6.1 - 3.6.4. For amplification of target sequences 10 ng of synthesized cDNA was added to 10  $\mu$ l KAPA SYBR FAST qPCR mix and added up to 20  $\mu$ l with nuclease-free H<sub>2</sub>O. As a final step 20  $\mu$ l of this master-mix was loaded per well of the 96 well plate, where lyophilized primers were already present in each well. The plate was loaded in the LightCycle 480 II instrument and run under the program listed in Table 15.

**Table 15: PCR array cycling conditions.**

Step	Temperature [°C]	Time	Repetitions
1	95	2 min	} 40
2	95	5 sec	
3	60	30 sec	
4	95	0.06 °C/sec starting at 65 °C	
5	40	hold	

### 3.7 FLUORESCENCE ACTIVATED CELL SORTING (FACS)

FACS analysis was performed to study the different immune cell populations. For this, BMDCs were stained for the surface markers CD11c, CD80 and CD86. First, cells were harvested at the desired time point and  $0.5 \times 10^6$  cells were transferred into a 1.5 ml tube per sample. For unstained, isotype and single stain controls a BMDC pool was collected with cells from each sample. Cells were then washed with 1x PBS, resuspended in 150  $\mu$ l PBS with 2 % formaldehyde and incubated for 20 min at RT in the dark. Then 600  $\mu$ l FACS buffer were added and the cells were centrifuged at 480 rcf for 5 min. Cells were resuspended in an appropriate amount of FACS buffer, so that they could be easily distributed on the different antibody staining samples, e.g. 100  $\mu$ l per sample. Once distributed, they were centrifuged again at 480 rcf for 5 min and resuspended in 20  $\mu$ l of FACS buffer. For staining 10  $\mu$ l of the respective fluorophore-conjugated antibody diluted 1:25 in FACS buffer was added to the cells, incubated for 30 min at 4 °C in the dark and subsequently washed with 200  $\mu$ l FACS buffer. Finally cells were resuspended in 500  $\mu$ l FACS buffer and analyzed using a BD™ LSR II.

### 3.8 DETECTION OF ROS

For the analysis of reactive oxygen species a ROS assay was performed. First, cells were carefully harvested with a cell scraper and collected in a 15 ml tube. Cells were centrifuged at 480 rcf for 5 min and resuspended in PBS with a cell density of  $0.5 \times 10^6$  cells/ml. Per group 1 ml of cell suspension was stained with 2  $\mu$ M DCFDA solution in DMSO. After incubation for 30 min at 37 °C in the dark 500  $\mu$ l PBS were added and the cell suspension was centrifuged at 480 rcf for 5 min. Cells were then resuspended in 1 ml DMEM cell culture medium and could be treated with e.g. DMF or other compounds for the desired time period. Analysis was then directly performed using a BD™ LSR II without any further washing of the cells.

### 3.9 ANALYSIS OF THIOREDOXIN REDUCTASE ACTIVITY

For analysis of the enzymatic activity of thioredoxin reductase the commercially available “Thioredoxin Reductase (TrxR) Assay Kit” was used, following the manufacturer’s protocol. For this,  $7 \times 10^6$  BMDCs were gently harvested using a cell scraper, homogenized in 300  $\mu$ l cold assay buffer and centrifuged at 13 000 rcf for 15 min at 4 °C. From the supernatant generated here 50  $\mu$ l from each sample were used for TrxR assay. Thereby a TrxR inhibitor was added to one set of samples and another set was measured without the inhibitor to analyze background enzyme activity. The reaction mixture was composed of 50  $\mu$ l of sample with or without 10  $\mu$ l TrxR inhibitor, 30  $\mu$ l Assay Buffer, 8  $\mu$ l DTNB solution and 2  $\mu$ l NADPH solution. Additionally a TNB standard curve was created. The plate was measured as fast as possible using a Multiskan EX at 405 nm and a second time after 20 min incubation at RT in the dark.

### 3.10 STATISTICAL ANALYSIS

Unless otherwise stated, the data were reported as mean with standard deviation (SD). Statistical analysis of the data was performed using a one-way or two-way ANOVA with Tukey post-hoc test to compare between three or more treatment groups. In the case of only two treatment groups, an unpaired Student's t test was carried out. P

values of  $\leq 0.05$  were considered significantly different. P values were marked with stars according to the following criteria: \*,  $p = \leq 0.05$ ; \*\*,  $p = \leq 0.01$ ; \*\*\*,  $p = \leq 0.001$ ; \*\*\*\*,  $p = \leq 0.0001$ . If not otherwise indicated in the graph, the p values refer to the corresponding DMSO control.

## 4 RESULTS

### 4.1 DMF-MEDIATED ANTI-INFLAMMATORY EFFECTS IN WILDTYPE BMDCs

In this initial chapter, the anti-inflammatory effects of DMF treatment will be assessed. These were previously substantiated by an oxidative stress-mediated induction of type II dendritic cells, which in turn trigger a  $T_H2$  response [137]. As a first step, the stability of the system was therefore verified in order to provide a basis for further work in this thesis.

For all experiments carried out in this thesis, bone marrow-derived dendritic cells were used as a cell system in order to more accurately decipher the mechanisms of action as well as the effectiveness of DMF or CO treatment. To this end, dendritic cells were isolated from the bone marrow of wildtype C57BL/6 mice. The protocol used for this is shown in Figure 8A and will be briefly explained in the following. After isolation of the cells from the femurs of mice, they were cultivated in a special differentiation medium for seven days. During this time, fresh medium was administered to the cells on both day three and day six. After differentiation for seven days, the non-adherent cells were carefully harvested and analyzed for purity by flow cytometry. This procedure yielded an average of 81.2 % pure cell population being positive for the DC marker CD11c. Furthermore, the harvested cells were predominantly immature DCs, as only 13.8 % were also positive for the activation marker CD86 (Figure 8B).

After successful characterization of the harvested BMDCs these cells were treated with DMF for 4 h and effects on redox homeostasis were monitored. The first step was the analysis of intracellular glutathione, the cells most abundant non-enzymatic ROS scavenger. Here a significant decrease from 29.5  $\mu\text{M}$  in DMSO-treated cells to 6.2  $\mu\text{M}$  after incubation with DMF could be observed after 4 hours. Through additional incubation with the antioxidant NAC this inhibition of GSH was completely reversed (Figure 9A).

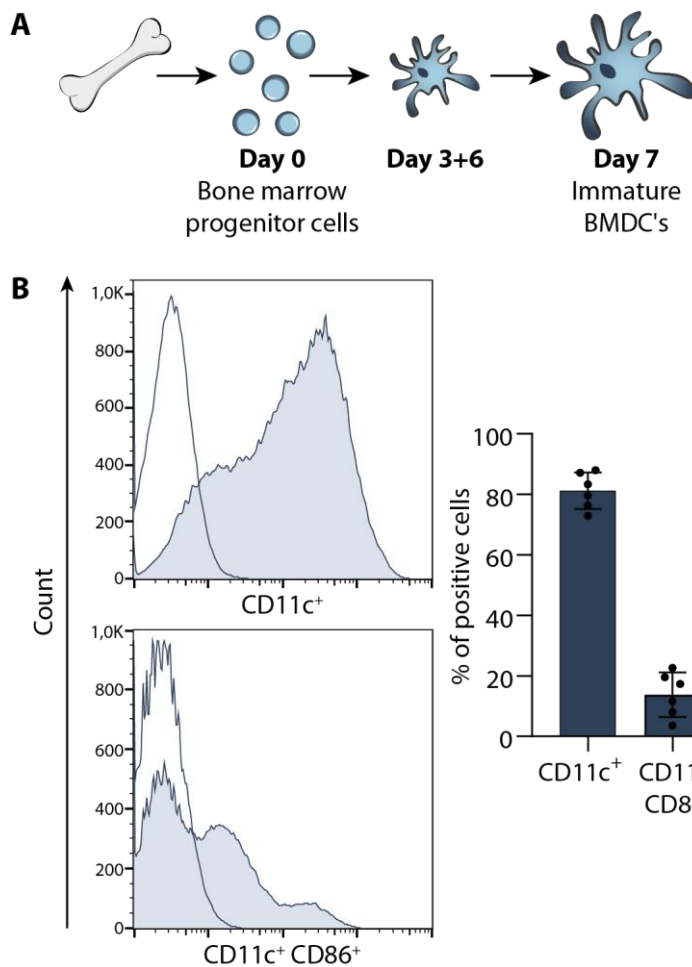


**Figure 8: Isolation of DCs from bone marrow of mice.**

(A) BMDCs were isolated from femurs of mice and cultured in DMEM culture media supplemented with 20 ng/ml GM-CSF in uncoated culture dishes. Replenishment with fresh culture medium took place on day 3 and 6. Immature BMDCs were harvested on day 7. (B) Harvested BMDCs were stained for CD11c and CD86, and DC culture purity was determined by FACS analysis. Shown are representative histograms (left) and quantitative analysis (right) (n=6). Isotype control, open, DC markers, filled.

Similar effects on redox homeostasis could be observed in the analysis of intracellular ROS levels. For this purpose, BMDCs were treated with DMF for 4 h and then the formation of reactive oxygen species was analyzed by staining with DCFDA, showing that DMF treatment leads to an increase in ROS and thus to the induction of oxidative stress. Also in this case the DMF-mediated effect can be completely prevented by co-incubation with the antioxidant NAC (Figure 9B).



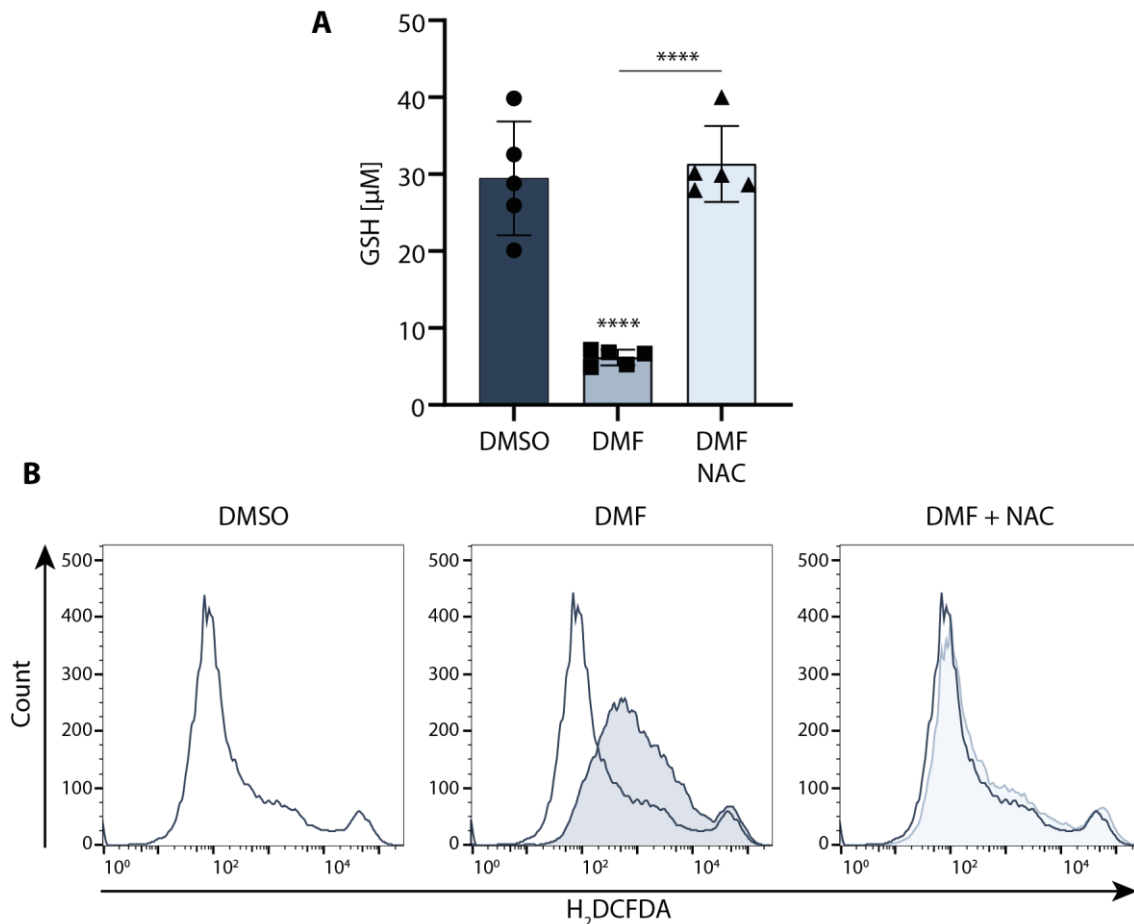


**Figure 9: DMF treatment induces oxidative stress in wildtype BMDCs.**

(A) BMDCs were treated with DMSO, 70  $\mu$ M DMF or 1 mM NAC for 4 h and GSH content was analyzed by a spectrometric assay ( $n=5$ ; ANOVA with Tukey post-hoc test). (B) Furthermore harvested DCs were incubated with DMSO, 70  $\mu$ M DMF or 1 mM NAC for 4 h and intracellular ROS levels were determined by staining with 2',7'-dichlorodihydrofluorescein diacetate (H<sub>2</sub>DCFDA). DMSO-treated control, open; treatment groups, filled ( $n=3$ ).

It was previously shown by Ghoreschi et al. that two crucial pathways, modulated during DMF treatment, are the STAT1 and the HO-1 pathway [137]. Therefore, their signal transduction was investigated on the protein level to confirm the effects in own experiments. For this purpose, immature BMDCs were first pretreated with DMF and NAC and then STAT1 phosphorylation was investigated over a time span of 1 h after additional LPS supplementation. The samples were harvested at 0, 15, 30 and 60 minutes after LPS stimulation and analyzed by Western blot. In the case of LPS stimulation alone without prior DMF or NAC treatment, there was a time-dependent increase in STAT1 phosphorylation, with the strongest signal after 60 min. Overall levels of unphosphorylated STAT1 remained constant (Figure 10A). Thus, it is not a regulation of the STAT1 basal levels, but rather an increase in this protein's phosphorylation. This LPS-mediated induction could be inhibited by DMF treatment. In

protein lysates of cells incubated with DMF, the levels of pSTAT1 remained unchanged over the period of 60 min. However, in accordance with the previously obtained data on redox homeostasis, this DMF-mediated effect was reversed by co-treatment with NAC. Thus, in cells treated with DMF and NAC, the pSTAT1 levels increased once again (Figure 10A).

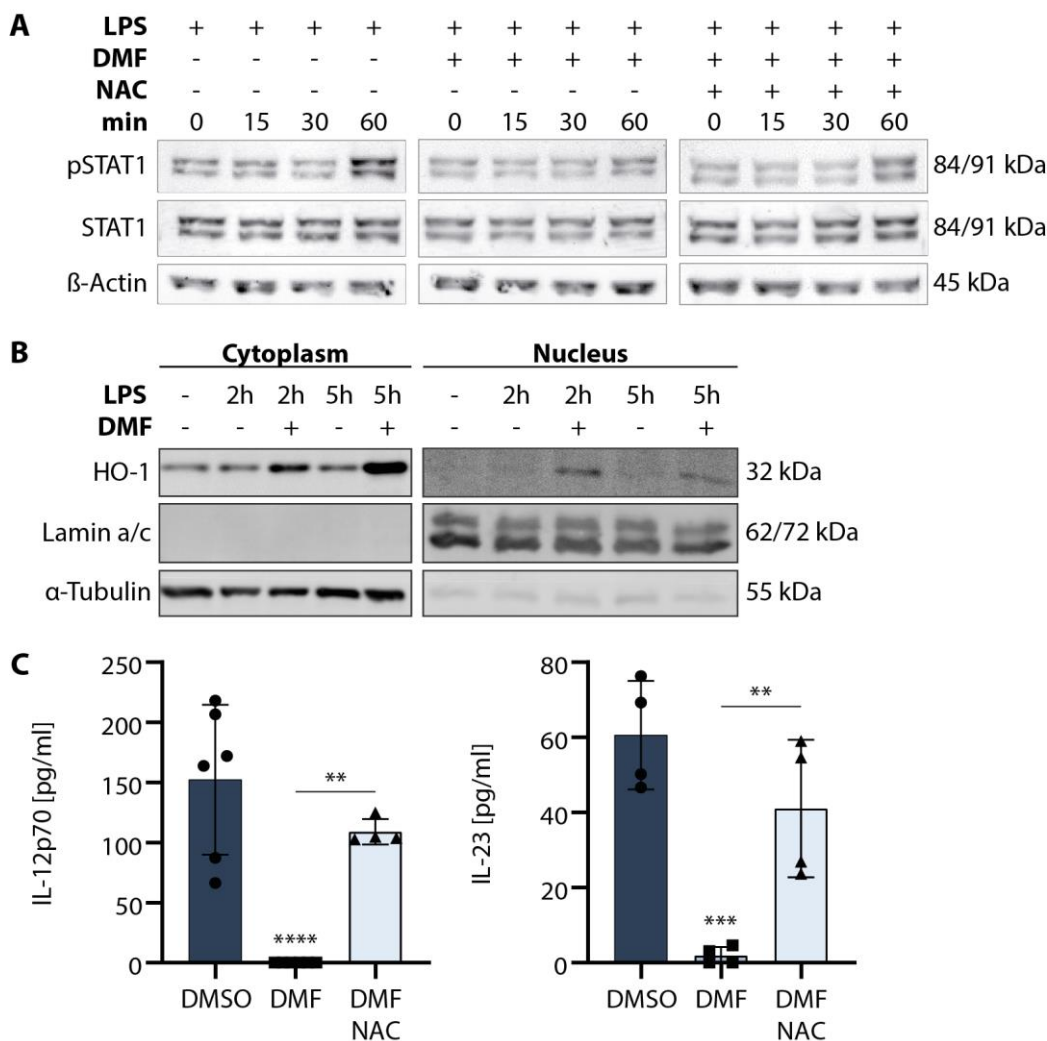


**Figure 10: DMF modulates the HO-1 and STAT1 signaling pathway.**

(A and B) For monitoring of protein expression DCs were pretreated with DMSO, 70  $\mu$ M DMF or 70  $\mu$ M DMF + 1 mM NAC for 1 h and then stimulated with 1  $\mu$ g/ml LPS for the indicated time periods. Cell lysates were harvested and analyzed for STAT1 and pSTAT1 levels (A) and HO-1 expression (B) by Western blot. Representative Western blots are shown (n=3). (C) BMDCs were pre-incubated with DMSO, 70  $\mu$ M DMF or 70  $\mu$ M DMF + 1 mM NAC for 1 h and then stimulated with 1  $\mu$ g/ml LPS for 24 h. Cell culture supernatants were harvested and IL-12p70 and IL-23 levels were determined by ELISA (n=4; ANOVA with Tukey post-hoc test).

HO-1 signal transduction was investigated as the second central signaling pathway for DMF treatment. After treatment with DMF, induction of the protein occurred. In addition, the protein was translocated into the cell nucleus, where it can act

as a transcription factor. This effect was observed at both time points investigated, namely after 2 h and 5 h (Figure 10B).

The inflammatory cytokines IL-12p70 and IL-23 were identified as downstream targets of the STAT1 and HO-1 signaling pathway by Ghoreschi et al. [137]. Also, in own experiments, a modulation of the secreted cytokine levels by incubation with DMF could be detected. After treatment for 24 h, both IL-12p70 and IL-23 were strongly inhibited. Again, this effect could be prevented by the addition of NAC, whereby high cytokine concentrations were detected in the supernatants of the equivalently treated cells (Figure 10C).

These experiments show that the effects of DMF treatment found by Ghoreschi et al. represent a robust system. The modulations of intracellular GSH levels, as well as STAT1 and HO-1 signaling pathways, could be reproduced in these own experiments. Thus, the induction of type II dendritic cells, with low levels of proinflammatory cytokines IL-12p70 and IL-23, could be verified by treatment with DMF. This provides a solid basis to gain a more detailed insight into the mechanisms of action of the fumarate in the further course of this thesis.

## 4.2 FUMET-CORMS AS POWERFUL ANTI-INFLAMMATORY AGENTS

As already described in chapter 1.3.4, the role of carbon monoxide as an anti-inflammatory modulator has gained increasing acceptance in recent years. In a collaboration project with the Institute for Organic Chemistry in Cologne, it was possible to obtain novel CO-releasing substances. These molecules released not only CO but also various fumaric acid esters. The project's objective was to obtain a characterization of the biological effects of these CORMs and investigate whether the anti-inflammatory properties of CO and FAEs can complement or even enhance each other. Parts of this work have already been published in a peer-reviewed journal [178].

## 4.2.1 INDUCTION OF TYPE II DENDRITIC CELLS BY FUMET-CORMS

An overview of the four different substances used is shown in Figure 6 and Table 9. Generally, these substances can be categorized into two different classes. Firstly, classical CORMs, namely substance **8** and *rac-5*, were used. In aqueous solution, these substances would already release CO and additionally fumaric acid or dimethyl fumarate, respectively. The second group used was the so-called FumET-CORMs. They are represented by the molecules *rac-7a* and *rac-7b*. These substances are enzyme-triggered CORMs because they require transport into the cell to be cleaved by esterases, followed by release of CO and monomethyl fumarate directly into the cytoplasm.

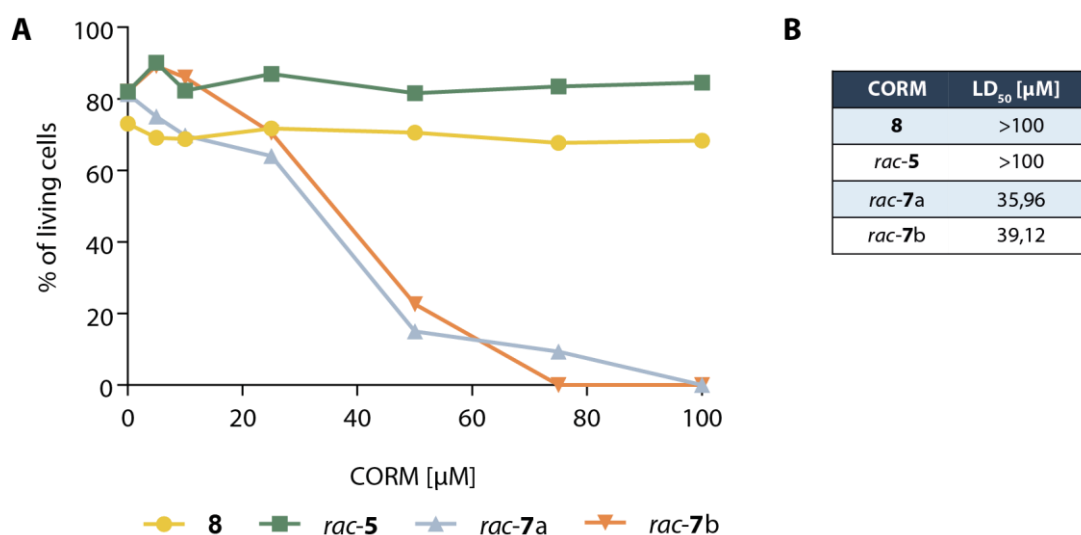


**Figure 11: Analysis of CORM toxicity on BMDCs.**

(A) Harvested BMDCs were treated with DMSO, 1 μg/ml LPS and the indicated concentrations of CORMs for 24 h. Cells were then harvested and counted with a Neubauer chamber. Live/death discrimination of cells was assessed by trypan blue staining. Shown is the percentage of living cells in each group (n=3). Calculated LD<sub>50</sub> values are depicted in (B). Figure modified from [178].

As a first step before general use of these substances in BMDCs, a toxicity assessment was carried out to determine the concentration up to which they can be used *in vitro*. For this purpose, BMDCs were incubated with the CORMs and LPS for 24 h and then a trypan blue exclusion assay was performed. Cells that appeared blue due to the loss of membrane integrity were classified as not viable. It was found that the substances **8** and *rac-5* showed no cytotoxicity at the tested concentrations up to 100 μM (Figure 11). In contrast, the use of the FumET-CORMs *rac-7a* and *rac-7b* leads

to the rapid death of cells with an LD<sub>50</sub> value of 35.96  $\mu$ M and 39.12  $\mu$ M, respectively (Figure 11). However, at the applied concentration of 25  $\mu$ M of each FumET-CORM, the molecules show an acceptable toxicity profile with only a few dead cells after 24 h. Because of this, the FumET-CORMs were used in all following experiments at a maximum of 25  $\mu$ M. However, for the substances **8** and *rac-5*, a higher concentration of up to 75  $\mu$ M was chosen, since no toxicity could be observed with these molecules. This also allows better comparability with the positive control DMF concentration of 70  $\mu$ M, which is often published and was also chosen for own experiments.

To test the efficacy of the substances, their impact on the levels of inflammatory cytokines was first investigated. After 24 h stimulation with LPS, the BMDCs had a basal level of 478.08 pg/ml of IL-12p70 and 216.08 pg/ml of IL-23, which was significantly reduced by incubation with just 25  $\mu$ M DMF (Figure 12). However, it should be noted that treatment with both FumET-CORMs also resulted in a strong reduction of IL-12p70 and IL-23 levels. This inhibition was even more pronounced than by DMF treatment with an equivalent concentration alone. There was a significant difference between the DMF treatment and the one using FumET-CORMs. Thereby the IL-12p70 levels for *rac-7a* and *rac-7b* were decreased to only 21.89 and 20.08 pg/ml, respectively. For IL-23 the concentrations were 29.33 pg/ml for *rac-7a* and 32.32 pg/ml for *rac-7b* (Figure 12). With both CORMs **8** and *rac-5*, which already release CO and fumaric acid in the cell culture medium, no or only a poor inhibition of the cytokines could be detected. Despite their use at a higher concentration of 75  $\mu$ M, these CORMs proved to be not particularly effective. Therefore, further investigations focused on the two FumET-CORMs *rac-7a* and *rac-7b*, which turned out to be promising compounds.

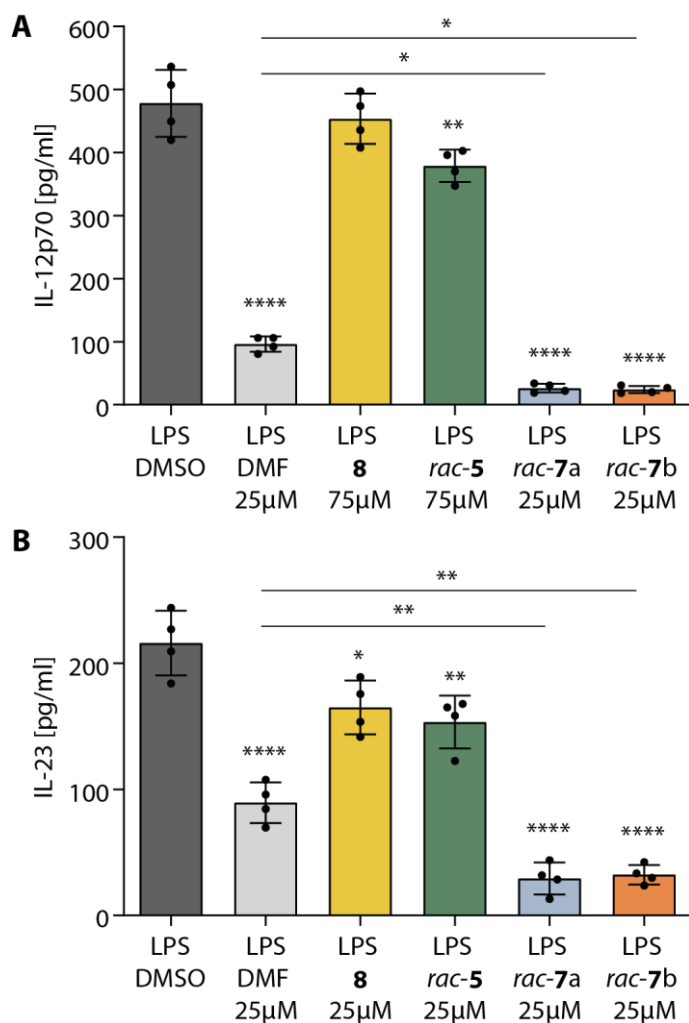


**Figure 12: Inhibition of inflammatory cytokine secretion by FumET-CORMs.**

For detection of inflammatory cytokines BMDCs were pretreated with DMSO or the indicated concentrations of DMF or CORMs for 1 h and subsequently stimulated with 1 μg/ml LPS for 24 h. Cell culture supernatants were harvested and IL-12p70 (A) and IL-23 (B) levels were determined by ELISA (n=4; ANOVA with Tukey post-hoc test). Figure modified from [178].

In order to obtain a more detailed understanding of the underlying mechanisms, the HO-1 and STAT1 signaling pathways were also analyzed in this system (Figure 13-Figure 14). As it is already known that HO-1 plays a central role in CO signaling and is also up-regulated by DMF, the expression levels of this protein were first investigated at the protein level. As already observed in Figure 10, HO-1 was induced after treatment with 70 μM DMF. Treatment with all four CO-releasing substances resulted in an upregulation of the protein as well. This was most noticeable for the molecule *rac-7b*, even if it was used at a significantly lower concentration than DMF, namely 25 μM (Figure 13).

Next, the ability of FumET-CORMs to inhibit phosphorylation of STAT1 was investigated. BMDCs were treated with the different substances in increasing concentrations and then stimulated with LPS for 1 h. The inhibition of pSTAT1 was observed for DMF as well as for *rac-7a* and *rac-7b* (Figure 14). Similar to the previous experimental results, this inhibition occurred at significantly lower concentrations of

FumET-CORMs compared to DMF treatment alone. Figure 14A shows that the use of 25  $\mu$ M DMF resulted in only a weak decline of the pSTAT1 levels, whereas 25  $\mu$ M *rac-7a* and *rac-7b* resulted in the detection of only a weak signal in the Western blot.

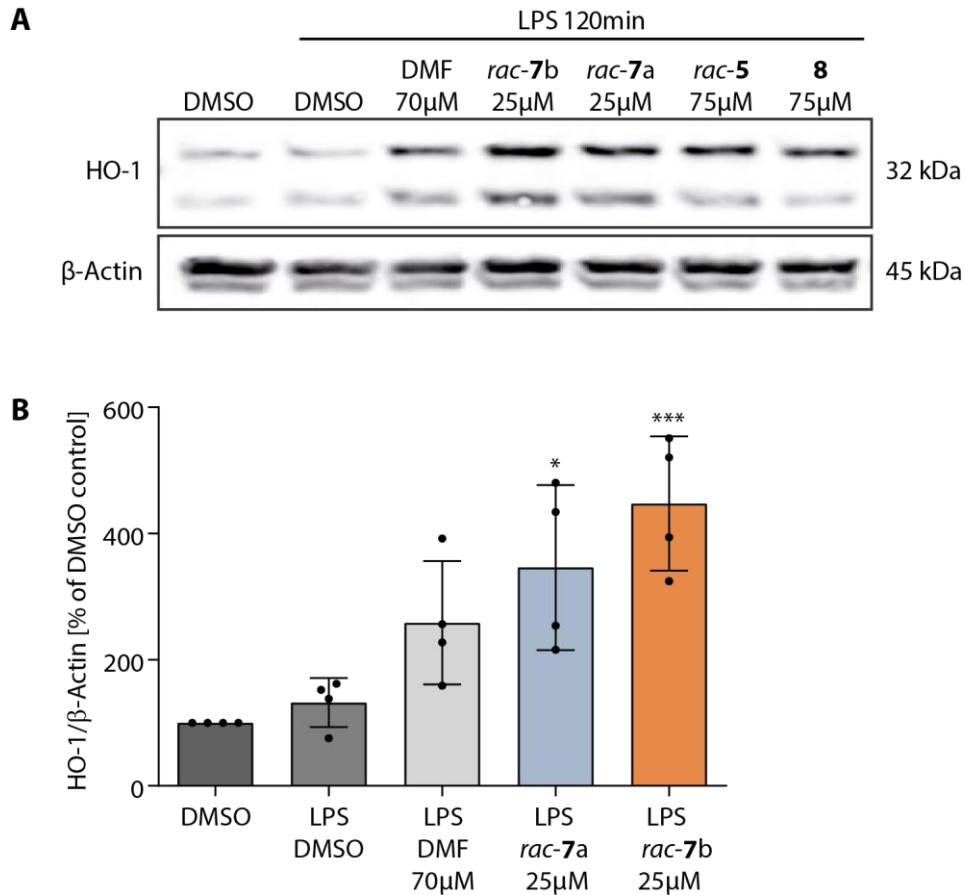


**Figure 13: FumET-CORM treatment induces HO-1.**

(A) For monitoring of protein expression DCs were pretreated with DMSO or the indicated concentrations of DMF or CORMs for 1 h and then stimulated with 1  $\mu$ g/ml LPS. Cell lysates were prepared after 2 h and analyzed for HO-1 expression by Western blot.  $\beta$ -Actin was used as loading control. A representative Western blot is depicted (n=4). (B) Densitometric quantification of the HO-1/ $\beta$ -actin ratio is shown in percent of DMSO control (n=4; ANOVA with Tukey post-hoc test). Figure modified from [178].

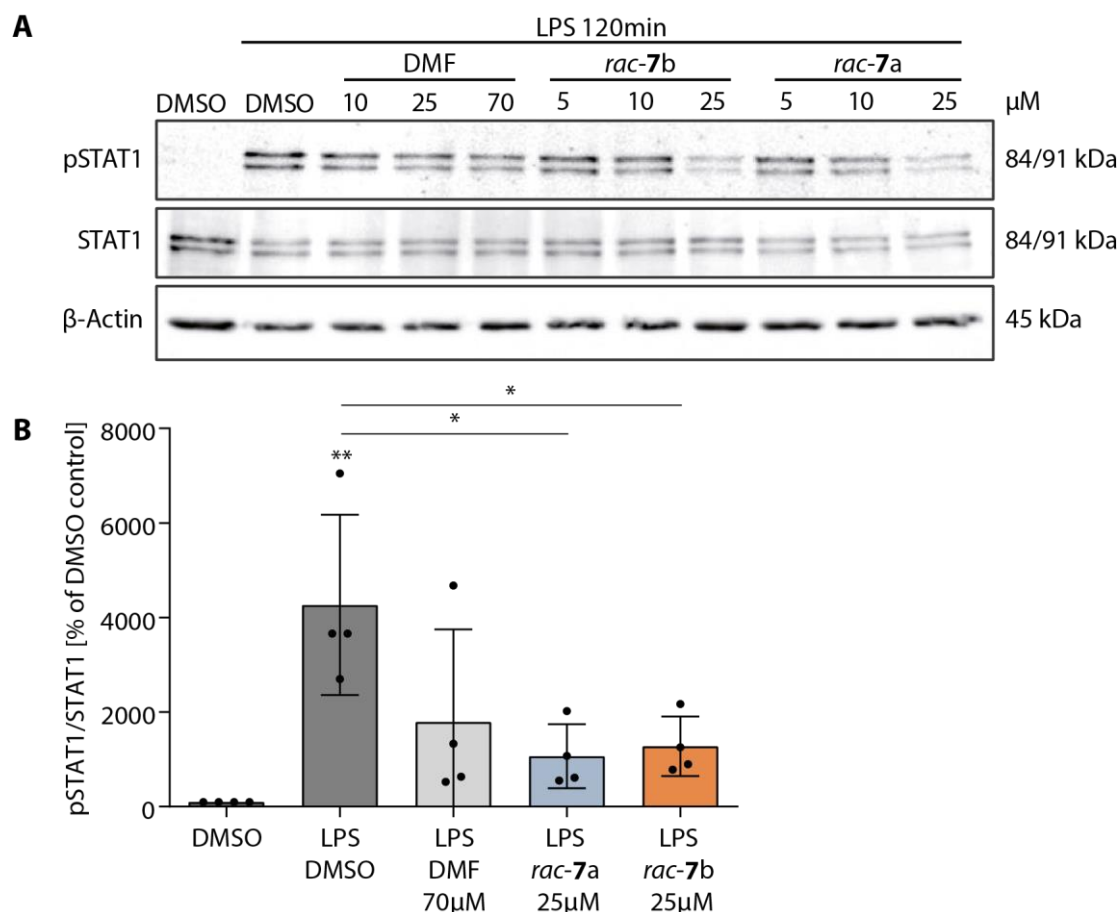


**Figure 14: Inhibition of STAT1 phosphorylation by FumET-CORMs.**

(A) Harvested BMDCs were pre-incubated with DMSO or with the indicated concentrations of DMF or CORMs for 1 h and subsequently stimulated with 1 μg/ml LPS for 2 h. Cell lysates were analyzed for pSTAT1 and STAT1 levels and β-actin served as loading control. A representative Western blot is shown (n=4). (B) Densitometric quantification of the pSTAT1/STAT1 ratio is shown in percent of DMSO control (n=4; ANOVA with Tukey post-hoc test). Figure modified from [178].

Next, we investigated whether these FumET-CORM-mediated effects can be reversed by additional incubation with the antioxidant NAC similar to DMF treatment, thus suggesting a ROS-mediated mechanism. For this purpose, the STAT1 and HO-1 signaling pathways were examined once again at the protein level using Western blot. It was found that after DMF and FumET-CORM treatment, there was an increase in HO-1 in the BMDCs (Figure 15A). Again, the induction of the protein by FumET-CORMs was stronger than by DMF treatment with a higher concentration. Coincubation with NAC produced a weaker induction of HO-1, although the levels did not completely return to baseline. Especially for *rac-7a*, hardly any effects could be observed by NAC (Figure 15A). Similarly, when looking at pSTAT1 levels, the effects described above could be reproduced by DMF and FumET-CORMs. Both fumarate and the molecules *rac-7a* and *rac-7b* mediated a potent inhibition of STAT1 phosphorylation, while the



STAT1 ground levels remained unchanged. Simultaneous incubation with NAC resulted in a renewed increase of pSTAT1 after LPS stimulation (Figure 15B). Again, this effect was only weak for the substance *rac-7a*.

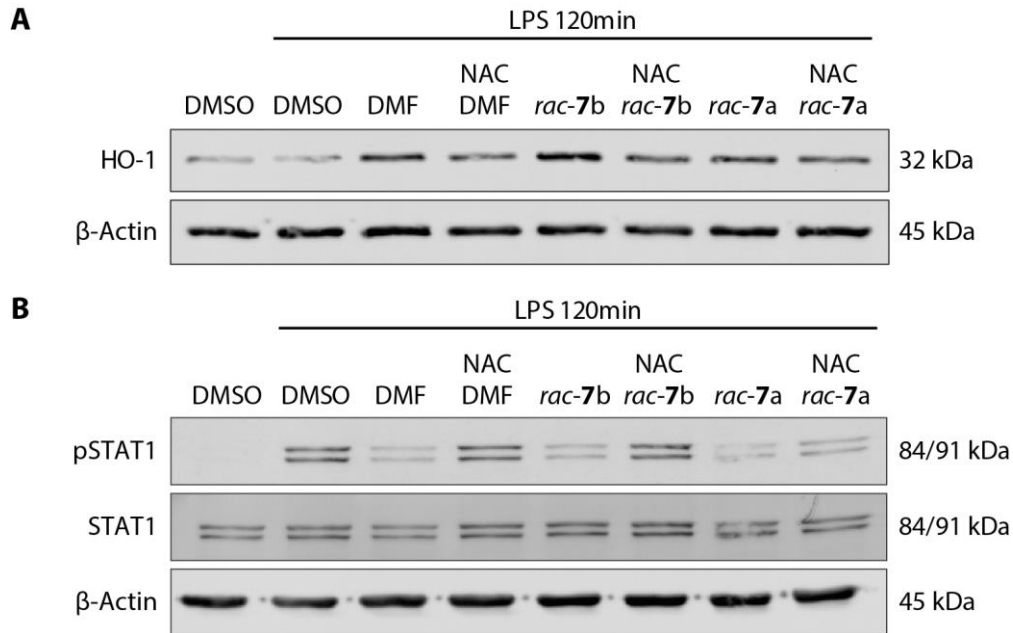


**Figure 15: Effects of CORMs and anti-oxidant treatment on signaling pathways.**

BMDCs were pretreated for 1 h with DMSO, 70  $\mu$ M DMF, 1 mM NAC, 25  $\mu$ M FumET-CORMs or a combination thereof. Afterwards cells were stimulated with 1  $\mu$ g/ml LPS and cell lysates were harvested after 2 h. Protein levels of HO-1 (A) or pSTAT1 and STAT1 (B) were analyzed by Western blotting, whereas  $\beta$ -actin served as loading control. Representative Western blots are shown (n=2).

Subsequently, we investigated the downstream regulated cytokines. The suppression of IL-12p70 and IL-23 inhibition by both FumET-CORMs was reversed by coincubation with NAC (Figure 16). While NAC did not normalize the HO-1 and pSTAT1 levels for *rac-7a* in Western blots, cytokine production showed a reversion comparable to DMF and *rac-7b* treated cells. In contradiction to the ELISA in Figure 12, the detected cytokine levels after DMF treatment were lower than after incubation with FumET-CORM. However, this can be explained by the concentrations applied. In Figure 12, a concentration of 25  $\mu$ M DMF was used to allow a direct comparison of the efficacy with FumET-CORMs. In this ELISA, DMF was only used as a positive control with a concentration of 70  $\mu$ M, which subsequently led to a stronger cytokine inhibition. In addition, the control substances *rac-8* and *rac-12* were used, which are not coupled to monomethyl fumarate and therefore release only CO and no fumaric acid ester into the cytoplasm of the cells. Thereby *rac-8* served as a control for *rac-7a* and *rac-12* was the

control substance for *rac-7b*. No significant cytokine inhibition could be determined for substances *rac-8* and *rac-12* (Figure 16).

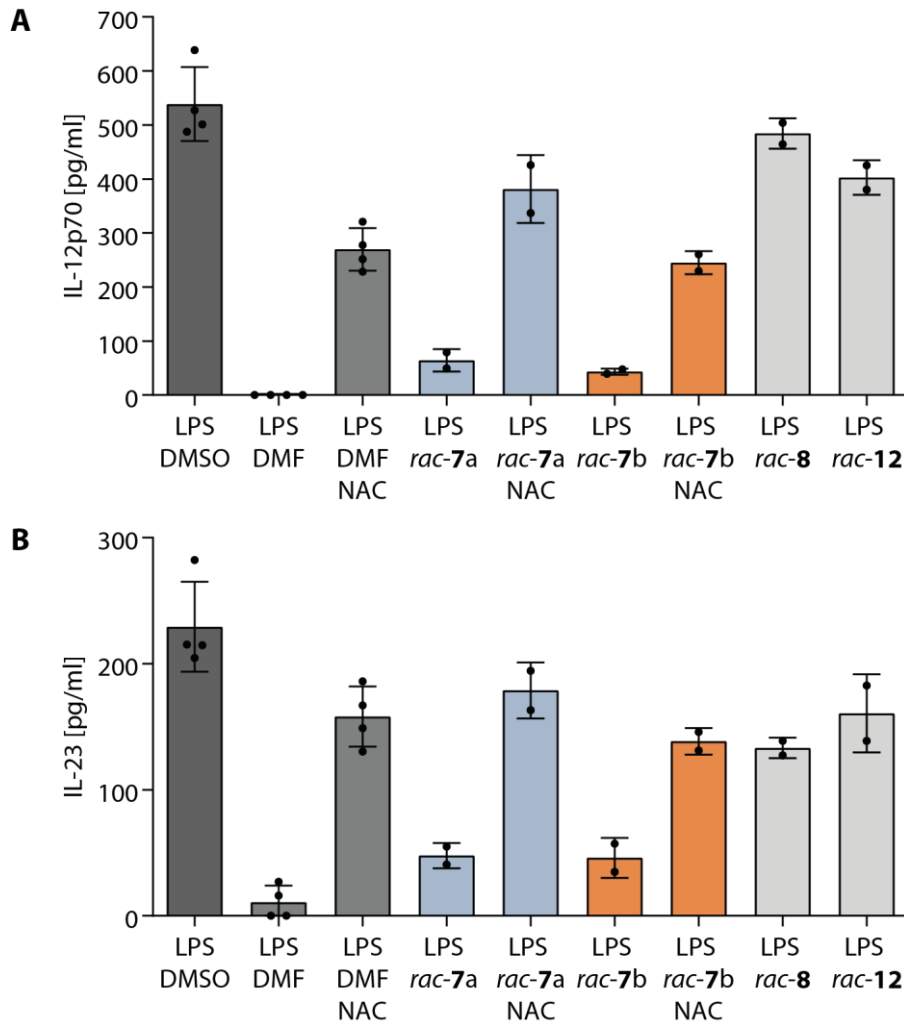


**Figure 16: NAC treatment reverses inflammatory cytokine inhibition by FumET-CORMs.**

Harvested immature DCs were stimulated with 1  $\mu$ g/ml LPS after pre-incubation with DMSO, 70  $\mu$ M DMF, 1 mM NAC, 25  $\mu$ M CORMs or a combination thereof for 1h. Cell lysates were collected after 24 h of stimulation and analyzed for IL-12p70 (A) and IL-23 (B) levels by ELISA (n=2).

In summary, the FumET-CORMs *rac-7a* and *rac-7b* represent molecules with potent anti-inflammatory properties. Both were able to effectively induce a DC type II immune response with low levels of proinflammatory cytokines IL-12p70 and IL-23. Furthermore, they showed improved efficacy compared to DMF treatment alone, as the same benefits occurred at significantly lower concentrations. On the other hand, the non-enzyme-activated substances **8** and *rac-5* did not show considerable anti-inflammatory properties and were not able to influence the investigated signaling pathways in a similar manner to the FumET-CORMs *rac-7a* and *rac-7b* or DMF.

## 4.2.2 MODULATION OF REDOX HOMEOSTASIS BY FUMET-CORMS

As a reversal of the effects from the addition of the antioxidant NAC was monitored in previous experiments, a modulation of the redox homeostasis by the FumET-CORMs was investigated in the following subchapter.

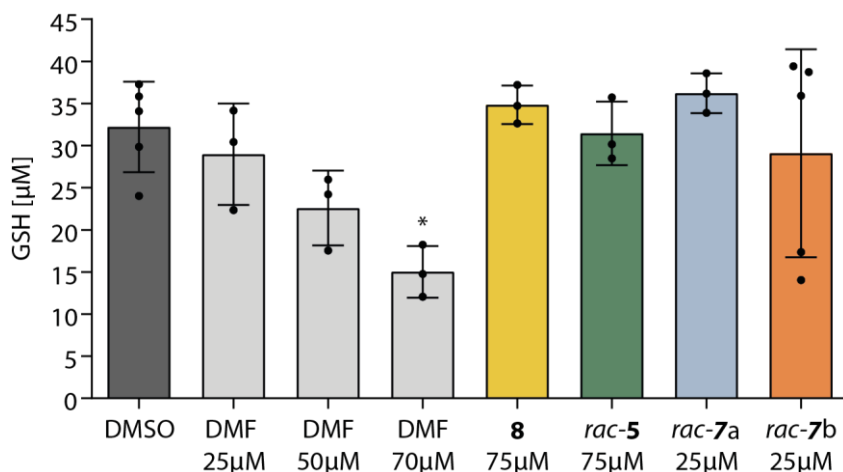


**Figure 17: CORM treatment doesn't diminish intracellular GSH level.**

BMDCs were treated with DMF or CORMs and intracellular GSH levels were determined after 4 h of incubation by a spectrometric assay (n=3; ANOVA with Tukey post-hoc test).

As already known from previous studies and also shown in own work, the use of DMF leads to a decrease of intracellular GSH levels (Figure 9A) [137]. Since the substances **8**, *rac-5*, *rac-7a* and *rac-7b* also release a fumaric acid ester in addition to CO, their influence on detectable GSH levels was analyzed in the following section. For this purpose, immature BMDCs were treated with increasing DMF concentrations as a positive control or with the different CO-releasing substances. After 4 h of incubation, intracellular glutathione was detected using a spectrometric assay. However, for none of the tested CORMs, a regulation of GSH levels could be determined (Figure 17). Only in two replicates of the *rac-7b* treated cells, there was a drop in the measured concentration. However, it should be noted that due to their toxicity, the compounds *rac-7a* and *rac-7b* were only used at 25 µM. If one examines the levels for the comparable DMF treatment at 25 µM, no regulation could be observed here either. Only when 70 µM DMF was applied, significant inhibition of the ROS scavenger was observed. Thus, a lack of regulation of the GSH levels is possibly due to the low concentrations administered. However, as described in the previous chapter, these are still sufficient to achieve a modulation of the STAT1 and HO-1 signaling pathways and their downstream cytokines (Figure 12-Figure 14). This is achieved despite the lack of

GSH inhibition. Such inhibition was also not detectable for the CORMs **8** and *rac-5* (Figure 17). In the case of these substances, however, there was no subsequent suppression of IL-12p70 or IL-23, as observed for the FumET-CORMs (Figure 12- Figure 14).

The next step was to investigate whether the induction of ROS in BMDCs occurs despite the lack of glutathione level modulation. For this purpose, cells were treated with 70  $\mu$ M DMF as a positive control or the FumET-CORMs once more. In addition, the previously mentioned control substances *rac-8* and *rac-12* were used, which only release CO and no fumaric acid ester into the cytoplasm of the cells. Also, a coincubation with NAC was performed for all samples. It could be observed that, as expected, incubation with DMF led to an increase in intracellular ROS levels. The addition of NAC could entirely reverse the increase in ROS. Despite a lack of adjustment of glutathione levels, the treatment with *rac-7a* and *rac-7b* also led to an increase of ROS. This induction was even more robust than the one observed during DMF treatment. Thereby the highest increase was observed for *rac-7b*. Additional incubation with NAC resulted in a partial decline of reactive oxygen species, but they could not be returned to the baseline level. In addition, the control substances, which only release CO, also showed comparable effects on ROS induction (Figure 18). This suggests that the observed modulations are not fumaric acid-specific effects. Instead, the release of CO already leads to an induction of oxidative stress.

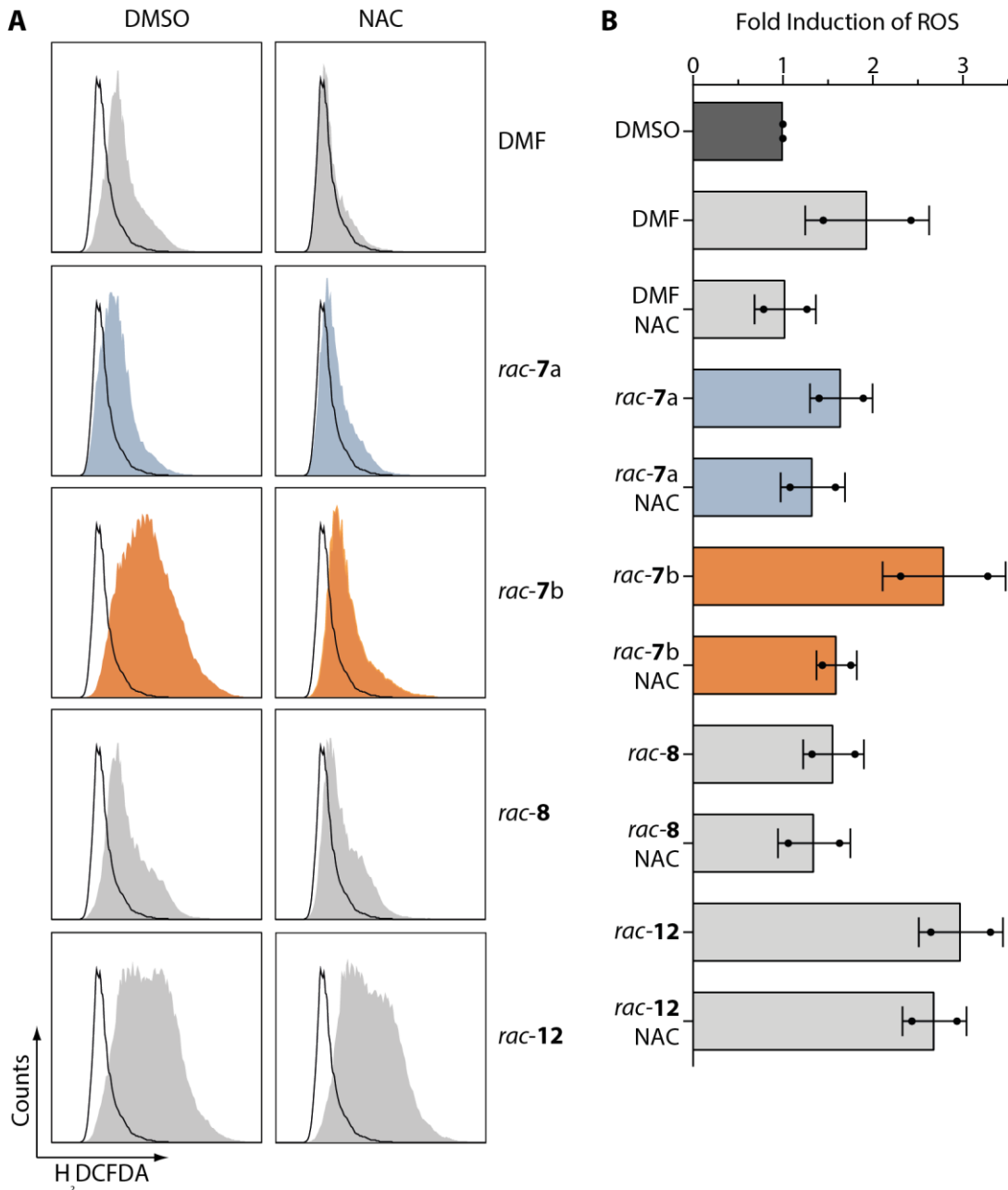


**Figure 18: Strong induction of reactive oxygen species in FumET-CORM-treated DCs.** Immature DCs were incubated with DMSO, 70  $\mu$ M DMF, 1 mM NAC, 25  $\mu$ M CORMs or a combination thereof for 4 h and intracellular ROS levels were determined by staining with 2',7'-dichlorodihydrofluorescein diacetate (H<sub>2</sub>DCFDA). Representative histograms are shown in (A) (n=2). DMSO-treated control, open; treatment groups, filled. (B) Quantitative analysis of geometric means as fold induction compared to DMSO control.

These results showed that the FumET-CORM had divergent effects on redox homeostasis of the treated BMDCs. On the one hand, treatment with these substances does not lead to any regulation of intracellular glutathione, one of the most important ROS scavengers in the cell (Figure 17). On the other hand, there still is a massive induction of oxidative stress, which can be observed by the increase in ROS (Figure

18). In the following chapter, a more detailed look is taken at the mechanistic principles of treatment with especially fumaric acid esters, which are also released by the FumET-CORMs, and the influence of oxidative stress involved.

### 4.3 EFFECTS OF ENDOGENOUS ROS STRESS ON DENDRITIC CELL DIFFERENTIATION

In the following chapters, the mechanistic background of DMF treatment should be examined more closely. In particular, the role of glutathione and reactive oxygen species for effective treatment with fumarate was examined. The exact mechanism of action of FAEs is not yet known as they induce varying effects in different cell types (Figure 3). However, a central point is an immune deviation from an inflammatory T<sub>h</sub>1/T<sub>h</sub>17 response towards the induction of T<sub>h</sub>2 cells [136, 137]. This is accomplished by the differentiation of anti-inflammatory type II DCs, as described in the previous chapters. In this context, the DMF-mediated inhibition of glutathione and the resulting accumulation of ROS have been discussed as important mechanisms [137]. Consequently, the central relevance of redox homeostasis for an effective DMF treatment should now be assessed.

#### 4.3.1 CHARACTERIZATION OF CYSTINE/GLUTAMATE ANTIPORTER KNOCKOUT CELLS

To investigate the influence of glutathione deficiency on DC differentiation without obtaining further off-target effects from DMF, cells of a cystine/glutamate antiporter knockout mouse model were used for the following experiments. This xCT antiporter is usually responsible for transporting cystine into the cell in exchange for glutamate. If the cells lack this antiporter, an intracellular deficiency of cystine occurs, which in the further course is essential for the synthesis of glutathione. Therefore, cells of these mice should not be able to produce GSH (Figure 19). However, it should be noted that it has already been shown for *in vitro* experiments that it is essential to cultivate KO cells without  $\beta$ -mercaptoethanol (2ME) in the medium. In the presence of

this 2ME, cystine can otherwise enter the cell in the form of a mixed disulfide via other amino acid transporters and thus render the knockout ineffective [251].

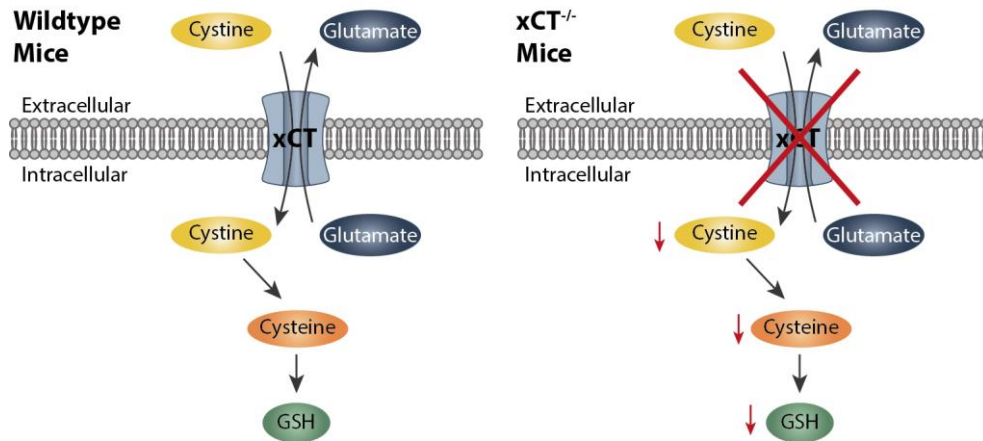


**Figure 19: Postulated effects of cystine/glutamate antiporter knockout on intracellular GSH levels.** Genetic knockout of the cystine/glutamate antiporter (xCT) results in an impaired transport of cystine into the cell. As cystine is an essential molecule for glutathione (GSH) synthesis, this leads to diminished intracellular glutathione levels.

However, this posed problems for the cultivation of the BMDCs used in the experiments, as without 2ME, no effective isolation of these cells was achieved. Figure 20A shows the effectiveness of BMDC isolation by calculation of an isolation rate. For this purpose, the cell count of the immature BMDCs harvested on day seven was correlated to the stem cells isolated and plated from the bone marrow on day zero. In the case of the cultivation of KO cells without 2ME, only a very low isolation rate was obtained (Figure 20A). Most of the cells had previously died during the seven days of differentiation.

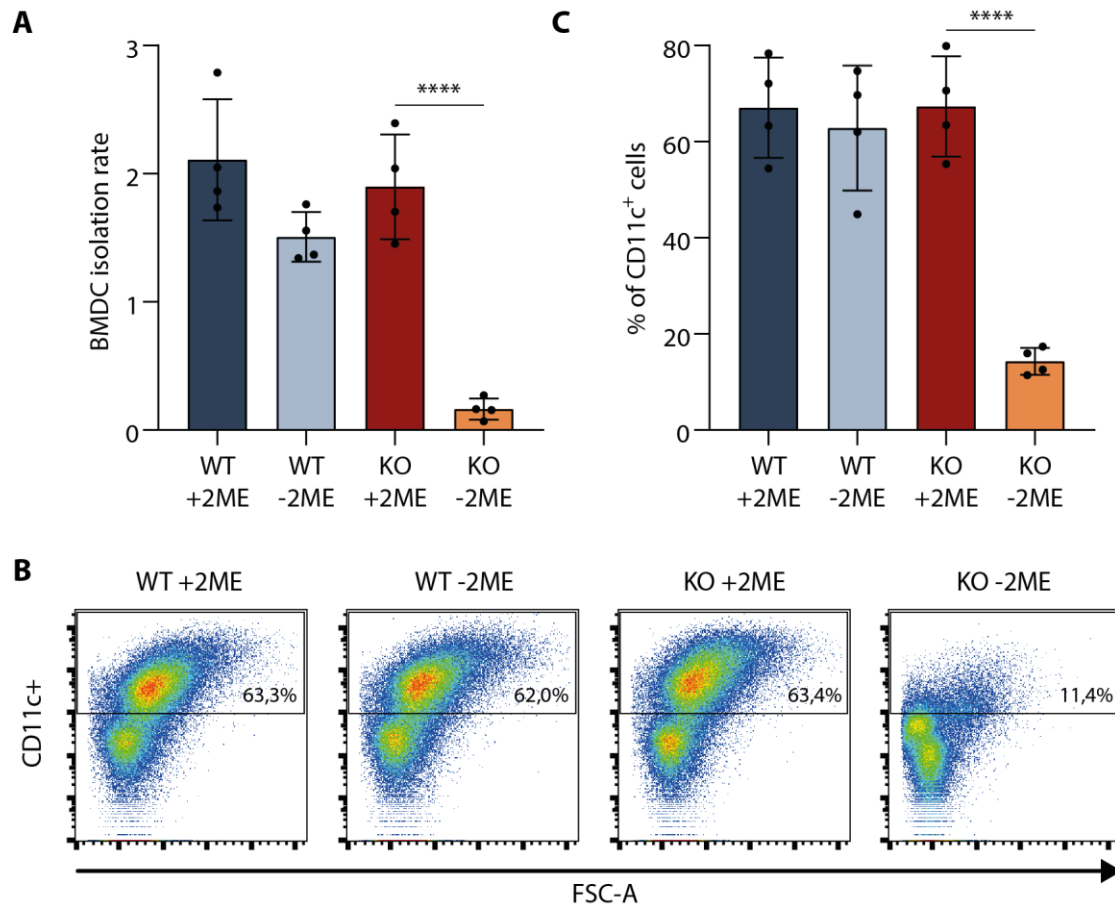


**Figure 20: Generation of BMDCs from xCT knockout mice requires  $\beta$ -mercaptoethanol.**

(A) Cells were isolated from bone marrow of WT and xCT.KO mice and cultivated in differentiation medium with or without 2ME. After 7 days immature BMDCs were harvested and cell count was determined. Depicted is the ratio of harvested cells on day 7 divided by the seeded cells on day of isolation. (B and C) Harvested BMDCs were stained for CD11c and analyzed by flow cytometry. Representative dot plots (B) and quantitative analysis (C) are shown. (n=4; ANOVA with Tukey post-hoc test)

In a subsequent step, these isolated cells were tested for the DC marker CD11c to check the population's purity. For both WT cells and KO cells cultivated with 2ME, the purity was approximately 67%. In contrast, the few harvested cells of the KO culture without 2ME were only 14.33% CD11c positive (Figure 20B-C). Consequently, the differentiation of BMDCs after isolation from bone marrow was performed under culture conditions with 2ME. After harvesting the cells on day 7, the medium was changed to one without  $\beta$ -mercaptoethanol. This compromise allowed the efficient isolation of BMDCs as well as the analysis of antiporter loss in the later course of the experiments.



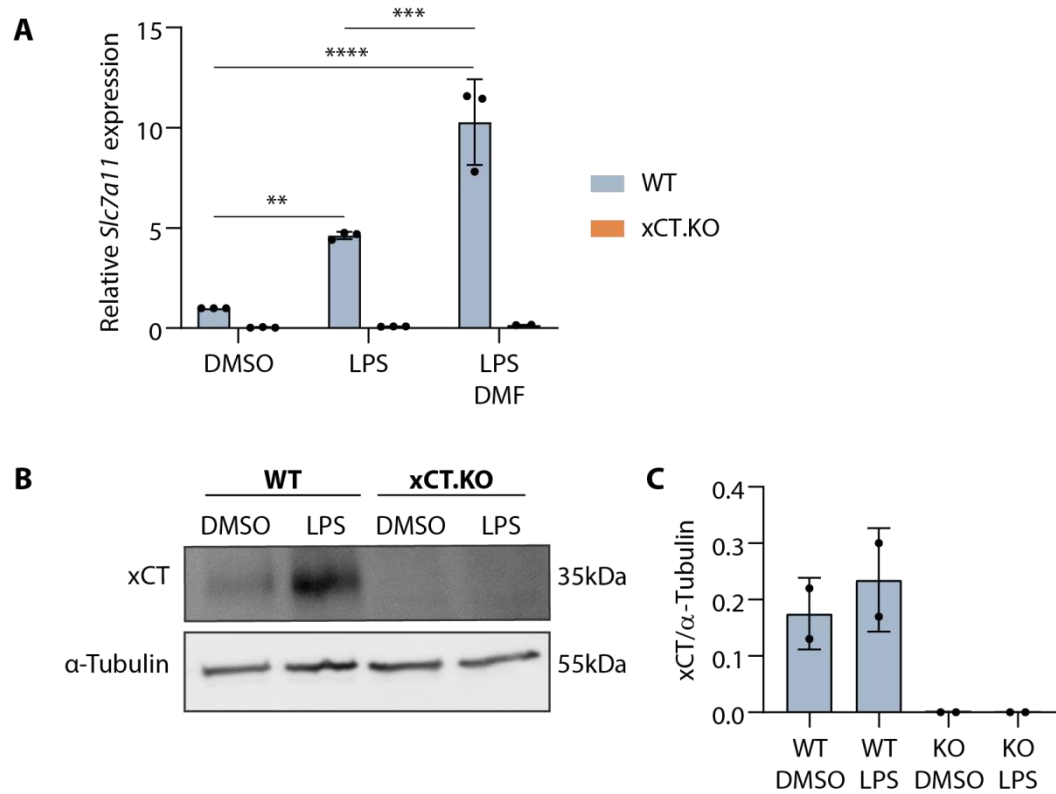


**Figure 21: Verification of xCT knockout in BMDCs.**

(A) Harvested WT and xCT.KO BMDCs were pretreated with DMSO or 70  $\mu$ M DMF for 1 h and subsequently stimulated with 1  $\mu$ g/ml LPS. After 2 h RNA samples were isolated and mRNA expression was analyzed by quantitative RT-PCR. *Slc7a11* expression was normalized to  $\beta$ -actin, *HRPT*, *Eef1a1* and *GAPDH* housekeeping gene expression (n=3; ANOVA with Tukey post-hoc test). (B and C) Protein expression of the xCT antiporter was determined by treating BMDCs with DMSO or 1  $\mu$ g/ml LPS. Cell lysates were harvested after 2 h of incubation and analyzed for xCT. As loading control  $\alpha$ -tubulin was used. A representative Western blot (B) and densitometric quantification (C) are shown (n=2).

Before using xCT knockout BMDCs in the experimental work to elucidate the role of oxidative stress on DC differentiation, their genetic characterization was conducted. The first step was to investigate whether the knockout can be detected at the RNA level. For this purpose, expression of *Slc7a11*, the gene coding for the cystine/glutamate antiporter was analyzed. BMDCs were treated with DMF and additionally stimulated with LPS. After 2 hours, the RNA samples were harvested. The treatment with LPS resulted in an induction of *Slc7a11* expression in wildtype cells, which could be further increased by treatment with DMF. In contrast, none of the knockout lysates showed any antiporter expression (Figure 21A). As a next step the knockout was verified on the protein level via analysis of xCT expression by Western blot. Also, at the protein level, wildtype BMDCs showed a clear signal, whereas, in the knockout cells, no band was visible in the Western blot (Figure 21B). Thus, the

knockout could be detected on both protein and RNA levels, allowing the use of xCT.KO mice BMDCs for further experiments.

#### 4.3.2 DIFFERENTIAL REGULATION OF REDOX HOMEOSTASIS AFTER XCT KNOCKOUT

The next step was the analysis of a possible imbalance of redox homeostasis in the cells of xCT.KO mice. Since no glutathione should be produced due to the loss of the antiporter, the first step was the detection of the ROS scavengers in various organs from said animals. On the one hand, organs were selected for which high expression of xCT was known in the respective murine tissue, such as thymus, spleen and brain. However, the liver, lung, heart and kidney, for which only low expression of the antiporter was described, were selected as controls [252]. In addition, bone marrow stem cells were analyzed directly after isolation without prior differentiation into dendritic cells for one week. In these *ex vivo* analyses, no difference in GSH concentrations of organs and cells was found between wildtype and knockout mice (Figure 22). Despite the previously successfully demonstrated loss of the antiporter (Figure 21), normal levels of glutathione were formed in all organs investigated. Apparently, compensatory mechanisms seem to exist *in vivo* to transport cystine into the cell even without the antiporter.

However, a different picture emerges when looking at the *in vitro* analyses. Again immature BMDCs were used. Due to the problems described in chapter 4.3.1, these cells were only subjected to a medium change after being harvested. Cultivation without 2ME was performed for 8 h and 24 h. However, DMF-mediated inhibition of intracellular glutathione occurs quickly after treatment, with a maximum effect after about 3 h. Therefore, this time point of DMF treatment was chosen as a positive control in the wildtype cells. It can be seen that the cultivation of wildtype cells without 2ME did not affect GSH levels. Knockout cells, which were kept in the presence of 2ME, showed similar scavenger concentrations as wildtype BMDCs. However, when these xCT.KO BMDCs were cultivated in the absence of 2ME, the intracellular GSH concentration was severely diminished after only 8 hours. The effect was even more pronounced after 24 hours when almost no GSH could be detected (Figure 23A). The delayed time kinetics of this inhibition can be explained by the fact that the scavenger is

not actively inactivated as in the case of DMF treatment. Here the decrease is due to the effect that no new glutathione can be synthesized after the medium change.

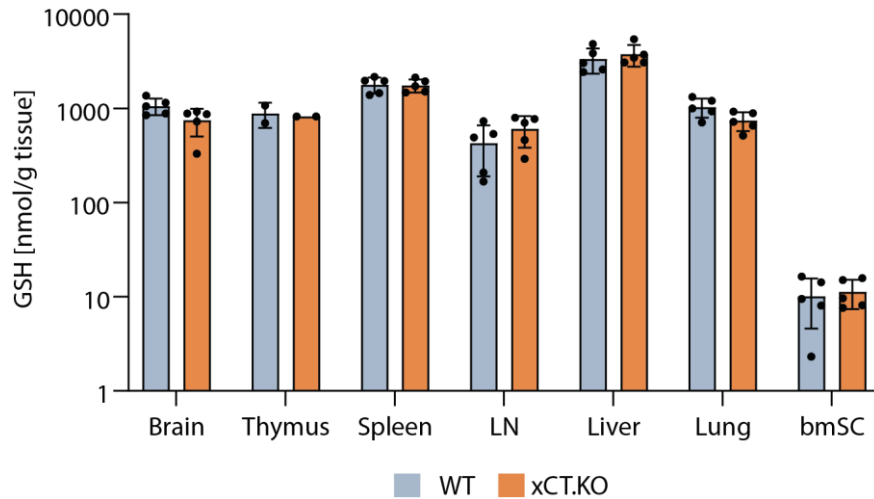


**Figure 22: No modulation of GSH levels by xCT knockout *ex vivo*.**

WT and KO mice were sacrificed and the indicated organs were removed and weighed. Intracellular GSH levels were directly analyzed and normalized to organ weight, or in the case of bmSC to  $\mu\text{g}$  of isolated protein. LN, lymph node; bmSC, bone marrow-derived stem cells. (n=5; thymus n=2)

Since there was a significant decrease in GSH levels in the knockout cells, it should now be evaluated whether this causes further implications for redox homeostasis. Therefore intracellular ROS levels were detected 24 h after a medium change without 2ME. It was found that only xCT.KO BMDCs, which had been cultivated without 2ME, showed an increase in ROS. In contrast, both wildtype groups and the knockout cells with 2ME show a comparably low level of ROS (Figure 23B).

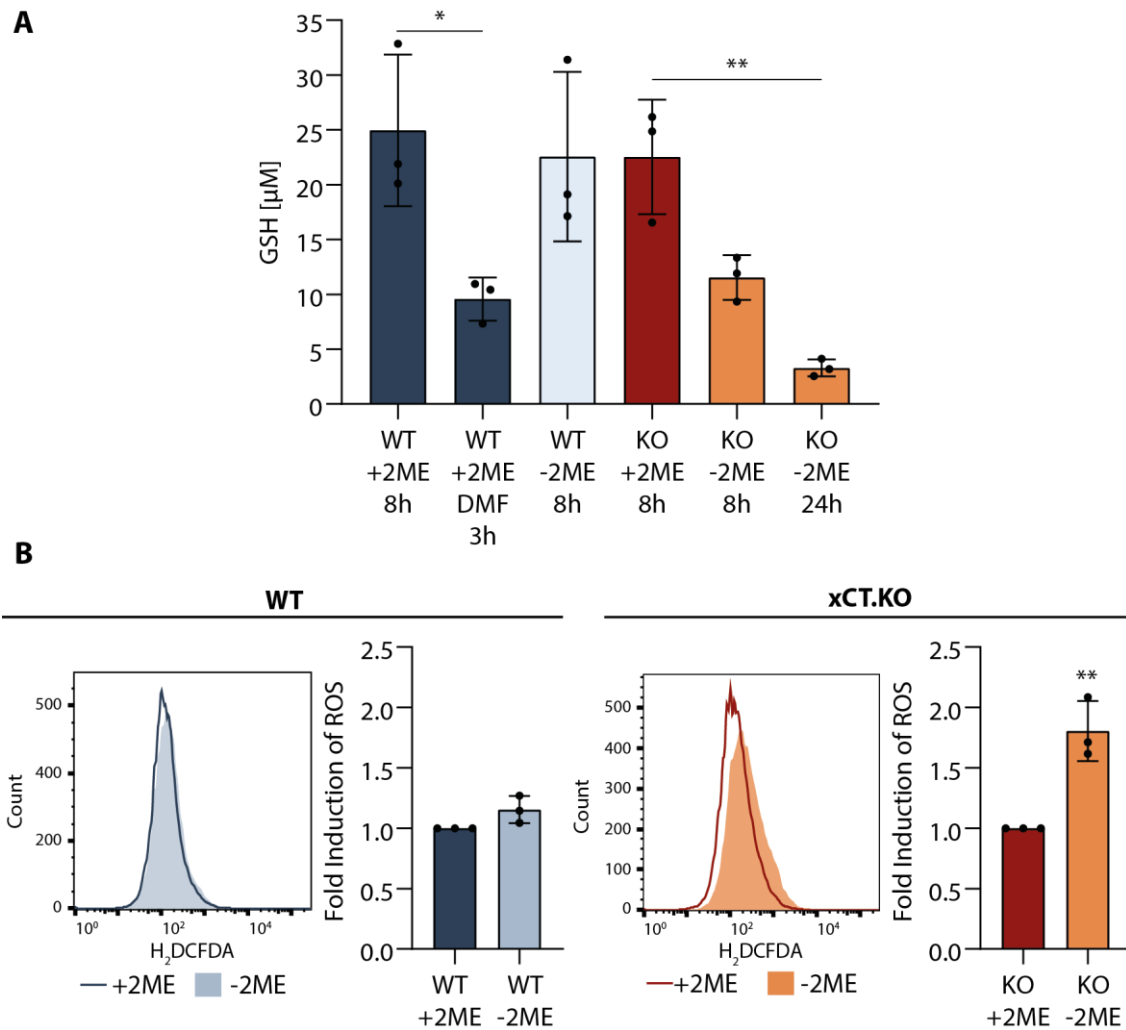


**Figure 23: Modulation of redox homeostasis in xCT knockout cells.**

(A) Harvested BMDCs were cultured in medium with or without 2ME for 8 h and 24 h. As a positive control WT cells were treated with 70  $\mu$ M DMF for 3 h. GSH content was analyzed by a spectrometric assay ( $n=3$ ; ANOVA with Tukey post-hoc test). (B) Immature DCs from WT or KO mice were cultured in medium with or without 2ME for 24 h and intracellular ROS levels were assessed by staining with 2',7'-dichlorodihydrofluorescein diacetate ( $H_2DCFDA$ ). Representative histograms (left) and geometric means as fold induction of +2ME control (right) are shown ( $n=3$ ; unpaired Student's t test).

Thus, it could be shown that the genetic loss of the cystine-glutamate antiporter reproduces the DMF-mediated effects on redox homeostasis. An inhibition of intracellular GSH occurred, with the simultaneous induction of reactive oxygen species. Thus it is now possible to investigate the effects of oxidative stress on DC differentiation without further side effects caused by DMF treatment.

### *4.3.3 EFFECTS OF xCT KNOCKOUT ON DENDRITIC CELL DIFFERENTIATION*

Based on the previously obtained data, the treatment protocol was adjusted, as depicted in Figure 24A. After isolation of stem cells from the bone marrow of both wildtype and xCT knockout mice, they were grown in medium with 2ME. Seven days later, the harvest of the immature dendritic cells was performed as usual. These cells were subjected to a medium change and plated out on cell culture plates according to the respective groups in medium with or without 2ME. After 24 h, a possible pretreatment with DMF or NAC for 1 h was applied, as after this time, the inhibition of GSH in the knockout cells was at its highest. Finally, the cells were stimulated with LPS, the duration of which depended on the particular assay performed.

Since the stem cells died after isolation from the bone marrow when cultivated in medium without 2ME, the first step was to analyze whether this was also the case for the immature BMDCs harvested at a later stage. However, using the above protocol, neither wildtype nor xCT knockout cells showed signs of toxicity after 24 h incubation with LPS (Figure 24B). Since the majority of BMDCs were viable after this time period, this treatment regimen could be further pursued.

As in the subproject of FumET-CORM characterization, the analysis of the HO-1 and STAT1 signaling pathways was used to gain a more detailed understanding of the underlying mechanisms. Using Western blotting, it could be shown that both a strong induction of HO-1 and an inhibition of STAT1 phosphorylation after DMF treatment were achieved in wildtype cells (Figure 25). Knockout BMDCs cultivated with 2ME exhibited similar basal levels of these proteins as wildtype cells. This was expected as the presence of 2ME allows cystine to enter the cell without the antiporter and thus, the cells maintain normal glutathione levels, as shown above (Figure 23A).

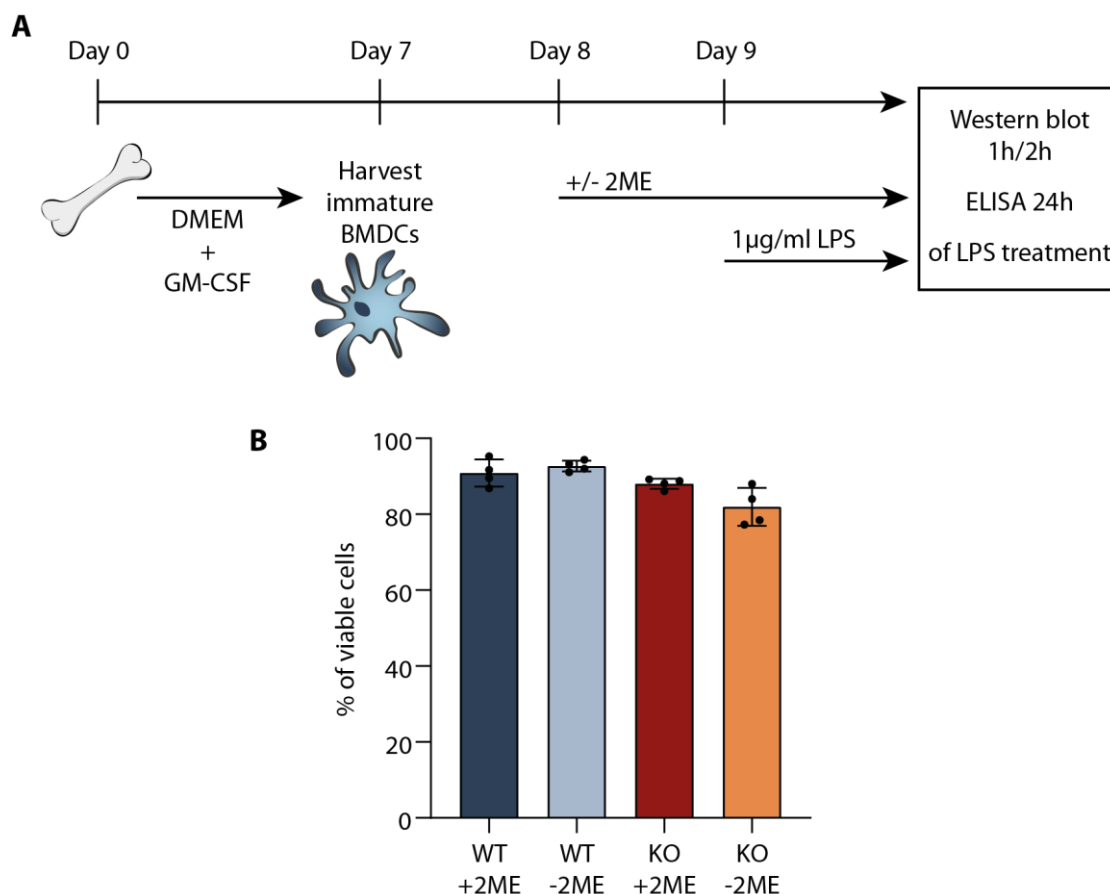


**Figure 24: Treatment regimen of wildtype and xCT knockout BMDCs.**

(A) The treatment regimen used for the succeeding experiments is shown. Immature DCs were generated as described previously (Figure 8). The cells were harvested on day 7 after isolation and plated onto suitable cell culture dishes with a concentration of  $1 \times 10^6$  cells/ml. One day later the medium was exchanged to medium with or without 2ME. After additional 24 h incubation the cells were stimulated with LPS for a period of 1-24 h depending on the desired assay. (B) BMDCs treated as described above were analyzed for cell viability by trypan blue assay after 24 h of culture in medium with or without 2ME (n=4).

The hypothesis was that xCT knockout BMDCs cultivated without 2ME should experience modulations similar to those observed in fumarate treatment if these DMF-mediated effects are attributable to inhibition of GSH. However, it turned out that the depletion of GSH in these knockout cells is insufficient to affect the signaling pathways. Instead, xCT.KO BMDC without 2ME showed comparable protein levels of HO-1 or STAT1 compared to the direct control group of knockout cells with 2ME, as well as to wildtype cells. The additional incubation of the knockout cells with the antioxidant NAC did not result in significant effects either (Figure 25).

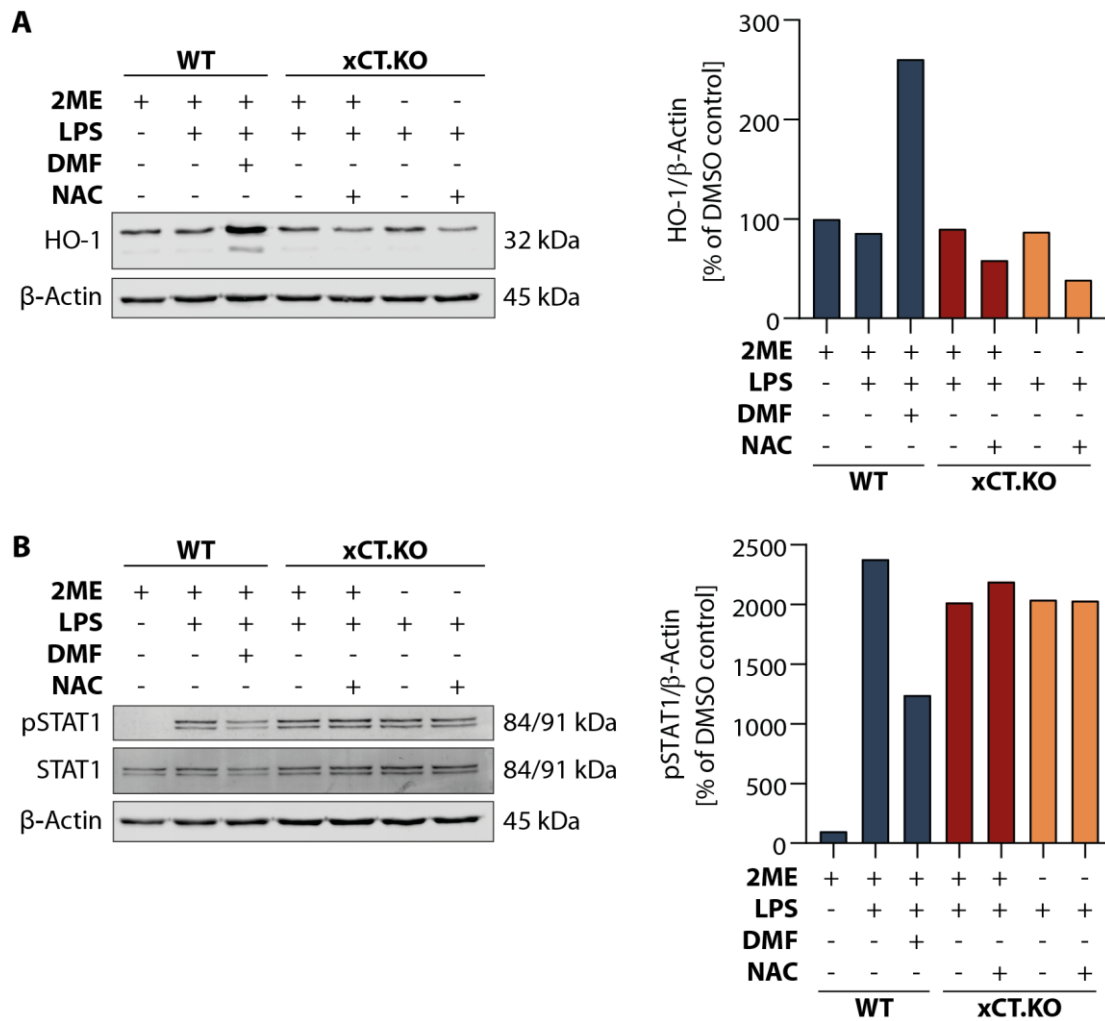


**Figure 25: Effects of xCT knockout on HO-1 and STAT1 signaling pathways.**

For monitoring of protein expression BMDCs were cultured as described in Figure 24. After 24 h of culture in medium with or without 2ME cells were pretreated with DMSO, 70  $\mu$ M DMF or 1 mM NAC for 1 h and then stimulated with 1  $\mu$ g/ml LPS for 2 h. Cell lysates were prepared and analyzed for HO-1 (A) or STAT1 and pSTAT1 (B) expression, whereas  $\beta$ -actin served as loading control. Representative Western blots and densitometric quantification are shown (n=3).

Next, it should be evaluated whether an additional DMF treatment can induce changes in the signaling cascades despite the already existing GSH depletion in the knockout cells. Regarding the HO-1 expression, a marked induction of the protein was visible after 2 h treatment with DMF. This was evident for both treatment groups of the wildtype cells as well as for the knockout BMDCs (Figure 26). However, it was also demonstrated once more that depletion of GSH alone was not sufficient to induce HO-1 since no regulation was visible between the knockout cells with and without 2ME.

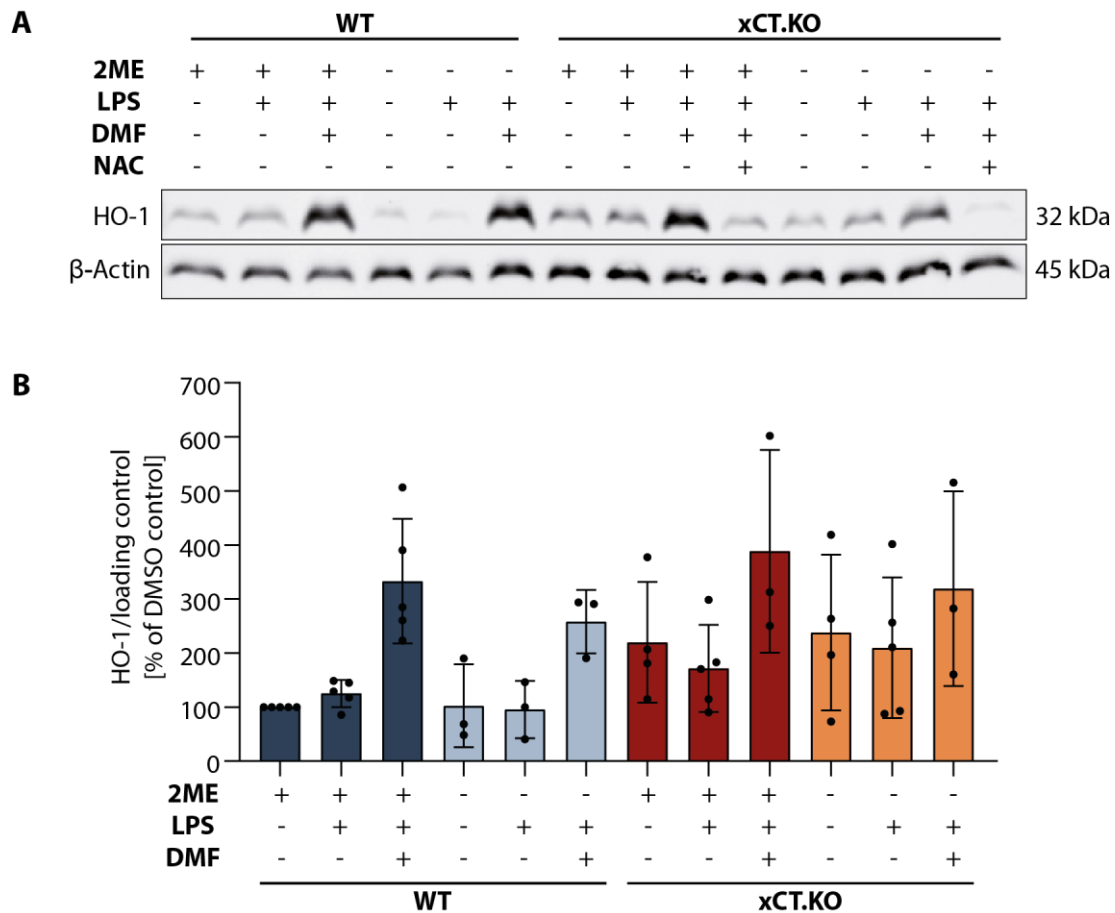


**Figure 26: HO-1 induction is not influenced by genetic loss of xCT antiporter alone.**

After 24 h of BMDCs culture with or without 2ME cells were pre-incubated with DMSO, 70  $\mu$ M DMF, 1 mM NAC or a combination thereof for 1 h. Subsequently 1  $\mu$ g/ml LPS was added, after 2 h of stimulation cell lysates were harvested and HO-1 expression was analyzed by Western blotting. A representative Western blot (A) and the semi-quantitative densitometric analysis (B) are shown (n=3). HO-1 protein levels were normalized to loading controls, for which  $\beta$ -actin or  $\alpha$ -tubulin were used.

Furthermore, in the xCT.KO BMDCs, the additional incubation with DMF resulted in an upregulation of HO-1. This effect was slightly weaker than in the other three treatment groups but was still clearly detectable (Figure 26). It is important to note that these cells already had depleted levels of intracellular GSH and an accumulation of ROS due to cultivation without 2ME (Figure 23). This means that in this case, the upregulation caused by DMF was not based on the simple induction of oxidative stress, as hypothesized before. The difference may be due to compensatory effects resulting from the genetic knockout or from other factors of the fumarate treatment. The Western blot also showed that the knockout cells had a slightly higher basal level of HO-1. However, this was rather due to the fact that the knockout animals have a mixed C57BL/6J and C57BL/6N background, whereas wildtype control cells were isolated from C57BL/6J mice. Therefore, more important than the comparison between wildtype



and knockout is the one between knockout cells cultivated with and without 2ME, since these cells were derived from the same background.

Looking at the STAT1 phosphorylation, a comparable result was obtained. Once again, both wildtype groups and knockout cells with 2ME should show a similar expression pattern. This was found to be the case, with all three groups showing a pronounced inhibition of pSTAT1 after DMF treatment, while maintaining comparable basal levels. Furthermore, the loss of GSH alone was not sufficient to achieve a reduction of STAT1 phosphorylation. However, the additional treatment of these knockout cells without 2ME with DMF was able to induce signal modulation (Figure 27). In contrast to the HO-1 signaling pathway, where the DMF effect was weak in knockout cells without 2ME, the inhibition of pSTAT1 was more robust in this group. After additional DMF incubation, almost no pSTAT1 could be detected, whereas the levels in the other three control groups decreased by at most up to 50 %. Again, additional mechanisms complementing GSH inhibition must be responsible for the modulation of the signaling pathway. The protein levels of unphosphorylated STAT1 remained unchanged in all groups (Figure 27).

To conclude the analysis of the signaling cascades involved in the induction of DC type II response, the downstream cytokines IL-12p70 and IL-23 were examined (Figure 28). As mentioned before, xCT.KO cells had slightly elevated basal levels of HO-1 compared to wildtype BMDCs. However, this was not reflected in the detected cytokine concentrations. The baseline levels of IL-12p70 and IL-23 compared between both wildtype and knockout cells, as well as between those with and without 2ME, are all on a constant level. However, this also means that no changes were caused by GSH depletion on the level of cytokine expression. Knockout cells cultivated without 2ME exhibited no change in the measured cytokine concentrations. Instead, as in the previous Western blots, additional treatment with DMF was required to achieve inhibition of IL-12p70 and IL-23. Cytokine levels could be completely suppressed in all four groups by incubation with DMF and were partially reversed by additional treatment with NAC (Figure 28).

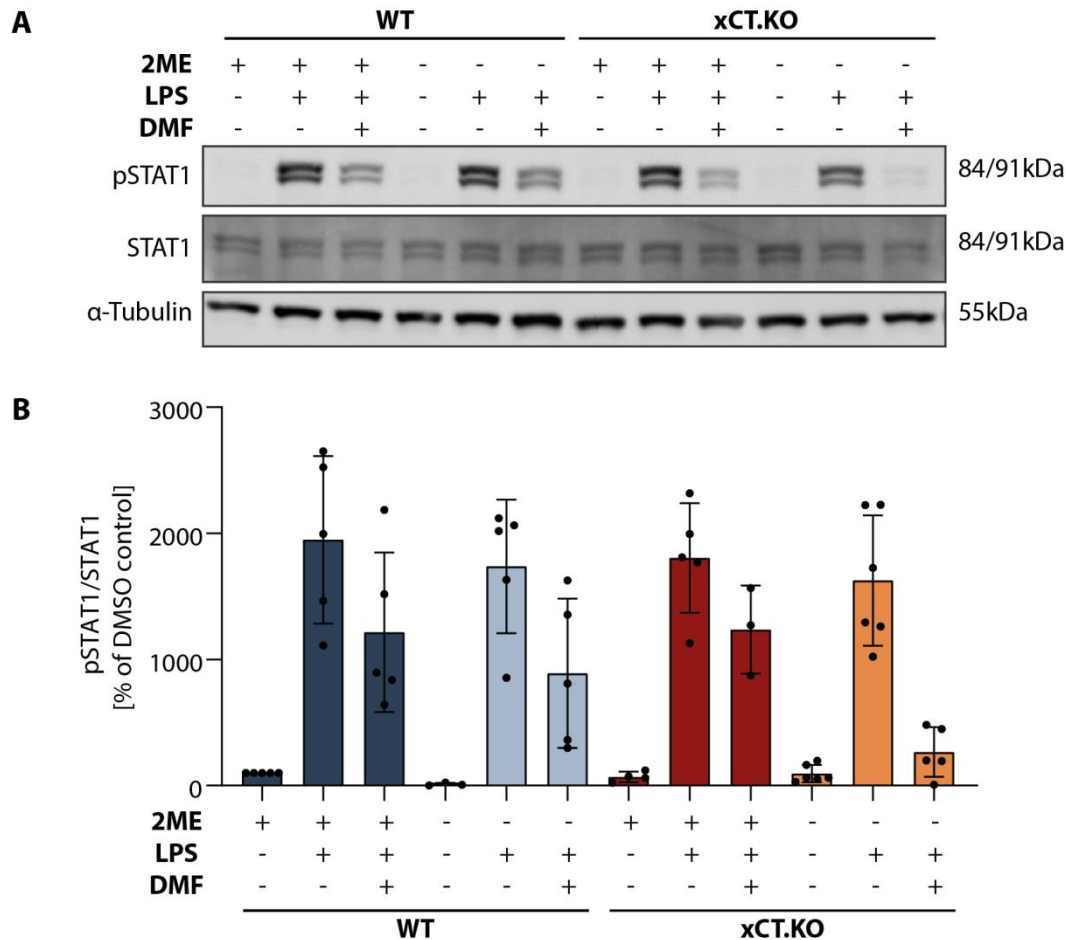


**Figure 27: STAT1 phosphorylation is not influenced by genetic loss of xCT antiporter alone.**

BMDCs cultured for 24 h with or without 2ME were pretreated with DMSO, 70  $\mu$ M DMF, 1 mM NAC for 1 h and then stimulated with 1  $\mu$ g/ml LPS for 2 h. Cell lysates were analyzed for STAT1 expression and phosphorylation by Western blotting. A representative Western blot (**A**) and the semi-quantitative densitometric analysis (**B**) are shown (n=5). Levels of pSTAT1 were normalized to overall STAT1 levels.

In conclusion, these findings indicate that the permanent inhibition of GSH alone does not induce differentiation towards a DC type II phenotype. Although oxidative stress is induced in xCT knockout cells, it does not lead to the induction of HO-1, the inhibition of pSTAT1 and the downstream inhibition of IL-12p70 and IL-23 as it is associated with the DMF treatment. Instead, additional treatment with DMF is required. This either suggests the involvement of additional effects of the fumarate or the compensation of the deficient GSH synthesis.

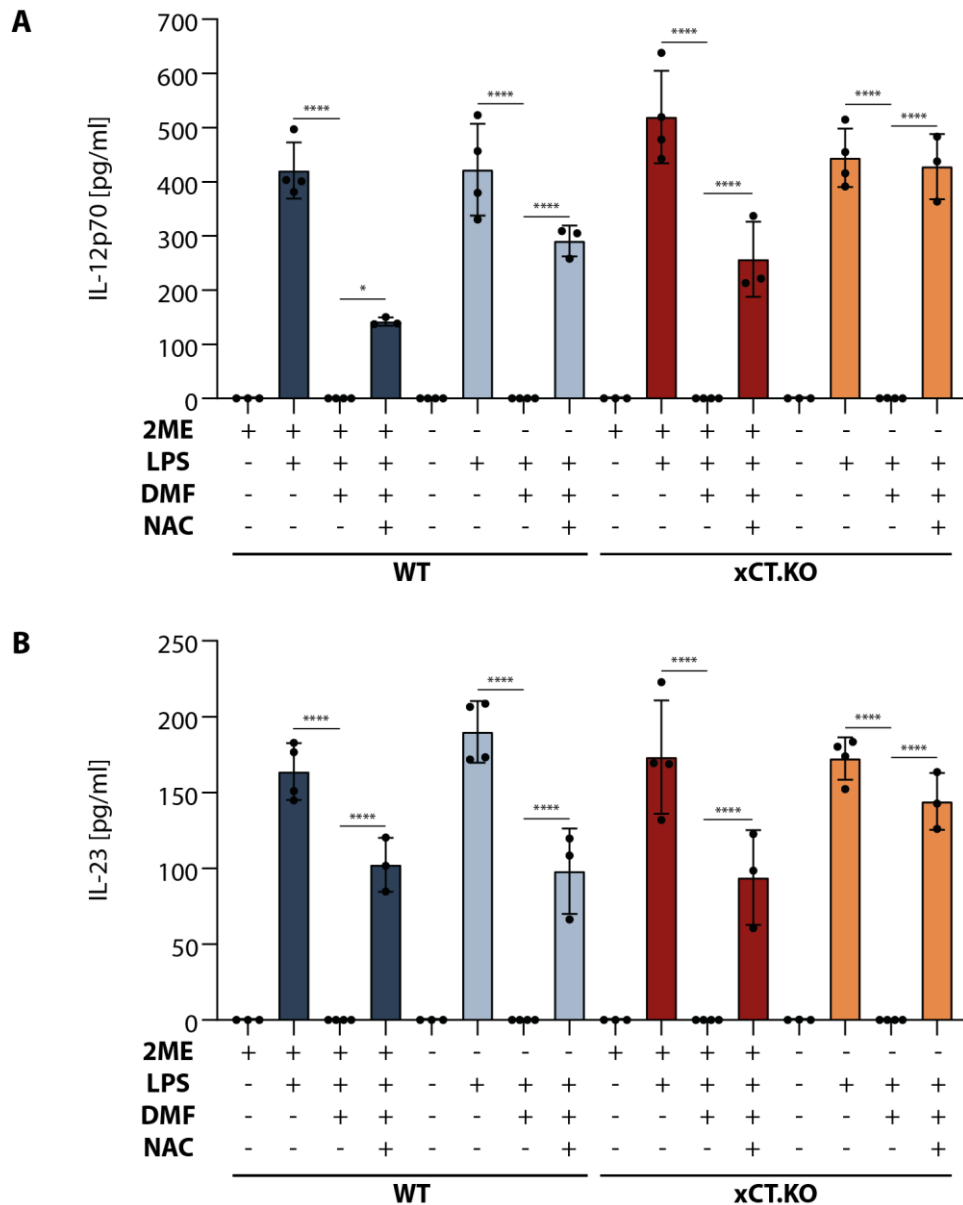


**Figure 28: Knockout of xCT antiporter is not sufficient to inhibit inflammatory cytokine secretion.** BMDCs were cultured as described in Figure 24. Before LPS-stimulation, cells were pre-incubated with DMSO, 70  $\mu$ M DMF, 1 mM NAC or a combination thereof. After 24 h of stimulation cell culture supernatants were harvested and IL-12p70 (A) and IL-23 (B) levels were determined by ELISA (n=4; ANOVA with Tukey post-hoc test).

#### 4.3.4 POSSIBLE OVERCOMPENSATION AFTER XCT KNOCKOUT BY OTHER REDOX PATHWAYS

One explanation of why the inhibition of intracellular glutathione alone is not sufficient to induce type II DCs could be that other contributing factors are also involved in DMF treatment. Another possibility is that in xCT knockout cells, overcompensation by other redox systems occurs. Strict regulation of reactive oxygen

species is indispensable for cellular survival, as excessive concentrations result in cell death induction (Figure 20). Therefore, it would hardly be surprising if other mechanisms compensate for the loss of one of the most important ROS scavenger. This question will be addressed in the following two chapters.

To get an overview of the numerous signaling pathways and effector molecules involved in the regulation of oxidative stress, a broadly designed PCR screen with 89 different genes of the redox system was performed in cultured immature BMCDs 24 h after 2ME depletion and subsequent LPS and DMF treatment as indicated in the figure legend. The genes in which regulation was detected were clustered according to their expression pattern (Figure 29).

One group of genes was found to have a generally higher expression in the knockout cells than the respective wildtype treatment groups (Figure 29A). Among these genes were some associated with increased ROS stress as well as the anti-apoptotic Bcl-2. This illustrates the finding that xCT.KO BMDCs are in a state of oxidative stress due to their proven increase in ROS and, thus, among other things, upregulate genes that ensure cellular survival. In this group, however, it was not evident that there is significant overcompensation by a particular redox pathway. There also existed some genes which showed a lower expression in the xCT knockout cells across all treatment groups (Figure 29B). These were often genes that are associated with a protective role in oxidative stress, such as *Cat*, *Dhcr24*, *Gpx4*, *Hp* or *Lcn2*. The decline in their expression thus leads to a loss of further protective mechanisms against oxidative stress. However, to reach a more precise conclusion, an additional investigation would also have to be carried out at the protein level.

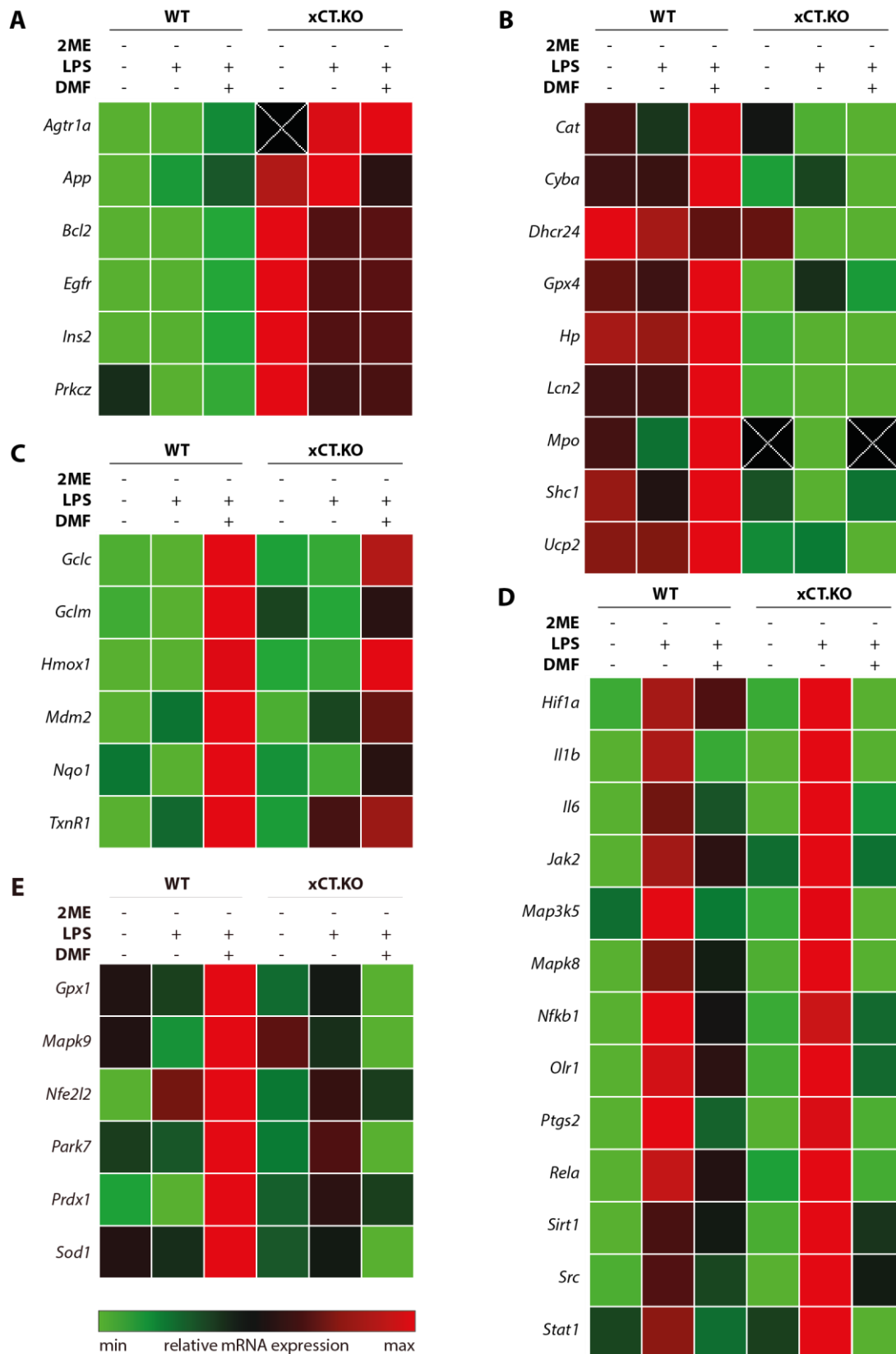


**Figure 29: Differential expression of genes related to oxidative stress response.**

(A-E) Immature DCs were cultured without 2ME for 24 h, pretreated with 70  $\mu$ M DMF for 1 h and then stimulated with 1  $\mu$ g/ml LPS for 2 h. RNA samples were isolated and mRNA expression was analyzed with a qPCR array containing 89 different target genes involved in oxidative stress response. The clustergrams of selected targets, divided according to their expression pattern, are shown.

Furthermore, expression patterns were found, which were already known to be involved in DMF treatment and which were equally regulated in both wildtype and knockout BMDCs (Figure 29C and D). These include the induction of *Hmox1* but also of *Gclc* and *Gclm*, which are the two subunits of the ligase involved in the synthesis of GSH. The induction by LPS and subsequent inhibition by DMF of *IL6*, *IL1b* and *NF- $\kappa$ B1* can be classified in this category. The reproduction of these effects already known from wildtype cells confirms the validity of the array and demonstrates the stability of DMF treatment in wildtype cells and the analyzed xCT.KO BMDCs.

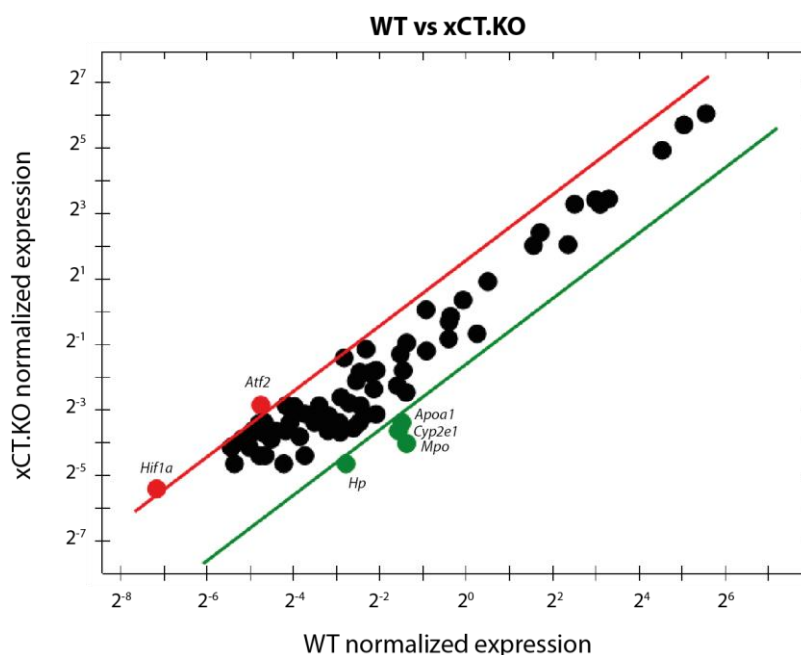


**Figure 30: Ex vivo analysis of oxidative stress response in wildtype and xCT knockout cells.**

Bone marrow derived stem cells were isolated from femurs of wildtype or xCT knockout mice and RNA purification was performed immediately. Expression of mRNA was analyzed by RT-PCR using a qPCR array containing 89 target genes involved in oxidative stress response. Scatter plot shows upregulated (red) and downregulated (green) targets in xCT knockout cells compared to wildtype cells.

Next, this array was performed with bone marrow stem cells directly after isolation, without prior differentiation into dendritic cells. This *ex vivo* analysis showed few significant modulations of the 89 genes analyzed (Figure 30). There was only a slight induction of *Atf2* and *Hif1a*, which can both be induced by oxidative stress. Besides, both anti-oxidative (*Apoa1*, *Hp*) and pro-oxidative (*Cyp2e1*, *Mpo*) genes were inhibited, which fits with the data formed *in vitro*. However, *ex vivo* all these regulations were weak. This suggests that the mice compensate for the loss of the antiporter and therefore, only very weak effects were detectable *ex vivo*. It is also possible that this involves compensations that were not detected by these arrays.

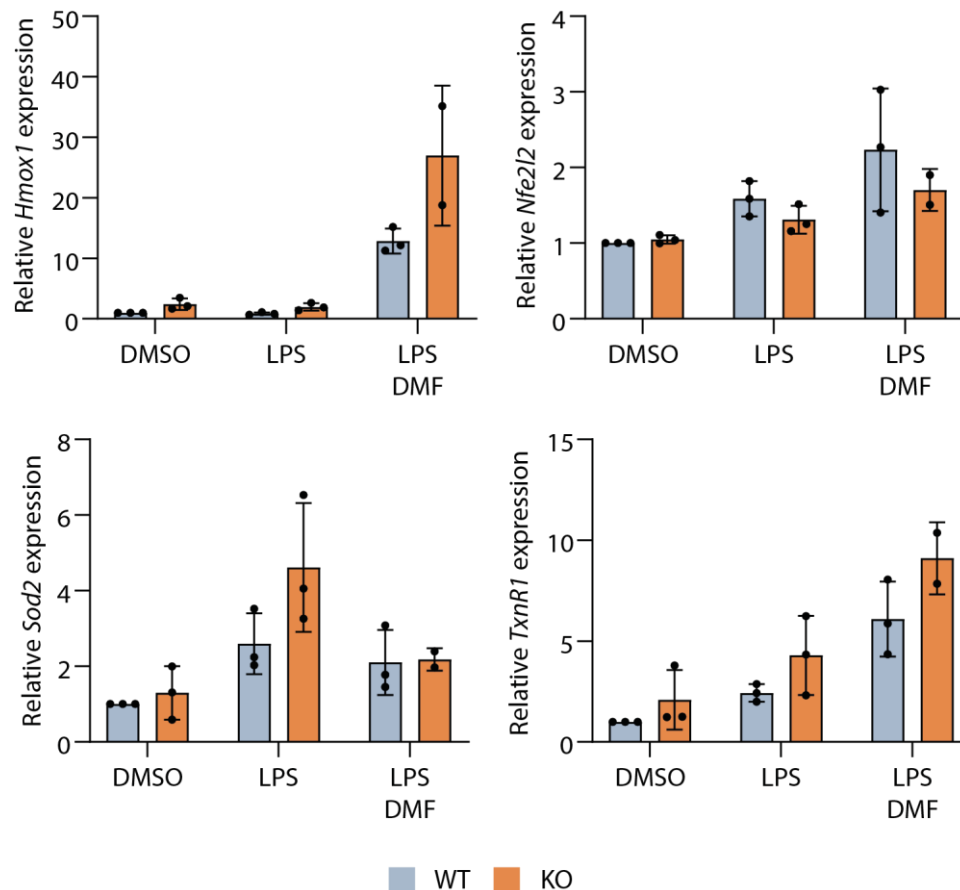


**Figure 31: Effects of DMF treatment and xCT knockout on mRNA expression.**

After cultivation of DCs without 2ME for 24 h, cells were pretreated with DMSO or 70  $\mu$ M DMF for 1 h and afterwards stimulated with 1  $\mu$ g/ml LPS for another 2 h. RNA samples were harvested and analyzed for mRNA expression of indicated target genes. The expression was normalized to  $\beta$ -Actin, HRPT, Eef1a1 and GAPDH housekeeping genes and is shown as fold change compared to the respective DMSO control (n=3).

For the more detailed analysis of different signaling pathways in the redox system and to confirm the PCR array results, further expression analysis was performed. Four different targets were selected for this (Figure 31). First, the heme oxygenase 1 (*Hmox1*) gene induction was analyzed, since it was known from the previously performed Western blots that the DMF treatment leads to an upregulation of HO-1 on the protein level (Figure 26). The investigation of the RNA expression could confirm this. In wildtype as well as in xCT.KO BMDCs the *Hmox1* expression was induced after incubation with DMF. These results are consistent with those obtained from the analysis of HO-1 protein expression. The second factor investigated was the gene coding for thioredoxin reductase (*TxnR1*). Besides glutathione, the thioredoxin system is one of the most important mechanisms to maintain cellular redox homeostasis. The treatment with DMF in both wildtype and knockout cells likewise induced the expression of *TxnR1* RNA (Figure 31). These results could already be demonstrated in

the PCR array, further confirming the results obtained in the experiment (Figure 29C). The antioxidant Sod2 is a molecule that catalyzes the dismutation of superoxide into either O<sub>2</sub> or hydrogen peroxide. It was shown that stimulation with LPS in the knockout cells led to an upregulation of the gene, which was subsequently reversed by DMF treatment. This effect was only very weak in wildtype cells (Figure 31). Finally, the (nuclear factor erythroid 2-related factor 2) *Nfe2l2* RNA expression was investigated. This gene codes for the protein Nrf2 which is considered one of the master regulators of oxidative stress, as it is involved in many different signaling pathways. However, no regulation on the RNA level was found in this experiment at the examined time point (Figure 31).

#### 4.3.5 EFFECTS OF THIOREDOXIN PATHWAY INHIBITION ON BMDC DIFFERENTIATION

Although no significant overcompensation was evident in the previous screens, the role of the thioredoxin pathway should be addressed by further analysis. For this purpose, auranofin, a thioredoxin reductase inhibitor, was used. Besides glutathione, the thioredoxin signaling pathway is considered one of the most important signaling cascades to maintain a normal redox balance in the cells. The objective was to determine whether the additional inhibition of the thioredoxin signaling pathway in xCT knockout cells, in contrast to wildtype cells, leads to a polarization towards a DC type II phenotype.

However, it should be noted that the use of higher dosages of auranofin in wildtype cells may already cause inhibition of inflammatory cytokines [253]. Therefore, the first step was to titrate the auranofin concentration to find one at which there are no toxic effects but still inhibition of thioredoxin reductase occurs. In this context, special attention was paid to whether the knockout cells were more sensitive towards the auranofin treatment than the wildtype control cells at the same concentration.



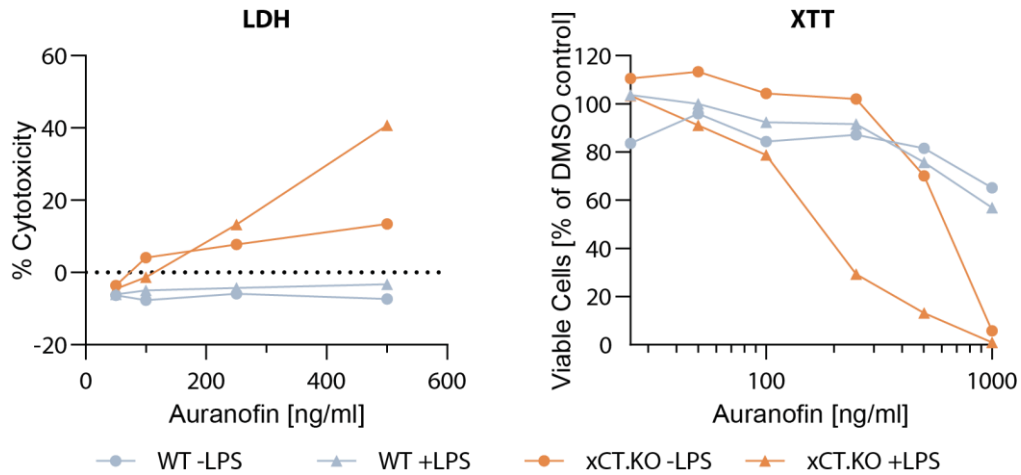


**Figure 32: Toxicity of auranofin on wildtype and xCT knockout BMDCs.**

Wildtype and xCT knockout BMDCs were cultured without 2ME for 24 h, followed by pretreatment with indicated concentrations of auranofin and stimulation with 1  $\mu$ g/ml LPS for another 24 h. Cell viability and cytotoxic effects of auranofin treatment were assessed by LDH (A) and XTT (B) assays (n=3).

Regarding the cytotoxicity, it was found that the xCT knockout BMDCs rapidly died after treatment with auranofin at only relatively low concentrations. In contrast, wildtype BMDCs showed no signs of toxicity after treatment with the same amounts of auranofin (Figure 32). Despite the minor changes found in the RNA-screen, the loss of a second antioxidant mechanism in the knockout cells quickly led to a strong decline in cell viability. Whether this increased sensitivity to auranofin treatment compared to wildtype cells was also reflected in other assays was investigated in the following experiments.

Initially, the baseline levels of thioredoxin reductase activity were determined and its inhibition after auranofin treatment was verified. It was noticeable that especially xCT knockout BMDCs cultivated without 2ME already had a decreased basal activity compared to the other control cells (Figure 33A). This was the first indication that there is insufficient compensation through this redox system. Additionally, the detected levels were further inhibited in both wildtype and knockout cells by treatment with DMF (Figure 33A).

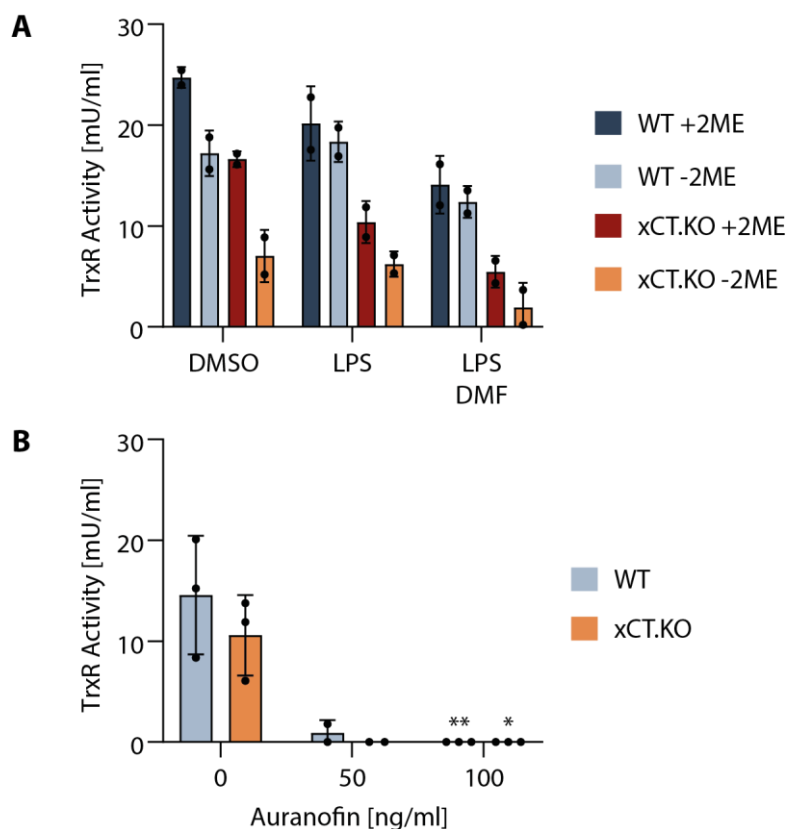
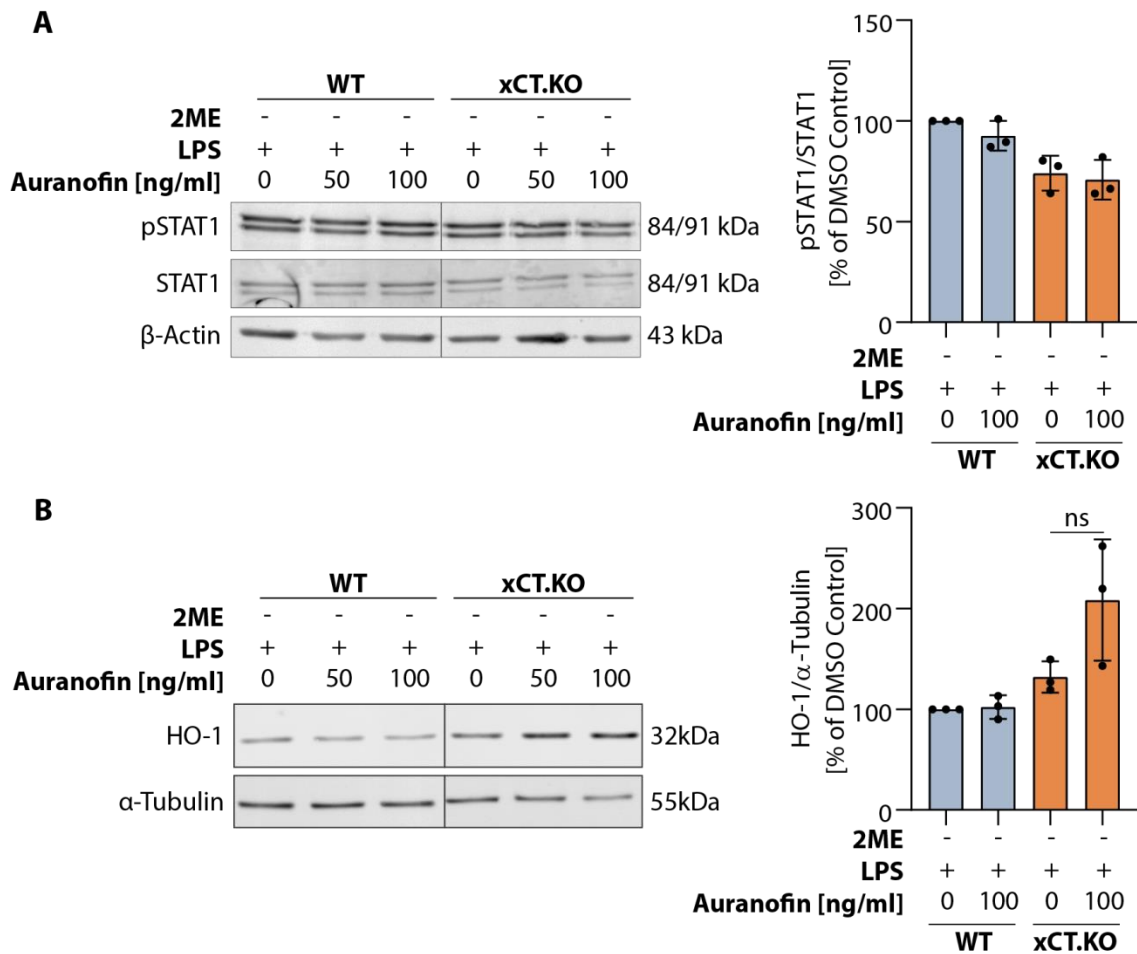


**Figure 33: Inhibition of thioredoxin reductase.**

(A and B) For monitoring of the thioredoxin antioxidant system the activity of thioredoxin reductase (TrxR) was determined. Thereby, one unit of TrxR is defined as the amount of enzyme that generates 0.5  $\mu\text{mol}$  of NADP. (A) Basal levels of TrxR were examined in cell lysates of BMDCs pretreated with DMSO or 70  $\mu\text{M}$  DMF for 1 h and stimulated with 1  $\mu\text{g}/\text{ml}$  LPS for 2 h ( $n=2$ ). (B) Efficiency of auranofin-mediated TrxR inhibition was tested by treatment of BMDCs cultured without 2ME for 24 h, followed by treatment with auranofin in the indicated concentrations for 5 h ( $n=3$ , ANOVA with Tukey post-hoc test).

Because of the toxicity observed in the knockout cells, only a very low concentration of a maximum of 100 ng/ml auranofin could be used. It should now be checked whether thioredoxin reductase activity was still inhibited. Figure 33B shows that despite the low concentrations applied, complete inhibition occurred in both the wildtype and the xCT.KO BMDCs. Hence, both 50 ng/ml and 100 ng/ml of auranofin could be used in either cell type to study the loss of the thioredoxin pathway without toxic effects.



After having defined the necessary parameters for an auranofin treatment, its effects on the STAT1 and HO-1 signaling pathways were investigated. As mentioned above, the hypothesis was made that in the case of an existing overcompensation by the thioredoxin signaling pathway in the xCT knockout cells, increased sensitivity to treatment with the inhibitor should occur. However, considering the STAT1 phosphorylation, this hypothesis could not be confirmed. Neither the wildtype nor the knockout cells showed a decrease in pSTAT1 levels (Figure 34A). In contrast, after incubation with the thioredoxin reductase inhibitor, the xCT.KO BMDCs responded by upregulating the HO-1 protein levels. This does not occur in wildtype cells at the same low concentrations applied (Figure 34B). Therefore, auranofin had divergent effects on

STAT1 phosphorylation and on HO-1. In order to address at this in more detail, the cytokines IL-12p70 and IL-23 regulated by those signaling pathways were investigated.

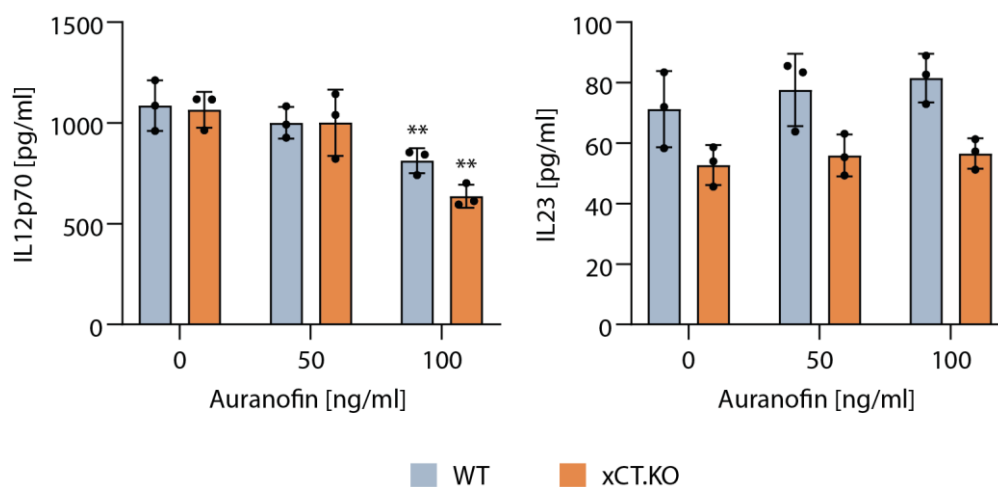


**Figure 35: Auranofin treatment has no influence on inflammatory cytokine release.**

Harvested BMDCs were cultivated for 24 h without 2ME as described in Figure 24 and then pretreated with the specified concentrations of auranofin or with DMSO for 1 h, after which the cells were stimulated with 1  $\mu$ g/ml LPS. Cell supernatants were harvested after 24 h and analyzed for IL-12p70 and IL-23 concentrations by ELISA (n=3, ANOVA with Tukey post-hoc test).

Although the Western blot showed a higher sensitivity of the knockout cells regarding HO-1 induction, this effect was not reflected in the detectable cytokine levels. The IL-23 levels in both wildtype and xCT.KO BMDCs remained unchanged after auranofin treatment. In the case of IL-12p70 regulation, a slight decrease in its concentration was observable. However, this occurred to the same extent in both investigated cell types (Figure 35). Thus, no increased sensitivity of the knockout cells can be considered either. The slight regulation of cytokine levels was achieved despite the lack of inhibition of STAT1 phosphorylation (Figure 34A).

Since IL-23 levels were not inhibited after auranofin treatment despite the increased HO-1 expression in knockout BMDCs, this aspect should be addressed in more detail. For the successful inhibition of the IL-23 by HO-1, the translocation of the protein into the cell nucleus is necessary, where it can act as a transcription factor. Thus, the next step was the analysis of HO-1 levels in both cytoplasmic and nuclear lysates. It could be shown that although auranofin treatment caused an induction and hence accumulation of the protein in the cytoplasm, no efficient translocation into the nucleus occurred (Figure 36). This may explain the subsequent lack of IL-23 inhibition.

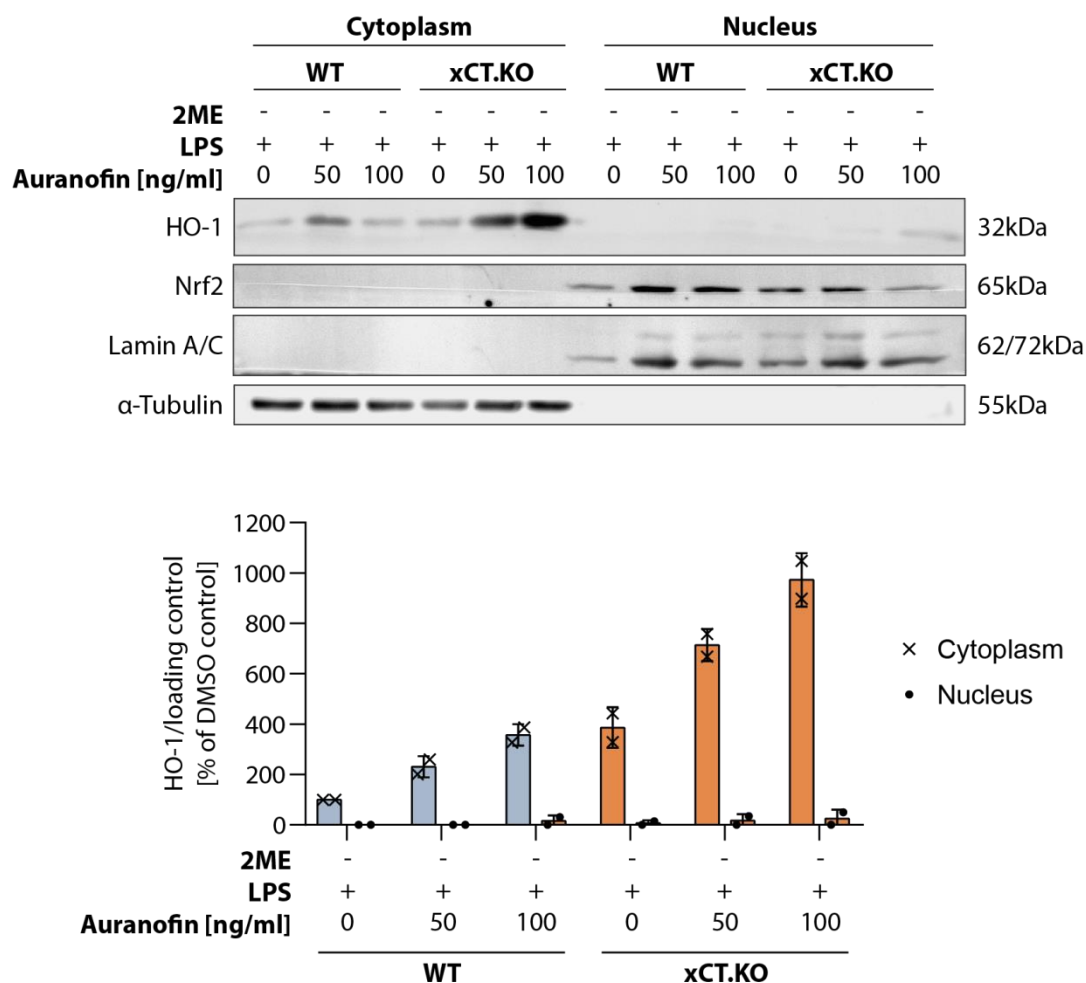


**Figure 36: No increased translocation of HO-1 into the nucleus after auranofin treatment.**

To investigate the translocation of HO-1 into the nucleus, its protein levels in cytoplasmic and nuclear fractions were investigated. Therefore immature DCs were cultivated for 24 h in absence of 2ME. Subsequently, a 1 h pretreatment with DMSO or the indicated concentrations of auranofin was performed as in the previous experiments. The following incubation with LPS was carried out for 6 h and then nuclear and cytoplasmic cell extracts were isolated. These were analyzed for HO-1 and Nrf2 expression by Western blotting. As loading controls for cytoplasm or nucleus,  $\alpha$ -tubulin and lamin A/C were used respectively. An exemplary Western blot and the semi-quantitative densitometric analysis of HO-1 are shown (n=2).

Since at the beginning of the chapter, the knockout cells reacted with considerably earlier toxicity after treatment with increasing auranofin concentrations, the question was raised whether this could be explained by a more pronounced induction of oxidative stress in these cells. Therefore, the analysis of intracellular ROS was performed. Nevertheless, only the non-toxic concentrations of 50 ng/ml or 100 ng/ml auranofin were applied. Once more it could be shown that the insufficient cystine import and the resulting GSH deficiency led to an accumulation of ROS. This became apparent since only the knockout cells cultivated without 2ME had a substantially increased basal level of ROS. Additional treatment with auranofin did not affect the ROS levels in all analyzed samples (Figure 37). However, it cannot be ruled

out that higher concentrations of auranofin may not trigger ROS induction, which subsequently results in increased cell death of knockout BMDCs.

In summary, it can be stated that in the case of xCT knockout BMDCs, overcompensation by the thioredoxin signaling pathway is unlikely. The cells neither show increased basic levels of thioredoxin reductase activity, nor could the additional inhibition of this enzyme enable the differentiation of DCs into a type II phenotype. Whether the DMF-mediated modulations of the signaling pathways are due to the fumarate's additional effects, as suspected in chapter 4.3.3, or whether there is still overcompensation in the xCT knockout cells through other redox pathways, remains unknown.

#### *4.3.6 EFFECTS OF NADPH OXIDASE KNOCKOUT ON DMF TREATMENT*

The last part of this thesis addressed the role of oxidative stress induction for successful treatment with DMF. For this purpose, a new mouse model was chosen. The following experiments were performed with BMDCs isolated from GP91 knockout mice. These mice have a defect in NADPH oxidase 2, the loss of which should result in a disturbed ROS formation and therefore were thought to allow the investigation of DMF treatment without the induction of oxidative stress.

As in the previous experiments, the HO-1 and STAT1 signaling pathways were initially examined on the protein level. In the case of a ROS-dependency of the DMF effects, incubation with the fumarate was not intended to result in a modulation of these pathways. However, both the induction of HO-1 and the inhibition of STAT1 phosphorylation could be achieved in GP91 knockout cells. Although the knockout BMDCs had low ground levels of HO-1, the upregulation was clearly visible (Figure 38).

The cytokine concentrations revealed a similar pattern. As usual, incubation with DMF led to an inhibition of IL-12p70 as well as IL-23 in the wildtype cells. However, this effect was observed to the same extent in the GP91 knockout cells. Furthermore, no difference in the basal levels of the two cytokines could be detected (Figure 39).

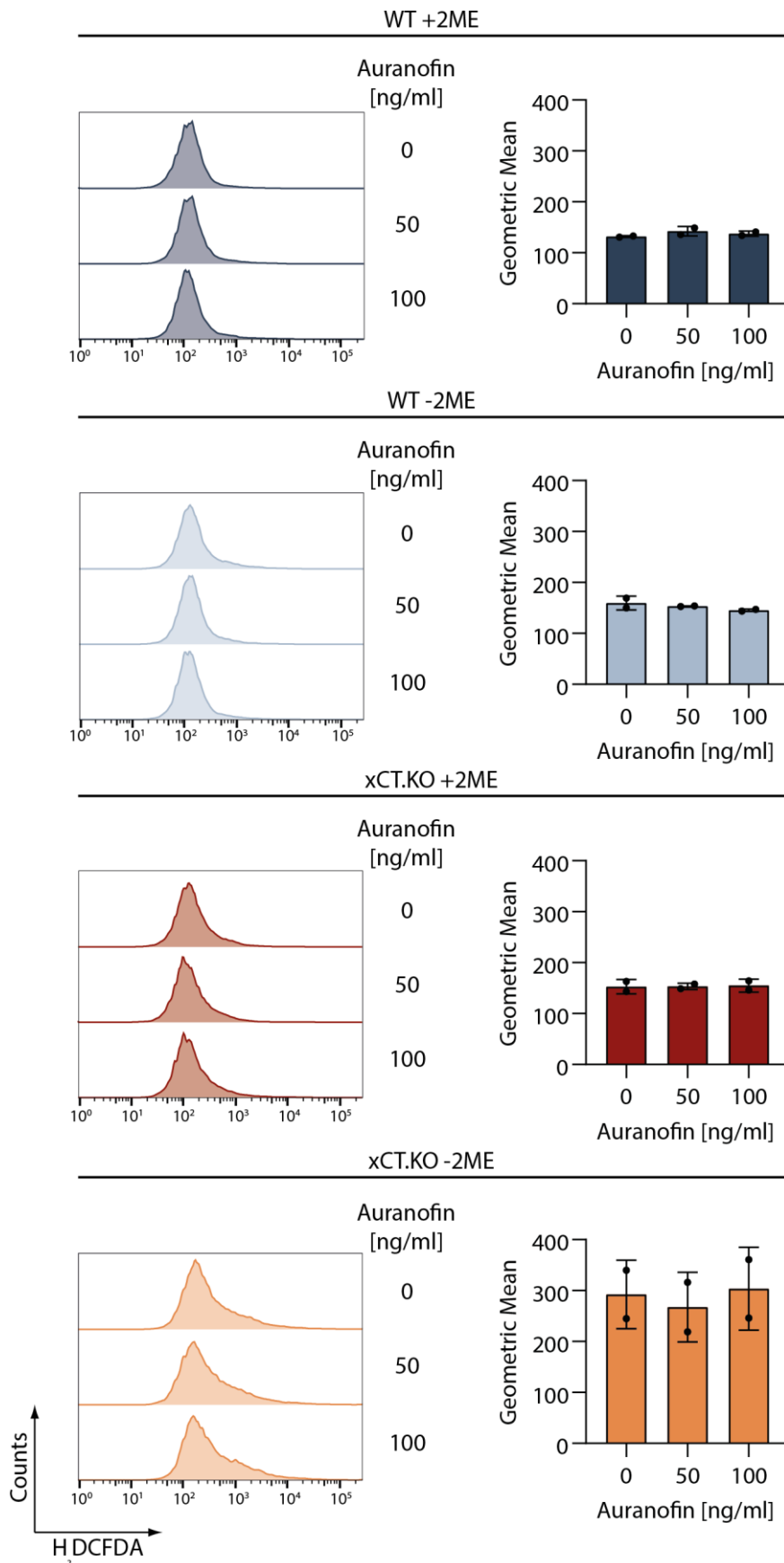


**Figure 37: No detectable modulation of ROS levels after auranofin treatment.** Immature DCs from wildtype or xCT knockout mice were cultured in medium with- out 2ME for 24 h. Subsequently cells were treated with DMSO or the indicated concentrations of auranofin and intracellular ROS levels were determined by stain- ing with 2',7'-dichlorodihydrofluorescein diacetate (H<sub>2</sub>DCFDA). Representative histograms (left) and geometric means (right) are shown (n=2).

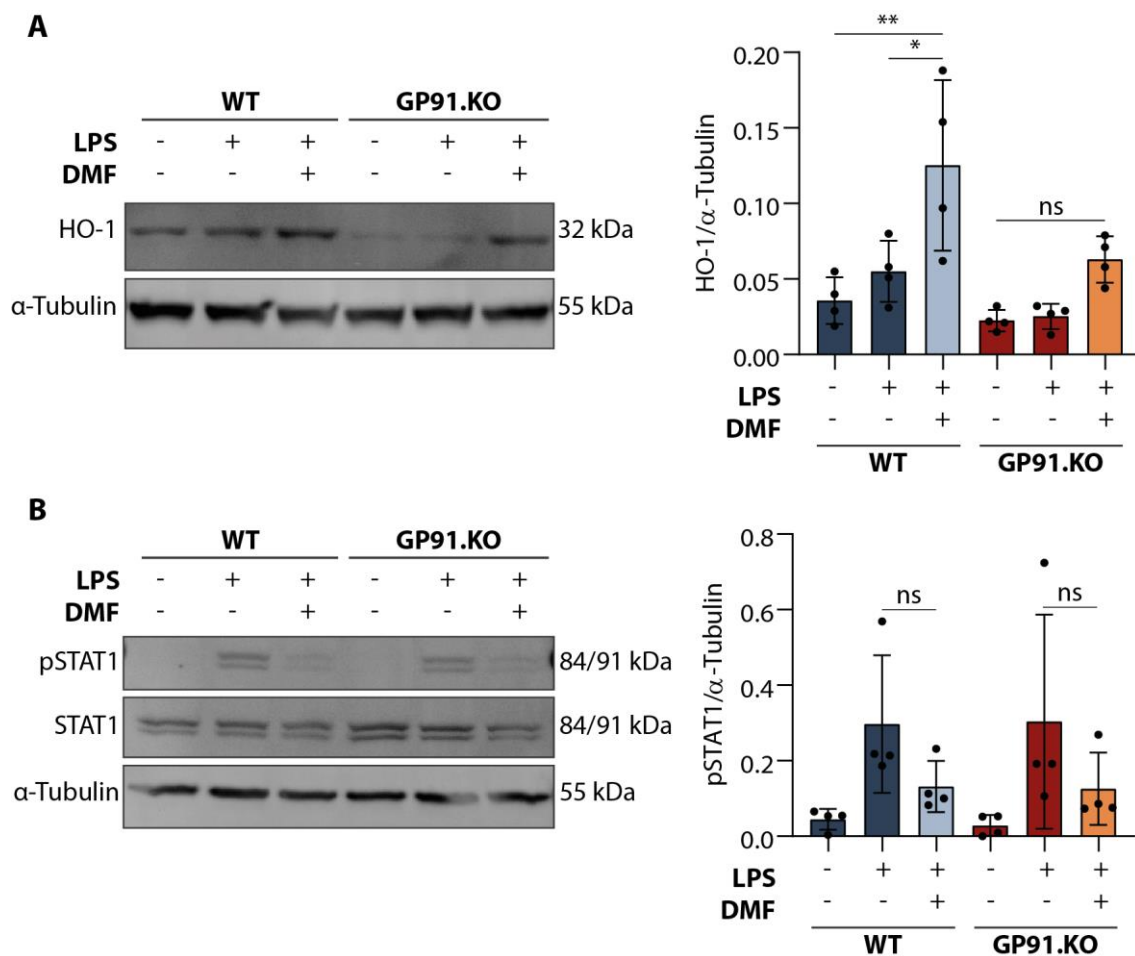


**Figure 38: Modulation of HO-1 and STAT1 signaling pathways in NADPH oxidase knockout cells.** Harvested immature BMDCs were pretreated with DMSO or 70 μM DMF for 1 h and subsequently stimulated with 1 μg/ml LPS for 1 h (B) or 2 h (A). Cell lysates were analyzed for HO-1 (A) or STAT1 and pSTAT1 (B) protein levels by Western blotting. As loading control α-tubulin was used. Representative Western blots (left) and the corresponding semi-quantitative densitometric analysis (right) are depicted (n=4, ANOVA with Tukey post-hoc test).

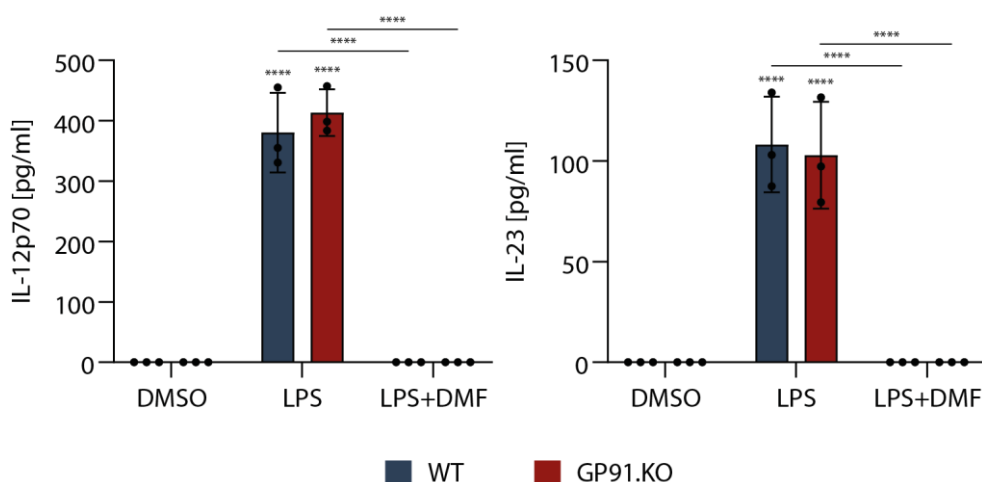


**Figure 39: Inhibition of inflammatory cytokines in wildtype and NADPH oxidase knockout cells.** Secreted cytokine levels were monitored by pre-incubation of BMDCs with DMSO or 70 μM DMF for 1 h, followed by stimulation of the cells with 1 μg/ml LPS for 24 h. Collected supernatants were then examined for IL-12p70 (left) and IL-23 (right) levels by ELISA (n=3, ANOVA with Tukey post-hoc test).



In order to determine, whether DMF treatment modifies redox homeostasis of BMDCs from GP91.KO mice, we analyzed the intracellular levels of reactive oxygen species in untreated and treated cells. Surprisingly, not only in the wildtype but also in the GP91 knockout cells induction of ROS after DMF treatment was detected (Figure 40). Although this increase was not statistically significant, there was a clear tendency observable. The lack of statistical significance is partly attributable to the few biological replicates of only  $n=2$ . Therefore, unlike previously assumed, the BMDCs of GP91.KO mice regulated intracellular ROS levels.

As to why the normal production of reactive oxygen species in GP91 knockout cells occurred despite the defect in NADPH oxidase requires further investigation. It is possible that this oxidase does not play a decisive role in the formation of ROS in the BMDCs utilized or whether other cellular mechanisms compensate for its loss. Independent of the underlying mechanisms, this in turn does not allow to analyze the dependency of DMF treatment on the induction of oxidative stress.

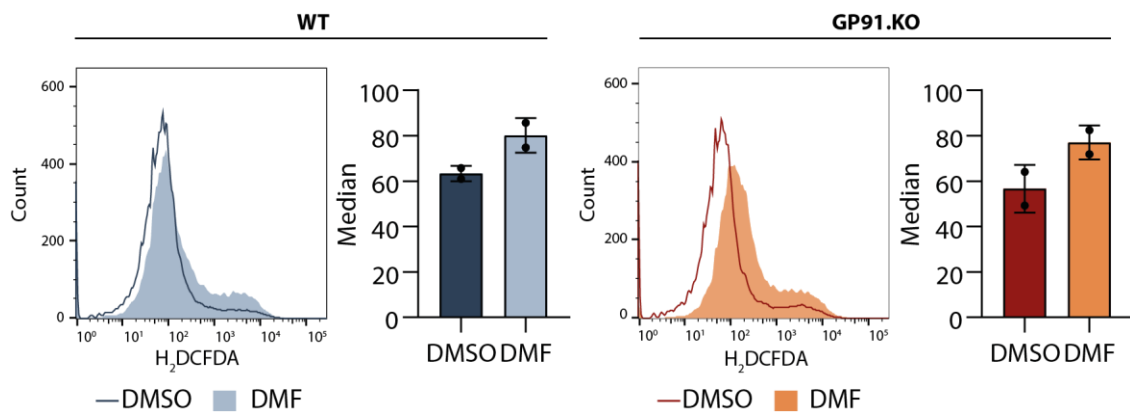


**Figure 40: NADPH oxidase knockout cells still show ROS induction after DMF treatment.**

For analysis of redox homeostasis immature DCs were treated with DMSO or 70  $\mu$ M DMF for 4 h. Adjacent determination of intracellular ROS levels was performed by staining with 2',7'-dichlorodihydrofluorescein diacetate (H<sub>2</sub>DCFDA). Representative histograms and quantitative analysis of medians are shown ( $n=2$ ).

## 5 DISCUSSION

### 5.1 FUMET-CORMS AS POWERFUL ANTI-INFLAMMATORY AGENTS

The successful therapy of T cell mediated autoimmune diseases such as multiple sclerosis or psoriasis, but also corresponding murine disease models such as EAE, can be achieved by the induction of an anti-inflammatory T<sub>h</sub>2 immune response [136, 137, 148, 254, 255]. Such a shift from the disease causing aberrant T<sub>h</sub>1/T<sub>h</sub>17 phenotype was first shown with recombinant IL-4 in mice and in humans and can also be achieved among others, by treatment with FAEs and the resulting modification of the differentiation of DCs into a type II phenotype [91, 135, 137, 256]. In order to enable an optimized treatment, to mitigate side effects and thereby increase patient compliance with the therapy, a continuous refinement of existing therapy options and a detailed understanding of their underlying mechanisms of action are indispensable. Therefore, the first part of this thesis aimed to investigate the effects of a combination of fumaric acid derivatives and carbon monoxide, with the focus on a possible improvement of therapy efficiency. Parts of the project have already been published in a scientific journal, but are supplemented by additional data in this thesis [178].

CO-releasing molecules (CORMs) were provided by a collaborating partner and were investigated for their biological activity and in particular their potential anti-inflammatory effects on BMDCs. Four different substances were investigated, which release different fumaric acid derivatives, but the main distinction is the type and kinetics of the delivery [178]. In the case of the substances *rac-5* and **8**, the molecules are already dissociated in aqueous solution, e.g. in cell culture medium. In contrast, the substances *rac-7a* and *rac-7b* are so-called enzyme-triggered CORMs (ET-CORMs). This type of CORM has to be transported into the cell first in order to be cleaved by esterases, followed by the release of their active components CO and monomethyl fumarate into the cytoplasm. This distinction also becomes evident when looking at the obtained data. For example, the substances *rac-5* and **8** do not exhibit any toxicity among the concentrations investigated, whereas the ET-CORMs could only be used up to a maximum concentration of 25  $\mu$ M (Figure 11). Since regulation of cytokine levels

is established for both CO and DMF, the effects of treatment on IL-12p70 and IL-23 secretion were investigated [137, 257, 258]. Again, biological inactivity, which was also seen in the toxicity measurements, was observed. Only the use of ET-CORMs resulted in a strong inhibition of inflammatory cytokines. Furthermore, as already described in the literature, a reduction of IL-12p70 and IL-23 levels under DMF treatment can be observed. However, the inhibitory effects of ET-CORMs were stronger than DMF treatment alone when a comparatively low concentration of the fumarate was used (Figure 12). This suggests a synergistic effect. Due to this fact the focus of further analyses was directed to the anti-inflammatory capabilities of *rac-7a* and *rac-7b*.

An overlapping factor that seems to play a central role for both DMF treatment and the therapeutic effects of CO is the HO-1 signaling pathway. In the case of DMF, both a strong induction of the protein and its translocation into the cell nucleus were previously described by Ghoreschi and coworkers and could also be shown here (Figure 10) [137]. HO-1 is influenced by CO at two levels. Firstly, CO is constantly being formed in the body through the cleavage of heme mediated by HO-1 [153]. On the other hand, an induction of HO-1 after CO treatment has also been described. In addition, no therapeutic effect was observed in HO-1 knockout cells after CO incubation, indicating a central role of this pathway for effective CO treatment [257]. The treatment of BMDCs with the CORMs likewise led to an induction of the protein (Figure 13). This was strongest after treatment with *rac-7b*, but could be observed for all substances. Again, the effects were considerably stronger than with DMF treatment alone.

Conflicting data to the literature was obtained by analysis of STAT1 phosphorylation. In the literature no effect on this signaling pathway after CO treatment is described. Instead, STAT3 activation has been shown to be inhibited [257]. However, analysis of the STAT1 signaling pathway in this work showed a well-defined inhibition of pSTAT1 levels by the ET-CORMs *rac-7a* and *rac-7b* in a concentration-dependent manner (Figure 14). This observed difference between the published CO-treatment and the one with FumET-CORMs is probably due to the additional release of the fumaric acid ester. This probably also explains the observed inhibition of IL-23 levels by FumET-CORM treatment, as this cannot be achieved by incubation with CO alone (Figure 16) [257]. However, contrary to the literature, no or only a mild effect on IL-12p70 levels could be observed in own experiments after CO incubation (Figure 16) [257, 259]. For this purpose, the control substances *rac-8* and *rac-12* were used, which

were not coupled to fumaric acid esters and thus only release CO into the cell following esterase cleavage. The lack of or only slight effect of these substances on the release of inflammatory cytokines is most probably caused by the very low concentration administered.

In summary, the substances that release CO and a fumaric acid ester only within the cell show the most potent biological activity. Especially *rac-7b* has substantial impacts on the HO-1 signaling pathway (Figure 13 and Figure 15). These enhanced effects may be partially due to the different kinetics of esterase cleavage. Thus, in the case of *rac-7a*, a linear release of smaller amounts of CO occurs over a prolonged period of time. In contrast, *rac-7b* rapidly releases higher amounts of CO into the cell [178]. Since the analysis of signaling pathways, in particular in Western blots, only occurs over short periods of 1-2 h, less CO and FAE were likely released into the cell in the case of *rac-7a*. This difference is compensated when observing the cytokine levels. Here a more extended period of 24 h is analyzed, whereby both FumET-CORMs cause an equally potent inhibition of IL-12 and IL-23 (Figure 12 and Figure 16).

Due to their promising efficacy in the performed *in vitro* experiments, the validation of their effectiveness in preclinical mouse models should also be tested in the project's future course. In this context, EAE as an *in vivo* model of multiple sclerosis is particularly suitable. As shown in a previous study by Chora *et al.* the administration of CO by inhalation of the gas led to an improvement of the clinical score in C57BL/6 mice [174]. However, so far, no modulation of cytokine levels in humans could be achieved after inhalation of CO [260]. One explanation for this was discussed in the route of administration. Therefore, in another work, the application of CORMs in an EAE mouse model was performed. Hereby, significant mitigation of disease progression could be achieved by prophylactic administration of the substances [261]. Since the FumET-CORMs used in this work released a fumaric acid ester in addition to CO, and since this ester is already used in the clinical treatment of MS, they should show an even further improved treatment profile compared to the already existing studies. However, this needs to be clarified in further experiments.

As one proposed mechanism of FAE activity in the literature is the inhibition of intracellular glutathione and thus the dysregulation of redox homeostasis, the influence of FumET-CORMS on this system should be investigated in the further course of the work. However, for none of the CORMs applied, a decrease in GSH levels could be

detected (Figure 17). This lack of GSH regulation despite the intracellular release of a fumaric acid ester, at least in the case of *rac-7a* and *rac-7b*, is probably due to the very low concentrations utilized. In comparison, no regulation occurred when the control peptide DMF was incubated with the BMDCs at 25  $\mu\text{M}$ . Only at the common standard concentration of 70  $\mu\text{M}$  significant effects were achieved (Figure 17). However, in contrast to the undetectable regulation of glutathione levels, there was a massive induction of reactive oxygen species after FumET-CORM treatment (Figure 18). This effect was particularly strong for *rac-7b*, probably due to the considerably faster and higher release kinetics of CO than *rac-7a*.

The increased ROS induction compared to the reference substance DMF is presumably caused by the additional carbon monoxide release. Accordingly, the ability of both exogenous and also endogenous CO produced in the mitochondria to induce the production of ROS is well established [179, 262, 263]. This is also reflected through the fact that the sole release of CO by the substances *rac-8* and *rac-12* led to a comparable increase in ROS (Figure 18).

The possible involvement of  $\text{Fe}^{2+}$ , which is released after esterase cleavage, in the formation of reactive oxygen species, should also be mentioned. As described in chapter 1.4.1, this is a pro-oxidative molecule that can contribute to the further formation of ROS, especially the hydroxyl radical, through Fenton reaction. However, this effect could already be counteracted by the CORM-mediated induction of HO-1. The up-regulation of this heme protein leads to ferritin induction, which can trap free iron molecules and thus prevent their pro-oxidative effects [264].

Whether this significantly more robust induction of oxidative stress is also responsible for the improved efficacy of the substances should be investigated in the further course of this thesis. In particular, the causal significance of redox modulation for treatment with the fumaric acid ester DMF was investigated.

## 5.2 ASSESSMENT OF XCT KNOCKOUT MICE AS MODEL SYSTEM FOR ENDOGENOUS ROS STRESS

In order to develop new therapeutic approaches and improve existing therapies, a detailed understanding of the mechanism of action of a drug is indispensable. Therefore, in the second part of this thesis the molecular pathways of DMF treatment should be addressed. In particular, the role of reactive oxygen species and the central ROS-scavenger glutathione were investigated.

From previously published studies it is known that DMF treatment leads to a decrease in intracellular glutathione levels and an increase in reactive oxygen species. Among other things, this induction of oxidative stress has been shown to cause the resulting immune deviation towards an anti-inflammatory type II phenotype [137]. These results could also be reproduced by first experiments in this thesis. DMF treatment led to low GSH levels in BMDCs (Figure 9) and subsequently to an induction of type II DCs via the induction of HO-1 and suppression of the STAT1 signaling pathway (Figure 10).

However, to investigate the importance of oxidative stress, mice with a knockout of the cystine/glutamate antiporter were used as a model system. This antiporter is responsible for the import of cystine into the cell, which is then converted intracellularly into cysteine, where it is essential for the synthesis of glutathione. With the help of this model, the effects of GSH loss are to be specifically simulated, since the disturbed cystine import is expected to result in impaired GSH production, excluding additional off-target effects mediated by pharmacological inhibition of GSH through DMF treatment (Figure 19).

In BMDCs, the knockout of the antiporter could be verified on RNA as well as on protein level (Figure 21). Nonetheless, it was also shown that the knockout does not lead to a change in GSH levels when organs of these mice were analyzed directly *ex vivo* (Figure 22). Thereby, organs with a known low expression of the antiporter, such as liver, lung, heart and kidney, as well as organs with a high expression of the antiporter, such as brain, thymus and spleen, were analyzed [252]. These data are consistent with the observations of a cooperation partner (personal communication) and also with already published literature on the characterization of these mice. For

example, although the analysis of GSH levels in the hippocampus showed an increase in GSH with age, no difference between wildtype and xCT knockout animals could be detected [265]. Also a second manuscript confirms that glutathione levels in liver, cerebrum, cerebellum, thymus and spleen were not decreased in knockout mice. Only in the plasma of the animals a significant inhibition could be found, for which the formation of a cysteine/GSH mixed disulfide (CySSG) is held responsible due to high cysteine concentrations in the plasma [251].

The situation is different, however, when isolated cells of knockout mice are examined *in vitro*. It should be noted that for *in vitro* experiments the cells must be cultivated without  $\beta$ -mercaptoethanol. Otherwise, cystine can be transported into the cell in the form of a mixed disulfide via other amino acid transporters, where it is then once again reduced to 2ME and cysteine. Thus, in the presence of 2ME, the xCT antiporter is bypassed, resulting in normal intracellular glutathione levels (Figure 23) [251]. Throughout this work BMDCs were used for the performed experiments. The protocol for obtaining these cells involves isolating progenitor cells from mouse bone marrow and after a week of cultivation under specific conditions immature DCs can be harvested (Figure 8). However, studies have shown that the presence of 2ME in the cell culture medium is essential for this process of DC isolation. If the cells were cultivated without this agent, the number of cells that could be harvested was significantly reduced and only a very small percentage of these cells were positive for the DC marker CD11c (Figure 20). For this reason, 2ME was added to the culture for the duration of the seven days during the differentiation of the DCs. After harvesting the immature BMDCs, the medium was changed to one with or without 2ME (Figure 24). It was found that at least a culture of 8 h or better 24 h is required to achieve the expected decrease of intracellular GSH levels. Furthermore, only in knockout, but not in wildtype DCs, an increase in ROS was observed when cultivating in medium without 2ME (Figure 23). Thus, the effects of xCT knockout on redox homeostasis are comparable to DMF treatment, which also results in an inhibition of GSH and induction of ROS (Figure 9) [137]. However, there is a big difference in the kinetics of these effects. Under DMF treatment a rapid decrease of intracellular GSH with a peak after about 3 h and a subsequent increase even beyond the original levels takes place [266, 267]. In contrast, a decrease in intracellular GSH levels in xCT knockout cells was detectable after 8 h at the earliest, since glutathione is not actively scavenged as in the case of DMF treatment. Instead, no new synthesis of the molecule can be performed. Furthermore, the decline in

glutathione levels persists over a long period of time, is not reversed and ultimately results in cell death.

Considering these results, the knockout of the cystine/glutamate antiporter is a valid model for the analysis of the influence of glutathione deficiency and the resulting induced oxidative stress for *in vitro* experiments. However, there are some limitations for the use of this model in *in vivo* experiments. For example, the fundamental assumption, namely an inhibition of intracellular GSH, cannot be effectively demonstrated. It is possible that *in vivo* the antiporter loss is compensated by other cystine or cysteine transporters, such as system alanine-serine-cysteine (ASC), system L or system X<sub>AG</sub> [268, 269]. For the performance of *in vivo* experiments it should therefore be considered to select another mouse model in which the required glutathione deficiency can also be detected in the tissue. One possibility would be the utilization of mice with a knockout of the catalytic subunit of glutamate cysteine ligase (GCLC) [270].

Moreover, on completion of the experimental work for this thesis, it was discovered that the utilized xCT knockout mice exhibit a mixed background of C57BL/6J and C57BL/6N. Since the genetic background of a mouse line can have a significant influence on the course of different disease models, backcrossing to, for example, a C57BL/6J background should be performed before further use of these mice. This fact should also be kept in mind when interpreting the *in vitro* experiments in this work and especially when comparing them with the wildtype controls, for which BMDCs from C57BL/6J mice were isolated.

### 5.3 THE RELEVANCE OF REDOX HOMEOSTASIS FOR EFFECTIVE DMF TREATMENT

After validation of the use of xCT knockout cells as a model system for glutathione deficiency *in vitro*, these BMDCs were used to investigate the relevance of redox homeostasis for successful DMF treatment. T cell-mediated autoimmune diseases such as multiple sclerosis or psoriasis are associated with an aberrant induction of T<sub>h</sub>1/T<sub>h</sub>17 cells. The aim of many therapeutic approaches, such as treatment with FAEs, is therefore to achieve an immune deviation towards an anti-inflammatory T<sub>h</sub>2 cell



population in order to positively influence the course of the disease [91, 135-137, 256]. This shift towards a T<sub>H</sub>2 dominated phenotype is based on the previous induction of type II DCs, featuring specific characteristics like strongly reduced secretion of inflammatory cytokines such as IL-12p70 or IL-23. Studies showed that treatment with DMF leads to a decrease in intracellular glutathione levels in both patients and dendritic cells *in vitro*. Furthermore, all these effects could be reversed by treatment with different antioxidants (NAC, GSH-OEt). Because of this it is likely that the inhibition of GSH and subsequent induction of oxidative stress is a central mechanism of action of DMF treatment [137].

It has also been shown that signal transduction by the induction and nuclear translocation of HO-1 and the inhibition of STAT1 phosphorylation is responsible for the regulation of IL-12p70 and IL-23 expression [137]. Therefore, the following analyses focused on these two signaling pathways. Contrary to the results obtained with DMF treatment, inhibition of intracellular GSH was not sufficient to achieve a modulation of these signal transduction molecules. No differences in HO-1 or pSTAT1 levels could be detected in knockout BMDCs cultivated with or without 2ME (Figure 25). Treatment of these cells with NAC, which is intracellularly cleaved to cysteine, did not show any effect on protein levels either (Figure 25). However, an additional treatment of knockout BMDCs, cultivated in the absence of 2ME, with DMF leads to the expected HO-1 induction and a strong attenuation of pSTAT1 (Figure 26 and Figure 27). Since these cells already exhibit depleted GSH levels, the modifications may result from additional off-target effects of DMF treatment. Examination of downstream regulated IL-12p70 and IL-23 showed a consistent pattern. Inhibition of GSH alone was not sufficient to result in a decrease of inflammatory cytokines. Instead the effects could be achieved by addition of DMF (Figure 28). There are several possible explanations for these findings. First, it may simply be that the role of oxidative stress is not the central mechanism of DMF-mediated immunodeviation towards a DC type II phenotype. However, it is also possible that in cells with an xCT knockout the effects from induced ROS stress are compensated by other signaling pathways supporting the maintenance of cellular redox homeostasis. Potential compensation mechanisms are discussed in chapter 5.4. Furthermore, it must be considered that glutathione inhibition is not the only therapeutic effect following DMF treatment, but rather involves the modification of many other targets, which may also be required for the induction of type II DCs. This question is addressed in more detail in chapter 5.5.

The fact that a single knockout of the cystine/glutamate antiporter and alterations in redox homeostasis are not sufficient to reproduce the protective effects of DMF treatment is also evident when observing the course of experimental autoimmune encephalomyelitis (EAE), an established model of multiple sclerosis in mice. Treatment with DMF can protect the animals from developing severe EAE due to an anti-inflammatory  $T_H2$  response [136, 137]. However, this ameliorated course of EAE is not observed in xCT knockout animals. This could be demonstrated by own experiments of the research group (data not shown), but is also shown in a published study [271]. In this paper no difference in the course of an EAE between wildtype C57BL/6 and xCT knockout animals was found. Only after bone marrow transplantation from knockout animals a slightly decreased EAE score was observed on two days of disease progression. However, there was no difference in demyelination or infiltration and activation of microglia. Overall, in accordance with own *in vitro* data, the data suggest that the genetic loss of glutathione alone is not sufficient to simulate effects of DMF treatment.

To further investigate the influence of reactive oxygen species, experiments were also conducted in GP91 knockout cells. This is a subunit of NADPH oxidase, the loss of which should result in a disrupted generation of ROS. If ROS was relevant for DMF treatment, no induction of type II DCs should occur in knockout cells after incubation with the fumaric acid derivative. However, in GP91 knockout BMDCs an unchanged modulation of the HO-1 and STAT1 signaling pathway as well as an inhibition of IL-12p70 and IL-23 could be induced in comparison to wildtype cells by DMF treatment (Figure 38 and Figure 39). However, in contrast to the predicted signaling pathway, DMF strongly increased free ROS in BMDCs (Figure 40). This result is surprising, since in experiments performed by the cooperation partner who provided the mice, no ROS induction was detected in knockout animals [272]. A possible explanation for the continued production of reactive oxygen species could include that NADPH oxidases might play only a minor role in DMF-induced ROS generation in dendritic cells. This is supported by the fact that dendritic cells produce significantly less ROS via NOX2 as compared to other phagocytes like macrophages or neutrophils [198]. Alternatively, the ROS production may occur predominantly via other pathways, for example, in the mitochondria. Indeed, there are conflicting studies that show that despite GP91 loss, ROS production remains unchanged [273]. Therefore,

the use of this model as a control to study redox dependency in BMDCs is problematic and requires further investigation.

As a justification for a ROS-dependency of DMF treatment, inversion of the effects by antioxidant treatment is usually mentioned [137]. This inhibition of DC type II induction could also be observed in own experiments (Figure 9 and Figure 10). One of the main effects of fumarates in general and DMF in particular is the covalent modification of free cysteine or of cysteine residues in proteins, the so-called succination. This chemical reaction occurs non-specifically in the cell and is irreversible [274]. For instance, also in the case of glutathione there is a decrease in detectable levels due to covalent binding of DMF to the tripeptide [275]. It should now be noted that frequently used antioxidants such as NAC or GSH-OEt also contain a modifiable cysteine residue [276]. It is therefore conceivable that the effects after treatment with these antioxidant control substances may not be due to the prevention of DMF-induced ROS induction, but due to scavenging of the fumarate by covalent binding before it can initiate alterations in the cell.

The central question is whether GSH inhibition and induction of reactive oxygen species is a direct causality or a secondary phenomenon of effective DMF treatment. There is ample evidence for both, which makes a final judgement difficult. An essential mechanism for successful treatment and prevention of  $T_h1/T_h17$  mediated autoimmune diseases such as multiple sclerosis or psoriasis is the induction of a  $T_h2$  cell response. However, many different mechanisms are possible for the induction of this immune deviation. For example, treatment with curcumin leads to an improvement of EAE together with the induction of HO-1. However, instead of the phosphorylation of STAT1, the phosphorylation of STAT3 is a crucial parameter [254]. There are also contradictory publications on the role of curcumin on glutathione levels. After treatment with the substance, both inhibition and induction of GSH could be demonstrated [277-279]. However, no effect on glutathione was found in the work with curcumin in our own group, which suggests a redox-independent mechanism (personal communication). As a further substance with anti-inflammatory properties, itaconate should be mentioned. Treatment with itaconate has many similarities with effects caused by DMF incubation. For instance, it also induces HO-1 and inhibits inflammatory cytokines such as IL-12 or IL-6 [280-282]. In contrast to DMF, however, itaconate treatment leads to a

significant decrease in ROS levels [280]. This again would be an indication for redox independence of the therapeutic process.

A property that DMF, curcumin and itaconate have in common is that they are considered to be Nrf2 activators. Nrf2 is regarded as an important regulator of many different mechanisms involved in cellular antioxidant defense. The fact that all these Th2 inducing substances also influence the Nrf2 signaling pathway suggests that redox homeostasis is of importance in this context. However, own analyses of BMDCs did not show an increase in Nrf2 protein after DMF treatment (data not shown), but an increase on the mRNA level (Figure 29 and Figure 31). This induction did not take place in xCT knockout cells, although the difference between treated wildtype and knockout BMDCs was not significant. Furthermore, there are conflicting publications in the literature on the dependence of DMF treatment on Nrf2 [141-143, 283]. A more detailed discussion of this issue is presented in the following chapter.

## 5.4 POSSIBLE COMPENSATORY MECHANISMS UNDER ENDOGENOUS ROS STRESS

An emerging question in the course of this thesis was whether DC type II induction in xCT knockout cells does not occur due to overcompensation by other redox signaling pathways. Since strict control of intracellular ROS levels is crucial for cellular survival, buffering of glutathione loss by one or more alternative pathways would be highly likely. As mentioned above, Nrf2 is one of the central regulators of many different antioxidant proteins and signaling pathways. Therefore, the importance of this transcription factor for DMF treatment will be briefly discussed below.

Conflicting opinions on this topic can be found in the literature. On the one hand, an Nrf2 dependency of DMF treatment has been observed [141, 142, 284]. However, publications exist showing the opposite as well [143, 283, 285]. Fumarates act as Nrf2 activators by inactivating its inhibitor kelch-like ECH-associated protein 1 (KEAP1) through modification of its cysteine residues [141, 286]. Thus, after DMF treatment, the induction of the transcription factor could be observed. In this work, Linker *et al.* observed an impaired DMF-mediated therapeutic efficiency in Nrf2 knockout mice suffering from EAE [141]. From this, an Nrf2 dependency of DMF

treatment was concluded. However, the treatment of chronic EAE was investigated using an attenuated protocol in the Nrf2 knockout mice, as these mice show a more severe disease course. Another study, which focused on the acute phase of EAE, found no differences in DMF-mediated effects between wildtype and knockout animals. Thus, in both lines, induction of type II monocytes with a typical cytokine profile with low levels of IL-12/23 (p40) and IL-6 occurred and protective effects of DMF in Nrf2-deficient animals were observed concerning EAE development [143].

This demonstrates that although induction of transcription factor occurs after fumarate treatment, its causative role in successful treatment needs further investigation. Similar to own data on ROS-dependence, it is possible that the activation of Nrf2 as a redox modulator partly contributes to DMF treatment. However, the knockout alone might not be sufficient to induce immune deviation towards type II dendritic cells and thus protect against the development of EAE.

In order to address this question, it was considered to establish a new transgenic mouse line with a knockout of both the cystine/glutamate antiporter and Nrf2. However, this particular double knockout mouse would be redundant. As a key player, Nrf2 plays a role in the regulation of many redox signaling pathways. Thereby, the transcription factor also controls the expression of many genes involved in the glutathione system, such as GCLC, GCLM, GPX2, GPX4 and even the xCT antiporter gene SLC7a11 [287]. Accordingly, the knockdown of Nrf2 alone already leads to a loss of cystine/glutamate antiporter expression on the RNA and protein levels [288]. Furthermore, Nrf2 knockout mice exhibit diminished glutathione levels [289]. Also, own analyses of Nrf2 knockout BMDCs showed a significant decrease in intracellular GSH levels comparable to DMF treatment or xCT knockout cells (data not shown). A further knockout of the glutathione system in Nrf2-deficient animals is therefore not required and would probably not provide new insights as to the investigation of a single Nrf2 knockout. Instead, an adequate second target should be chosen, which is not already modulated by the Nrf2 loss.

Nevertheless, in the context of tumor development, it has been shown that the blockage of multiple redox pathways is necessary to result in biological effects. Thereby, only the inhibition of both the glutathione and thioredoxin systems caused cancer cell death [290].

To investigate the possible involvement of the thioredoxin signaling pathway in the cystine/glutamate antiporter knockout cells, both redox pathways were simultaneously inactivated. To verify this theory before the extensive generation of a double-transgenic mouse line, auranofin, a pharmacological inhibitor of thioredoxin reductase, was applied in experiments. However, the inhibitor alone is already capable of inhibiting IL-12p70 and inducing a T<sub>h</sub>2 response [253]. Therefore, an initial titration was performed to the lowest possible auranofin concentrations at which these effects are not yet observed in wildtype cells. This study's objective was to determine whether xCT knockout BMDCs would be more sensitive to the loss of the thioredoxin pathway compared to wildtype cells. However, this could only be seen concerning the toxicity of the inhibitor. Increasing concentrations of auranofin in knockout BMDCs quickly resulted in cell death, whereas no toxicity was observed in wildtype cells (Figure 32). This showed that the thioredoxin signaling pathway acts as an important backup mechanism in xCT knockout cells already stressed by LPS. If this pathway is also deactivated, the cells die rapidly.

However, this increased sensitivity could not be confirmed in further experiments on BMDC differentiation. No immune deviation towards a type II phenotype of dendritic cells with low proinflammatory IL-12p70 and IL-23 levels could be induced (Figure 35). The fact that the known inhibition of IL-12p70 was not observed in the wildtype cells is attributable to the significantly lower concentrations administered. This effect has only been observed in the literature at concentrations starting at 0.5 µg/ml or 1 µg/ml auranofin [253]. In own experiments, we only used ten times lower dosage levels at which no toxic effects were observed in the knockout BMDCs. Despite the only very low auranofin concentrations, complete inhibition of thioredoxin reductase was observed (Figure 33). Taken together, these experiments show that even a double deficiency, both in the glutathione and thioredoxin pathway, is not sufficient to achieve the immune deviation observed in DMF treatment towards type II dendritic cells. It could also be shown that in xCT knockout cells, no overcompensation through the thioredoxin pathway occurs. In the case of a possible compensation, increased basic levels of players in this signaling pathway, such as thioredoxin reductase, would be expected. However, this is not the case. No evidence for this was found by analysis of the RNA levels of thioredoxin reductase (Figure 29 and Figure 31). In contrast, xCT knockout BMDCs even depict a marked decrease in the enzymes activity (Figure 33).

## 5.5 FURTHER CELLULAR IMPLICATIONS ASSOCIATED WITH FUMARATE TREATMENT

Although overcompensation by various redox paths cannot be excluded in the previous chapter, there must be further reasons for the lack of DC type II induction in the xCT knockout system. It was shown that the knockout of the antiporter alone is not sufficient to cause changes in, for instance, the cytokine levels (Figure 28). However, even more important is the fact that xCT knockout BMDCs still showed the typical DMF-mediated effects, even though these cells already showed a loss of glutathione and an associated ROS induction (Figure 23). This indicates that DMF must have other targets in addition to the ROS scavenger that act independently of ROS induction to mediate these effects.

One example would be the interaction of DMF with the IL-1R-associated kinase (IRAK) 4-MyD88 complex. IRAK4 is a protein kinase that is involved in TLR-mediated signaling pathways of the immune response. Treatment with DMF leads to the direct modification of a cysteine residue by the fumaric acid ester. This prevents the kinase from binding to MyD88, resulting in disturbed downstream signaling [283].

It is precisely these cysteine residues that can become the target of many posttranslational modifications. One of them is the so-called succination, whereby the sulfhydryl group reacts with endogenous or exogenous fumarates. In this process, an S-(2-succino)cysteine compound is formed, whereby the latter can either be formed with free cysteine or with cysteine groups that are located, for example, in active centers of enzymes. It is also assumed that the reaction is irreversible due to the stability of the formed product [276, 291]. The interactions between DMF and glutathione also results from this process of succination [138].

However, the modification of sulfhydryl groups is not limited to proteins of the redox signaling pathways. Depending on the model system chosen, numerous possible active cysteine residues susceptible to succination by fumarates could be found. Thus, the analysis in a knockout model system led to the identification of 94 succinated proteins, most of which were involved in metabolic processes [292].

Another study in T cells even identified more than 2400 DMF sensitive cysteine residues, although only a small fraction was altered by fumarate treatment. This

included the protein kinase C theta (PKC $\theta$ ), which blocked the association with the costimulatory receptor CD28 and thus influenced T cell activation [293].

Succination by DMF was also investigated in a study by Kornberg *et al.* They attributed the anti-inflammatory effects of DMF to GAPDH and aerobic glycolysis inhibition. Once again, a redox-independent mechanism was demonstrated, whereby the immunological effects of DMF treatment, such as the attenuation of an EAE *in vivo*, could be reproduced using a GAPDH inhibitor [294].

Accordingly, the succination of proteins represents an already well-characterized possibility of posttranslational modification by DMF. Thereby, reaction with proteins and enzymes of the redox system can occur, as in the case of the DMF-mediated inhibition of the Nrf2 inhibitor, KEAP1, already described in the previous chapter [295]. Succination through fumarates is not limited to these antioxidative signaling pathways but also interferes with metabolism, immune cell activation and many other cellular processes. Therefore, DMF treatment's mechanism of action probably cannot be limited to one single signaling pathway. As observed in own experiments, the sole inhibition of redox signaling pathways and the induction of oxidative stress is insufficient to replicate DMF-mediated modulations in dendritic cells (Figure 26-Figure 28). Rather, a variety of additional fumarate targets are likely to be important for the induction of these anti-inflammatory effects.



## 5.6 CONCLUSIONS AND PERSPECTIVES

In the first part of the study, new CO and fumaric acid ester releasing substances should be biologically characterized and evaluated for their potential suitability as anti-inflammatory drugs. Indeed, the two FumET-CORMs *rac-7a* and *rac-7b* showed promising modulations of the HO-1 and STAT1 signaling pathways and induced potent anti-inflammatory effects in dendritic cells. This resulted in a significant induction of the HO-1 signaling pathway with simultaneous inhibition of STAT1 phosphorylation. The inflammatory cytokines IL-12p70 and IL-23, regulated by these signaling pathways, were also strongly diminished. It should be noted that the induced effects were significantly stronger than those of DMF treatment alone. Accordingly, the effects listed above occurred at considerably lower concentrations of FumET-CORMs compared to single DMF treatment. Thereby it seems to be essential that CO and the fumaric acid ester are released within the cell. Only the enzyme-triggered molecules could induce the anti-inflammatory effects described above, whereas the non-activated substances *rac-5* and **8** showed very limited biological activity. As the next step for further characterization of these promising compounds, it should be investigated whether these FumET-CORM-induced type II dendritic cells also lead to an immune deviation towards a T<sub>h</sub>2 response. This shift is essential for the treatment of T<sub>h</sub>1/T<sub>h</sub>17-mediated autoimmune diseases. Accordingly, the efficacy of *rac-7a* and *rac-7b* should also be investigated in a corresponding *in vivo* model, such as EAE.

In the further course of the work, the more detailed DMF treatment mechanism was investigated. In particular, the dependency on oxidative stress induction should be clarified. For this purpose, a cystine/glutamate antiporter knockout model was employed. It was shown that the knockout of this antiporter led to a specific attenuation of intracellular glutathione levels and, thus, to the induction of reactive oxygen species. The present study provides evidence that this state of oxidative stress alone is not sufficient to convert dendritic cells to the expected type II phenotype. Instead, the additional treatment of these cells with DMF still resulted in the modulation of HO-1 and STAT1 signaling pathways and subsequent inhibition of the inflammatory cytokines IL-12p70 and IL-23.

Consequently, additional effects of the fumarate, besides the induction of oxidative stress, probably play an important role in the induction of type II BMDCs.

The possibility of overcompensation by other redox signaling pathways was also considered. However, even by additional inhibition of the thioredoxin signaling pathway by auranofin, no immune deviation towards an anti-inflammatory phenotype of dendritic cells could be achieved. In conclusion, the inhibition of glutathione and ROS induction by knockout of the cystine/glutamate antiporter alone is insufficient to reproduce the anti-inflammatory effects of DMF treatment. It is likely that, in addition to the induction of oxidative stress, other fumarate objectives, such as the modulation of proteins in the cell metabolism, play a significant role in mediating its mechanisms of action. However, in order to be able to make a more precise statement on this, possible overcompensation by other redox pathways should be excluded in xCT knockout cells by further experiments, as in the present study, this was only achieved for the thioredoxin signaling pathway. Therefore, a more detailed investigation of the interaction between GSH levels, ROS levels and antioxidant molecules like e.g. Nrf2 is also needed in the future.

## 6 ABBREVIATIONS

%	Percent
°C	Degree Celsius
µg	Microgram
µl	Microliter
µM	Micromolar
2ME	β-mercaptoethanol
2VP	2-Vinylpyridine
aa	Amino acid
APC	Antigen presenting cell
APS	Ammonium persulfate
Atg4	Autophagy-related protein 4
ATP	Adenosine triphosphate
Batf3	Basic leucine zipper transcription factor ATF-like 3
BCA	Bicinchoninic acid
BMDC	Bone marrow-derived dendritic cell
bp	Base pair
BSA	Bovine serum albumin
CCL	CC-chemokine ligand
CCR	CC-chemokine receptor
CD	Cluster of differentiation
cDC	Classical DCs
cDNA	Complementary DNA
CDP	Common DC precursor
cGMP	Cyclic guanosine monophosphate
cm	Centimeter
CNS	Central nervous system
CO	Carbon monoxide
CO <sub>2</sub>	Carbon dioxide
COHb	Carboxyhemoglobin
CORM	CO-releasing molecule
DCFDA	2',7' -dichlorofluorescein diacetate
DMEM	Dulbecco's Modified Eagle's Medium
DMF	Dimethyl fumarate
DMSO	Dimethyl sulfoxide
DNA	Deoxyribonucleic acid
dNTP	Deoxynucleoside triphosphate
DTNB	5,5'-dithiobis-2-nitrobenzoic acid
E2-2	E-protein transcription factor 4
EDTA	Ethylenediamine tetraacetic acid
ELISA	Enzyme-linked Immunosorbent Assay
ER	Endoplasmic reticulum
ERK	Extracellular signal-regulated kinase

Ero1 $\alpha$	ER oxidoreductin
ET-CORM	Enzyme-triggered CO-releasing molecule
EtOH	Ethanol
FAD	flavin adenine dinucleotide
FAE	Fumaric acid ester
FCS	Fetal calf serum
Flt3	Fms-related tyrosine kinase 3
FumET-CORM	Fumarate-derived iron carbonyl complexes
g	Gram
GAPDH	Glyceraldehyde 3-phosphate dehydrogenase
GCLC	Glutamate-cysteine ligase catalytic subunit
GCLM	Glutamate-cysteine ligase regulatory subunit
GM-CSF	Granulocyte-macrophage colony-stimulating factor
GPX	Glutathione peroxidase
GR	Glutathione reductase
GSH	Glutathione
GSSG	Glutathione disulfide
h	Hour
H <sub>2</sub> O	Water
H <sub>2</sub> O <sub>2</sub>	Hydrogen peroxide
HCl	Hydrochloric acid
HIF-1 $\alpha$	Hypoxia-inducible factor 1-alpha
HO $\cdot$	Hydroxyl radical
HO-1	Heme oxygenase 1
HSC	Hematopoietic stem cell
Id2	E-protein inhibitor of DNA binding 2
IFN	Interferon
IL	Interleukin
IRAK	IL-1R-associated kinase
Irf	Interferon regulatory factor
JNK	C-Jun N-terminal kinase
kb	Kilobases
KCl	Potassium chloride
kDa	Kilodalton
KEAP1	Kelch-like ECH-associated protein 1
Klf4	Kruppel-like factor 4
KO	Knockout
LDH	Lactate dehydrogenase
LPS	Lipopolysaccharide
M	Molar
mA	Milliampere
MAPK	Mitogen-activated protein kinase
MBP	Myelin basic protein
MD-2	Myeloid differentiation factor-2
MDP	Macrophage and DC precursor
MeOH	Methanol

MgCl <sub>2</sub>	Magnesium chloride
MHC	Major histocompatibility complex
min	Minute
ml	Milliliter
mM	Millimolar
MMF	Monomethyl fumarate
MOG	Myelin oligodendrocyte glycoprotein
mol	Mole
MP	Myeloid precursor
mRNA	Messenger RNA
MS	Multiple sclerosis
mtDNA	Mitochondrial DNA
mtROS	Mitochondrial reactive oxygen species
MyD88	Myeloid differentiation primary response gene 88
NAC	N-acetyl-L-cysteine
NaCl	Sodium chloride
β-NADPH	β-Nicotinamide adenine dinucleotide 2'-phosphate
NaOH	Sodium hydroxide
NF-κB	Nuclear factor kappa-light-chain-enhancer of activated B cells
ng	Nanogram
nM	Nanomolar
Notch-2	Neurogenic locus notch homolog protein 2
NOX	NADPH oxidase
NP-40	Nonidet™ P 40 Substitute
Nrf2	Nuclear factor erythroid 2-related factor 2
O <sub>2</sub>	Oxygen
O <sub>2</sub> <sup>·-</sup>	Superoxide radical
PAMP	Pathogen-associated molecular pattern
PBS	Phosphate-buffered saline
PCR	Polymerase chain reaction
pDC	Plasmacytoid DCs
PDI	Protein disulfide isomerase
PI3K	phosphoinositide 3-kinase
PKCθ	protein kinase C theta
PLP	Myelin proteolipid protein
PPARγ	Peroxisome proliferator-activated receptor gamma
PPMS	Primary progressive multiple sclerosis
pre-cDC	Pre-classical dendritic cells
PRR	Pattern recognition receptor
pSTAT1	Phosphorylated signal transducer and activator of transcription 1
qRT-PCR	Quantitative real-time PCR
rcf	Relative centrifugal force
RNA	Ribonucleic acid
RNase	Ribonuclease
RORγt	Receptor-related orphan receptor γ-T
ROS	Reactive oxygen species
rpm	Rounds per minute

RRMS	Relapsing-remitting multiple sclerosis
RT	Room temperature
SD	Standard deviation
SDS	Sodium dodecyl sulfate
SDS-PAGE	Sodium dodecyl sulfate–polyacrylamide gel electrophoresis
sec	Second
sGC	Soluble guanylyl cyclase
SLC7a11	gene encoding the Cystine-Glutamate antiporter
SOD	Sodium dismutase
SPMS	Secondary progressive multiple sclerosis
SSA	Sulfosalicylic acid
STAT	Signal transducer and activator of transcription
T-bet	T-box expressed in T cells
TBS	Tris-buffered saline
TCR	T cell receptor
TEA	Triethanolamine
TEMED	Tetramethylethylenediamine
TGF- $\beta$	Transforming growth factor beta
T <sub>h</sub>	T helper cell
TIRAP	TIR domain-containing adaptor protein
TLR	Toll-like receptor
TNF	Tumor necrosis factor
TRAM	TRIF-related adaptor molecule
TRIF	TIR domain-containing adaptor inducing IFN- $\beta$
Trx	Thioredoxin
TrxR	Thioredoxin Reductase
U	Units
V	Volt
v/v	Volume per volume
w/v	Weight per volume
WT	Wildtype
xCT	Cystine-Glutamate antiporter

## 7 ACKNOWLEDGMENTS

Without the support of numerous people, my thesis could not have been realized in this form. I would like to take this opportunity to express my sincere gratitude for the help I received in many ways.

First and foremost, I would like to thank my supervisor, Prof. Dr. Martin Röcken, for giving me the opportunity to work on my thesis in the laboratories of the University Department of Dermatology and to become a part of his research group. I appreciate his trust to hire me for this interesting project, as well as my scientific training and professional input over all these years.

Secondly, I would like to take this opportunity to thank Prof. Dr. Robert Feil. His constructive suggestions, as well as the effortful work of proofreading, were of great help in the preparation of this thesis. Additionally, I greatly appreciate that Prof. Dr. Stefan Laufer and Prof. Dr. Thilo Stehle agreed to be examiners in my defense committee.

I would like to thank Prof. Dr. Thomas Wieder for his help with all my questions, for arranging and coordinating the joint project with the research group of Prof. Dr. Hans-Günther Schmalz and for the nice conversations during lunch breaks. I thank him and also Dr. Heidi Braumüller for their continuously sympathetic ear and guidance with all scientific matters.

One of the best experiences in this chapter of my life was the great atmosphere at the Röntgenweg. For that, I would like to thank all my colleagues. In particular Susanne Weidemann for her strict regime in the lab, apple tastings, the numerous nice talks and her amusing way of underlining each conversation with funny noises. Much appreciation to Max and Nadine aka the "Fensterbank-Crew". We were the tough core of the PhD room and together several long days became much more enjoyable. A very big thank you also goes out to Ellen, Katharina and Nadine, for the countless engaging debates and ideas (scientific and non-scientific) that have been instrumental in creating the thesis in its present form. Because of all of you, this time became not only a job, but a great life experience with many great memories and I am happy to be able to not only call you my colleagues, but also my friends.

Last but definitely not least, my highest gratitude goes to my parents for their unconditional support during my entire life journey. You have always been there for me and have been a great support and encouragement in many ways throughout all these years.



## 8 LITERATURE

1. Chaplin, D.D., *Overview of the immune response*. J Allergy Clin Immunol, 2010. **125**(2 Suppl 2): p. S3-23.
2. Murphy, K. and C. Weaver, *Janeway's Immunobiology*. Vol. 9th revised edition. 2016, New York: W. W. Norton & Company. 1-904.
3. Takeuchi, O. and S. Akira, *Pattern recognition receptors and inflammation*. Cell, 2010. **140**(6): p. 805-20.
4. Medzhitov, R., P. Preston-Hurlburt, and C.A. Janeway, *A human homologue of the Drosophila Toll protein signals activation of adaptive immunity*. Nature, 1997. **388**: p. 394-397.
5. Rock, F.L., et al., *A family of human receptors structurally related to Drosophila Toll*. PNAS, 1998. **95**(2): p. 588-593.
6. Poltorak, A., et al., *Defective LPS Signaling in C3H/HeJ and C57BL/10ScCr Mice: Mutations in Tlr4 Gene*. Science, 1998. **282**(5396): p. 2085-2088.
7. Kawai, T., et al., *Unresponsiveness of MyD88-Deficient Mice to Endotoxin*. Immunity, 1999. **11**(1): p. 115-122.
8. Hu, W., et al., *Differential outcome of TRIF-mediated signaling in TLR4 and TLR3 induced DC maturation*. Proc Natl Acad Sci U S A, 2015. **112**(45): p. 13994-9.
9. Yamamoto, M., et al., *Essential role for TIRAP in activation of the signalling cascade shared by TLR2 and TLR4*. Nature, 2002. **420**: p. 324-329.
10. Yamamoto, M., et al., *TRAM is specifically involved in the Toll-like receptor 4-mediated MyD88-independent signaling pathway*. Nat Immunol, 2003. **4**(11): p. 1144-50.
11. Kuper, C., F.X. Beck, and W. Neuhof, *Toll-like receptor 4 activates NF-kappaB and MAP kinase pathways to regulate expression of proinflammatory COX-2 in renal medullary collecting duct cells*. Am J Physiol Renal Physiol, 2012. **302**(1): p. F38-46.
12. Chien, Y.-h., et al., *Somatic recombination in a murine T-cell receptor gene*. Nature, 1984. **309**(5966): p. 322-326.
13. Siu, G., et al., *The human t cell antigen receptor is encoded by variable, diversity, and joining gene segments that rearrange to generate a complete V gene*. Cell, 1984. **37**(2): p. 393-401.
14. Turner, J.E., et al., *The Th17 immune response in renal inflammation*. Kidney Int, 2010. **77**(12): p. 1070-5.
15. Hu, X., et al., *Sensitization of IFN-gamma Jak-STAT signaling during macrophage activation*. Nature Immunology, 2002. **3**(9): p. 859-866.
16. Bradley, L.M., D.K. Dalton, and M. Croft, *A direct role for IFN-gamma in regulation of Th1 cell development*. The Journal of Immunology, 1996. **157**(4): p. 1350-1358.
17. Scott, P., *IFN-gamma modulates the early development of Th1 and Th2 responses in a murine model of cutaneous leishmaniasis*. The Journal of Immunology, 1991. **147**(9): p. 3149-3155.
18. Jacobson, N.G., et al., *Interleukin 12 signaling in T helper type 1 (Th1) cells involves tyrosine phosphorylation of signal transducer and activator of transcription (Stat)3 and Stat4*. J Exp Med, 1995. **181**(5): p. 1755-1762.

19. Ma, D., H. Huang, and Z. Huang, *STAT1 signaling is required for optimal Th1 cell differentiation in mice*. Chinese Science Bulletin, 2010. **55**(11): p. 1032-1040.
20. Lawless, V.A., et al., *Stat4 Regulates Multiple Components of IFN- $\gamma$ -Inducing Signaling Pathways*. The Journal of Immunology, 2000. **165**(12): p. 6803-6808.
21. Afkarian, M., et al., *T-bet is a STAT1-induced regulator of IL-12R expression in naïve CD4+ T cells*. Nature Immunology, 2002. **3**(6): p. 549-557.
22. Szabo, S.J., et al., *A novel transcription factor, T-bet, directs Th1 lineage commitment*. Cell, 2000. **100**(6): p. 655-69.
23. Röcken, M., et al., *Central role for TCR/CD3 ligation in the differentiation of CD4+ T cells toward a Th1 or Th2 functional phenotype*. The Journal of Immunology, 1992. **148**(1): p. 47-54.
24. Seder, R.A., et al., *CD28-mediated costimulation of interleukin 2 (IL-2) production plays a critical role in T cell priming for IL-4 and interferon gamma production*. J Exp Med, 1994. **179**(1): p. 299-304.
25. Zheng, W. and R.A. Flavell, *The transcription factor GATA-3 is necessary and sufficient for Th2 cytokine gene expression in CD4 T cells*. Cell, 1997. **89**(4): p. 587-96.
26. Pai, S.-Y., M.L. Truitt, and I.-C. Ho, *GATA-3 deficiency abrogates the development and maintenance of T helper type 2 cells*. Proceedings of the National Academy of Sciences, 2004. **101**(7): p. 1993-1998.
27. Ye, P., et al., *Requirement of Interleukin 17 Receptor Signaling for Lung Cxc Chemokine and Granulocyte Colony-Stimulating Factor Expression, Neutrophil Recruitment, and Host Defense*. Journal of Experimental Medicine, 2001. **194**(4): p. 519-528.
28. Rudner, X.L., et al., *Interleukin-23 (IL-23)-IL-17 Cytokine Axis in Murine Pneumocystis carinii Infection*. Infection and Immunity, 2007. **75**(6): p. 3055-3061.
29. Veldhoen, M., et al., *TGF $\beta$  in the Context of an Inflammatory Cytokine Milieu Supports De Novo Differentiation of IL-17-Producing T Cells*. Immunity, 2006. **24**(2): p. 179-189.
30. Bettelli, E., et al., *Reciprocal developmental pathways for the generation of pathogenic effector TH17 and regulatory T cells*. Nature, 2006. **441**(7090): p. 235-238.
31. Yang, X.O., et al., *STAT3 Regulates Cytokine-mediated Generation of Inflammatory Helper T Cells*. Journal of Biological Chemistry, 2007. **282**(13): p. 9358-9363.
32. Yang, X.O., et al., *T Helper 17 Lineage Differentiation Is Programmed by Orphan Nuclear Receptors ROR $\alpha$  and ROR $\gamma$* . Immunity, 2008. **28**(1): p. 29-39.
33. Aggarwal, S., et al., *Interleukin-23 Promotes a Distinct CD4 T Cell Activation State Characterized by the Production of Interleukin-17*. Journal of Biological Chemistry, 2003. **278**(3): p. 1910-1914.
34. Mangan, P.R., et al., *Transforming growth factor- $\beta$  induces development of the TH17 lineage*. Nature, 2006. **441**(7090): p. 231-234.
35. Zhou, L., et al., *IL-6 programs TH-17 cell differentiation by promoting sequential engagement of the IL-21 and IL-23 pathways*. Nature Immunology, 2007. **8**(9): p. 967-974.
36. Ghoreschi, K., et al., *Generation of pathogenic T(H)17 cells in the absence of TGF- $\beta$  signalling*. Nature, 2010. **467**(7318): p. 967-971.

37. Ohnmacht, C., et al., *Constitutive ablation of dendritic cells breaks self-tolerance of CD4 T cells and results in spontaneous fatal autoimmunity*. The Journal of experimental medicine, 2009. **206**(3): p. 549-559.
38. Jung, S., et al., *In Vivo Depletion of CD11c+ Dendritic Cells Abrogates Priming of CD8+ T Cells by Exogenous Cell-Associated Antigens*. Immunity, 2002. **17**(2): p. 211-220.
39. Gilliet, M., et al., *The Development of Murine Plasmacytoid Dendritic Cell Precursors Is Differentially Regulated by FLT3-ligand and Granulocyte/Macrophage Colony-Stimulating Factor*. Journal of Experimental Medicine, 2002. **195**(7): p. 953-958.
40. Karsunky, H., et al., *Flt3 Ligand Regulates Dendritic Cell Development from Flt3+ Lymphoid and Myeloid-committed Progenitors to Flt3+ Dendritic Cells In Vivo*. Journal of Experimental Medicine, 2003. **198**(2): p. 305-313.
41. Suzuki, S., et al., *Critical roles of interferon regulatory factor 4 in CD11b-high CD8 $\alpha$ - dendritic cell development*. Proceedings of the National Academy of Sciences, 2004. **101**(24): p. 8981-8986.
42. Nagasawa, M., et al., *Development of human plasmacytoid dendritic cells depends on the combined action of the basic helix-loop-helix factor E2-2 and the Ets factor Spi-B*. European Journal of Immunology, 2008. **38**(9): p. 2389-2400.
43. Jackson, J.T., et al., *Id2 expression delineates differential checkpoints in the genetic program of CD8 $\alpha$ + and CD103+ dendritic cell lineages*. The EMBO Journal, 2011. **30**(13): p. 2690-2704.
44. Li, H.S., et al., *The signal transducers STAT5 and STAT3 control expression of Id2 and E2-2 during dendritic cell development*. Blood, 2012. **120**(22): p. 4363-4373.
45. Hildner, K., et al., *Batf3 Deficiency Reveals a Critical Role for CD8 $\alpha$ + Dendritic Cells in Cytotoxic T Cell Immunity*. Science, 2008. **322**(5904): p. 1097-1100.
46. Grajales-Reyes, G.E., et al., *Batf3 maintains autoactivation of Irf8 for commitment of a CD8 $\alpha$ + conventional DC clonogenic progenitor*. Nature Immunology, 2015. **16**(7): p. 708-717.
47. Persson, Emma K., et al., *IRF4 Transcription-Factor-Dependent CD103+CD11b+ Dendritic Cells Drive Mucosal T Helper 17 Cell Differentiation*. Immunity, 2013. **38**(5): p. 958-969.
48. Williams, J.W., et al., *Transcription factor IRF4 drives dendritic cells to promote Th2 differentiation*. Nature Communications, 2013. **4**(1): p. 2990.
49. Tussiwand, R., et al., *Klf4 Expression in Conventional Dendritic Cells Is Required for T Helper 2 Cell Responses*. Immunity, 2015. **42**(5): p. 916-928.
50. Lewis, Kanako L., et al., *Notch2 Receptor Signaling Controls Functional Differentiation of Dendritic Cells in the Spleen and Intestine*. Immunity, 2011. **35**(5): p. 780-791.
51. Satpathy, A.T., et al., *Notch2-dependent classical dendritic cells orchestrate intestinal immunity to attaching-and-effacing bacterial pathogens*. Nature Immunology, 2013. **14**(9): p. 937-948.
52. den Haan, J.M.M., S.M. Lehar, and M.J. Bevan, *Cd8+ but Not Cd8- Dendritic Cells Cross-Prime Cytotoxic T Cells in Vivo*. Journal of Experimental Medicine, 2000. **192**(12): p. 1685-1696.
53. Saitoh, S.-I., et al., *TLR7 mediated viral recognition results in focal type I interferon secretion by dendritic cells*. Nature Communications, 2017. **8**(1): p. 1592.

54. Honda, K., et al., *IRF-7 is the master regulator of type-I interferon-dependent immune responses*. *Nature*, 2005. **434**(7034): p. 772-777.
55. Sallusto, F., et al., *Dendritic cells use macropinocytosis and the mannose receptor to concentrate macromolecules in the major histocompatibility complex class II compartment: downregulation by cytokines and bacterial products*. *Journal of Experimental Medicine*, 1995. **182**(2): p. 389-400.
56. von Delwig, A., et al., *Inhibition of macropinocytosis blocks antigen presentation of type II collagen in vitro and in vivo in HLA-DR1 transgenic mice*. *Arthritis Research & Therapy*, 2006. **8**(4): p. R93.
57. Reis e Sousa, C., P.D. Stahl, and J.M. Austyn, *Phagocytosis of antigens by Langerhans cells in vitro*. *Journal of Experimental Medicine*, 1993. **178**(2): p. 509-519.
58. Arnold-Schild, D., et al., *Cutting Edge: Receptor-Mediated Endocytosis of Heat Shock Proteins by Professional Antigen-Presenting Cells*. *The Journal of Immunology*, 1999. **162**(7): p. 3757-3760.
59. d'Ostiani, C.F., et al., *Dendritic Cells Discriminate between Yeasts and Hyphae of the Fungus *Candida albicans*: Implications for Initiation of T Helper Cell Immunity in Vitro and in Vivo*. *Journal of Experimental Medicine*, 2000. **191**(10): p. 1661-1674.
60. Inaba, K., et al., *Efficient Presentation of Phagocytosed Cellular Fragments on the Major Histocompatibility Complex Class II Products of Dendritic Cells*. *Journal of Experimental Medicine*, 1998. **188**(11): p. 2163-2173.
61. Blum, J.S., P.A. Wearsch, and P. Cresswell, *Pathways of Antigen Processing*. *Annual Review of Immunology*, 2013. **31**(1): p. 443-473.
62. Häcker, H., et al., *CpG-DNA-specific activation of antigen-presenting cells requires stress kinase activity and is preceded by non-specific endocytosis and endosomal maturation*. *The EMBO Journal*, 1998. **17**(21): p. 6230-6240.
63. Caux, C., et al., *Activation of human dendritic cells through CD40 cross-linking*. *Journal of Experimental Medicine*, 1994. **180**(4): p. 1263-1272.
64. Inaba, K., et al., *The tissue distribution of the B7-2 costimulator in mice: abundant expression on dendritic cells in situ and during maturation in vitro*. *Journal of Experimental Medicine*, 1994. **180**(5): p. 1849-1860.
65. Winzler, C., et al., *Maturation Stages of Mouse Dendritic Cells in Growth Factor-dependent Long-Term Cultures*. *Journal of Experimental Medicine*, 1997. **185**(2): p. 317-328.
66. Dieu, M.-C., et al., *Selective Recruitment of Immature and Mature Dendritic Cells by Distinct Chemokines Expressed in Different Anatomic Sites*. *Journal of Experimental Medicine*, 1998. **188**(2): p. 373-386.
67. Saeki, H., et al., *Cutting Edge: Secondary Lymphoid-Tissue Chemokine (SLC) and CC Chemokine Receptor 7 (CCR7) Participate in the Emigration Pathway of Mature Dendritic Cells from the Skin to Regional Lymph Nodes*. *The Journal of Immunology*, 1999. **162**(5): p. 2472-2475.
68. Patente, T.A., et al., *Human Dendritic Cells: Their Heterogeneity and Clinical Application Potential in Cancer Immunotherapy*. *Frontiers in Immunology*, 2019. **9**(3176).
69. Tussiwand, R. and E.L. Gautier, *Transcriptional Regulation of Mononuclear Phagocyte Development*. *Frontiers in Immunology*, 2015. **6**(533).
70. Comrie, W.A., et al., *The dendritic cell cytoskeleton promotes T cell adhesion and activation by constraining ICAM-1 mobility*. *Journal of Cell Biology*, 2015. **208**(4): p. 457-473.

71. Harjunpää, H., et al., *Cell Adhesion Molecules and Their Roles and Regulation in the Immune and Tumor Microenvironment*. *Frontiers in immunology*, 2019. **10**: p. 1078-1078.
72. Dolfi, D.V., et al., *Dendritic Cells and CD28 Costimulation Are Required To Sustain Virus-Specific CD8+ T Cell Responses during the Effector Phase In Vivo*. *The Journal of Immunology*, 2011. **186**(8): p. 4599-4608.
73. Shin, T., et al., *Cooperative B7-1/2 (CD80/CD86) and B7-DC costimulation of CD4+ T cells independent of the PD-1 receptor*. *The Journal of experimental medicine*, 2003. **198**(1): p. 31-38.
74. Umlauf, S.W., et al., *Regulation of interleukin 2 gene expression by CD28 costimulation in mouse T-cell clones: both nuclear and cytoplasmic RNAs are regulated with complex kinetics*. *Mol Cell Biol*, 1995. **15**(6): p. 3197-205.
75. Ragheb, J.A., M. Deen, and R.H. Schwartz, *CD28-Mediated Regulation of mRNA Stability Requires Sequences Within the Coding Region of the IL-2 mRNA*. *The Journal of Immunology*, 1999. **163**(1): p. 120-129.
76. Schoenberger, S.P., et al., *T-cell help for cytotoxic T lymphocytes is mediated by CD40-CD40L interactions*. *Nature*, 1998. **393**(6684): p. 480-483.
77. Jenkins, S.J., et al., *Dendritic Cell Expression of OX40 Ligand Acts as a Costimulatory, Not Polarizing, Signal for Optimal Th2 Priming and Memory Induction In Vivo*. *The Journal of Immunology*, 2007. **179**(6): p. 3515-3523.
78. Nossal, G.J. and B.L. Pike, *Functional clonal deletion in immunological tolerance to major histocompatibility complex antigens*. *Proceedings of the National Academy of Sciences of the United States of America*, 1981. **78**(6): p. 3844-3847.
79. Good, M.F., K.W. Pyke, and G.J. Nossal, *Functional clonal deletion of cytotoxic T-lymphocyte precursors in chimeric thymus produced in vitro from embryonic Anlagen*. *Proceedings of the National Academy of Sciences of the United States of America*, 1983. **80**(10): p. 3045-3049.
80. Luo, X., S.D. Miller, and L.D. Shea, *Immune Tolerance for Autoimmune Disease and Cell Transplantation*. *Annual Review of Biomedical Engineering*, 2016. **18**(1): p. 181-205.
81. Sinha, A.A. and T. Sajda, *The Evolving Story of Autoantibodies in Pemphigus Vulgaris: Development of the "Super Compensation Hypothesis"*. *Frontiers in medicine*, 2018. **5**: p. 218-218.
82. Dardalhon, V., et al., *Role of Th1 and Th17 cells in organ-specific autoimmunity*. *Journal of autoimmunity*, 2008. **31**(3): p. 252-256.
83. Orton, S.M., et al., *Association of UV radiation with multiple sclerosis prevalence and sex ratio in France*. *Neurology*, 2011. **76**(5): p. 425-431.
84. Huppke, B., et al., *Association of Obesity With Multiple Sclerosis Risk and Response to First-line Disease Modifying Drugs in Children*. *JAMA Neurology*, 2019. **76**(10): p. 1157-1165.
85. Hernán, M.A., M.J. Oleky, and A. Ascherio, *Cigarette Smoking and Incidence of Multiple Sclerosis*. *American Journal of Epidemiology*, 2001. **154**(1): p. 69-74.
86. Kampman, M.T. and M. Brustad, *Vitamin D: A Candidate for the Environmental Effect in Multiple Sclerosis – Observations from Norway*. *Neuroepidemiology*, 2008. **30**(3): p. 140-146.
87. van der Mei, I.A.F., et al., *Past exposure to sun, skin phenotype, and risk of multiple sclerosis: case-control study*. *BMJ*, 2003. **327**(7410): p. 316.
88. Ota, K., et al., *T-cell recognition of an immuno-dominant myelin basic protein epitope in multiple sclerosis*. *Nature*, 1990. **346**(6280): p. 183-187.

89. Ohashi, T., et al., *Analysis of proteolipid protein (PLP)-specific T cells in multiple sclerosis: identification of PLP 95–116 as an HLA-DR2,w15-associated determinant*. *International Immunology*, 1995. **7**(11): p. 1771-1778.
90. Genain, C.P., et al., *Identification of autoantibodies associated with myelin damage in multiple sclerosis*. *Nature Medicine*, 1999. **5**(2): p. 170-175.
91. Racke, M.K., et al., *Cytokine-induced immune deviation as a therapy for inflammatory autoimmune disease*. *J Exp Med*, 1994. **180**(5): p. 1961-6.
92. McDonald, W.I., K.J. Smith, and W.I. McDonald, *The pathophysiology of multiple sclerosis: the mechanisms underlying the production of symptoms and the natural history of the disease*. *Philosophical Transactions of the Royal Society of London. Series B: Biological Sciences*, 1999. **354**(1390): p. 1649-1673.
93. Lublin, F.D., et al., *Defining the clinical course of multiple sclerosis*. *Neurology*, 2014. **83**(3): p. 278.
94. Compston, A. and A. Coles, *Multiple sclerosis*. *The Lancet*, 2008. **372**(9648): p. 1502-1517.
95. Davies, F., et al., *The Transition to Secondary Progressive Multiple Sclerosis: An Exploratory Qualitative Study of Health Professionals' Experiences*. *International journal of MS care*, 2016. **18**(5): p. 257-264.
96. Filippini, G., et al., *Interferons in relapsing remitting multiple sclerosis: a systematic review*. *The Lancet*, 2003. **361**(9357): p. 545-552.
97. La Mantia, L., L.M. Munari, and R. Lovati, *Glatiramer acetate for multiple sclerosis*. *Cochrane Database of Systematic Reviews*, 2010(5).
98. Gold, R., et al., *Placebo-Controlled Phase 3 Study of Oral BG-12 for Relapsing Multiple Sclerosis*. *New England Journal of Medicine*, 2012. **367**(12): p. 1098-1107.
99. He, D., et al., *Teriflunomide for multiple sclerosis*. *Cochrane Database of Systematic Reviews*, 2016(3).
100. Riera, R., G.J.M. Porfírio, and M.R. Torloni, *Alemtuzumab for multiple sclerosis*. *Cochrane Database of Systematic Reviews*, 2016(4).
101. Polman, C.H., et al., *A Randomized, Placebo-Controlled Trial of Natalizumab for Relapsing Multiple Sclerosis*. *New England Journal of Medicine*, 2006. **354**(9): p. 899-910.
102. Giovannoni, G., et al., *A Placebo-Controlled Trial of Oral Cladribine for Relapsing Multiple Sclerosis*. *New England Journal of Medicine*, 2010. **362**(5): p. 416-426.
103. Kappos, L., et al., *A Placebo-Controlled Trial of Oral Fingolimod in Relapsing Multiple Sclerosis*. *New England Journal of Medicine*, 2010. **362**(5): p. 387-401.
104. Blair, H.A., *Dimethyl Fumarate: A Review in Relapsing-Remitting MS*. *Drugs*, 2019. **79**(18): p. 1965-1976.
105. Boehncke, W.-H. and M.P. Schön, *Psoriasis*. *The Lancet*, 2015. **386**(9997): p. 983-994.
106. Griffiths, C.E.M. and J.N.W.N. Barker, *Pathogenesis and clinical features of psoriasis*. *The Lancet*, 2007. **370**(9583): p. 263-271.
107. Wuepper, K.D., S.N. Coulter, and A. Haberman, *Psoriasis Vulgaris: A Genetic Approach*. *Journal of Investigative Dermatology*, 1990. **95**(5, Supplement): p. S2-S4.
108. Elder, J.T., *Genome-wide association scan yields new insights into the immunopathogenesis of psoriasis*. *Genes & Immunity*, 2009. **10**(3): p. 201-209.
109. Nickoloff, B.J., J.-Z. Qin, and F.O. Nestle, *Immunopathogenesis of Psoriasis*. *Clinical Reviews in Allergy & Immunology*, 2007. **33**(1): p. 45-56.

110. Santini, S.M., et al., *Interferon- $\alpha$ -Conditioned Human Monocytes Combine a Th1-Orienting Attitude with the Induction of Autologous Th17 Responses: Role of IL-23 and IL-12*. PLOS ONE, 2011. **6**(2): p. e17364.
111. Gregorio, J., et al., *Plasmacytoid dendritic cells sense skin injury and promote wound healing through type I interferons*. Journal of Experimental Medicine, 2010. **207**(13): p. 2921-2930.
112. Nestle , F.O., et al., *Plasmacytoid predendritic cells initiate psoriasis through interferon- $\alpha$  production*. Journal of Experimental Medicine, 2005. **202**(1): p. 135-143.
113. Nast, A., et al., *S3 – Guidelines on the treatment of psoriasis vulgaris (English version). Update*. JDDG: Journal der Deutschen Dermatologischen Gesellschaft, 2012. **10**(s2): p. S1-s95.
114. Kim, E.S. and J.E. Frampton, *Calcipotriol/Betamethasone Dipropionate Foam: A Review in Plaque Psoriasis*. Drugs, 2016. **76**(15): p. 1485-1492.
115. Mason, J., A.R. Mason, and M.J. Cork, *Topical preparations for the treatment of psoriasis: a systematic review*. British Journal of Dermatology, 2002. **146**(3): p. 351-364.
116. Lee, C.S. and J. Koo, *The efficacy of three class I topical synthetic corticosteroids, fluocinonide 0.1% cream, clobetasol 0.05% cream and halobetasol 0.05% cream: a Scholtz-Dumas bioassay comparison*. Journal of drugs in dermatology : JDD, 2009. **8**(8): p. 751-755.
117. Flytström, I., et al., *Methotrexate vs. ciclosporin in psoriasis: effectiveness, quality of life and safety. A randomized controlled trial*. British Journal of Dermatology, 2008. **158**(1): p. 116-121.
118. Gisondi, P., et al., *Combining etanercept and acitretin in the therapy of chronic plaque psoriasis: a 24-week, randomized, controlled, investigator-blinded pilot trial*. British Journal of Dermatology, 2008. **158**(6): p. 1345-1349.
119. Heydendael, V.M.R., et al., *Methotrexate versus Cyclosporine in Moderate-to-Severe Chronic Plaque Psoriasis*. New England Journal of Medicine, 2003. **349**(7): p. 658-665.
120. Papp, K.A., et al., *A global phase III randomized controlled trial of etanercept in psoriasis: safety, efficacy, and effect of dose reduction*. British Journal of Dermatology, 2005. **152**(6): p. 1304-1312.
121. Revicki, D., et al., *Impact of adalimumab treatment on health-related quality of life and other patient-reported outcomes: results from a 16-week randomized controlled trial in patients with moderate to severe plaque psoriasis*. British Journal of Dermatology, 2008. **158**(3): p. 549-557.
122. Blauvelt, A., et al., *Secukinumab is superior to ustekinumab in clearing skin of subjects with moderate-to-severe plaque psoriasis up to 1 year: Results from the CLEAR study*. Journal of the American Academy of Dermatology, 2017. **76**(1): p. 60-69.e9.
123. Kimball, A.B., et al., *Long-term efficacy of ustekinumab in patients with moderate-to-severe psoriasis: results from the PHOENIX 1 trial through up to 3years*. British Journal of Dermatology, 2012. **166**(4): p. 861-872.
124. Langley, R.G., et al., *Secukinumab in Plaque Psoriasis — Results of Two Phase 3 Trials*. New England Journal of Medicine, 2014. **371**(4): p. 326-338.
125. Walker, F., et al., *Fumaderm® in daily practice for psoriasis: dosing, efficacy and quality of life*. British Journal of Dermatology, 2014. **171**(5): p. 1197-1205.
126. Mrowietz, U., et al., *15 Jahre Fumaderm®: Fumarsäureester für die systemische Behandlung der mittelschweren und schweren Psoriasis vulgaris*.

- JDDG: Journal der Deutschen Dermatologischen Gesellschaft, 2009. **7**(s2): p. s3-s16.
127. Kappos, L., et al., *Efficacy and safety of oral fumarate in patients with relapsing-remitting multiple sclerosis: a multicentre, randomised, double-blind, placebo-controlled phase IIb study*. The Lancet, 2008. **372**(9648): p. 1463-1472.
  128. Hoefnagel, J.J., et al., *Long-term safety aspects of systemic therapy with fumaric acid esters in severe psoriasis*. British Journal of Dermatology, 2003. **149**(2): p. 363-369.
  129. Acha-Orbea, H., et al., *Limited heterogeneity of T cell receptors from lymphocytes mediating autoimmune encephalomyelitis allows specific immune intervention*. Cell, 1988. **54**(2): p. 263-73.
  130. Steinman, L., et al., *In vivo effects of antibodies to immune response gene products: prevention of experimental allergic encephalitis*. Proc Natl Acad Sci U S A, 1981. **78**(11): p. 7111-4.
  131. Waldor, M.K., et al., *Reversal of experimental allergic encephalomyelitis with monoclonal antibody to a T-cell subset marker*. Science, 1985. **227**(4685): p. 415-7.
  132. Brostoff, S.W. and D.W. Mason, *Experimental allergic encephalomyelitis: successful treatment in vivo with a monoclonal antibody that recognizes T helper cells*. The Journal of Immunology, 1984. **133**(4): p. 1938-1942.
  133. Röcken, M., J.H. Saurat, and C. Hauser, *A common precursor for CD4+ T cells producing IL-2 or IL-4*. The Journal of Immunology, 1992. **148**(4): p. 1031-1036.
  134. Röcken, M., J. Urban, and E.M. Shevach, *Antigen-specific activation, tolerization, and reactivation of the interleukin 4 pathway in vivo*. Journal of Experimental Medicine, 1994. **179**(6): p. 1885-1893.
  135. Ghoreschi, K., et al., *Interleukin-4 therapy of psoriasis induces Th2 responses and improves human autoimmune disease*. Nature Medicine, 2003. **9**(1): p. 40-46.
  136. Brück, J., et al., *Dimethyl fumarate-induced IL-17<sup>low</sup>IFN- $\gamma$ <sup>low</sup>IL-4<sup>+</sup> Th cells protect mice from severe encephalomyelitis*. European Journal of Immunology, 2018. **48**(9): p. 1588-1591.
  137. Ghoreschi, K., et al., *Fumarates improve psoriasis and multiple sclerosis by inducing type II dendritic cells*. Journal of Experimental Medicine, 2011. **208**(11): p. 2291-2303.
  138. Schmidt, T.J., M. Ak, and U. Mrowietz, *Reactivity of dimethyl fumarate and methylhydrogen fumarate towards glutathione and N-acetyl-l-cysteine—Preparation of S-substituted thiosuccinic acid esters*. Bioorganic & Medicinal Chemistry, 2007. **15**(1): p. 333-342.
  139. Lehmann, J.C.U., et al., *Dimethylfumarate Induces Immunosuppression via Glutathione Depletion and Subsequent Induction of Heme Oxygenase 1*. Journal of Investigative Dermatology, 2007. **127**(4): p. 835-845.
  140. Dibbert, S., et al., *Detection of fumarate–glutathione adducts in the portal vein blood of rats: evidence for rapid dimethylfumarate metabolism*. Archives of Dermatological Research, 2013. **305**(5): p. 447-451.
  141. Linker, R.A., et al., *Fumaric acid esters exert neuroprotective effects in neuroinflammation via activation of the Nrf2 antioxidant pathway*. Brain, 2011. **134**(3): p. 678-692.
  142. Scannevin, R.H., et al., *Fumarates Promote Cytoprotection of Central Nervous System Cells against Oxidative Stress via the Nuclear Factor (Erythroid-*



- Derived 2)-Like 2 Pathway*. Journal of Pharmacology and Experimental Therapeutics, 2012. **341**(1): p. 274-284.
143. Schulze-Topphoff, U., et al., *Dimethyl fumarate treatment induces adaptive and innate immune modulation independent of Nrf2*. Proceedings of the National Academy of Sciences, 2016. **113**(17): p. 4777-4782.
  144. de Martin, R., et al., *Dimethylfumarate Inhibits Tumor-Necrosis-Factor-Induced CD62E Expression in an NF- $\kappa$ B-Dependent Manner*. Journal of Investigative Dermatology, 2001. **117**(6): p. 1363-1368.
  145. Borgers, M., et al., *Dimethylfumarate is an Inhibitor of Cytokine-Induced Nuclear Translocation of NF- $\kappa$ B1, But Not RelA in Normal Human Dermal Fibroblast Cells*. Journal of Investigative Dermatology, 2001. **116**(1): p. 124-130.
  146. Loewe, R., et al., *Dimethylfumarate Inhibits TNF-Induced Nuclear Entry of NF- $\kappa$ B/p65 in Human Endothelial Cells*. The Journal of Immunology, 2002. **168**(9): p. 4781-4787.
  147. Peng, H., et al., *Dimethyl Fumarate Inhibits Dendritic Cell Maturation via Nuclear Factor  $\kappa$ B (NF- $\kappa$ B) and Extracellular Signal-regulated Kinase 1 and 2 (ERK1/2) and Mitogen Stress-activated Kinase 1 (MSK1) Signaling*. Journal of Biological Chemistry, 2012. **287**(33): p. 28017-28026.
  148. Brück, J., et al., *A review of the mechanisms of action of dimethylfumarate in the treatment of psoriasis*. Experimental Dermatology, 2018. **27**(6): p. 611-624.
  149. Ryter, S.W. and L.E. Otterbein, *Carbon monoxide in biology and medicine*. BioEssays, 2004. **26**(3): p. 270-280.
  150. Motterlini, R. and L.E. Otterbein, *The therapeutic potential of carbon monoxide*. Nature Reviews Drug Discovery, 2010. **9**(9): p. 728-743.
  151. Christopher, P.H., et al., *Where is the Clinical Breakthrough of Heme Oxygenase-1 / Carbon Monoxide Therapeutics?* Current Pharmaceutical Design, 2018. **24**(20): p. 2264-2282.
  152. Romão, C.C., et al., *Developing drug molecules for therapy with carbon monoxide*. Chemical Society Reviews, 2012. **41**(9): p. 3571-3583.
  153. Tenhunen, R., H.S. Marver, and R. Schmid, *The enzymatic conversion of heme to bilirubin by microsomal heme oxygenase*. Proceedings of the National Academy of Sciences, 1968. **61**(2): p. 748-755.
  154. Sjöstrand, T., *Endogenous Formation of Carbon Monoxide in Man*. Nature, 1949. **164**(4170): p. 580-581.
  155. Zayasu, K., et al., *Increased Carbon Monoxide in Exhaled Air of Asthmatic Patients*. American Journal of Respiratory and Critical Care Medicine, 1997. **156**(4): p. 1140-1143.
  156. Paredi, P., et al., *Exhaled Carbon Monoxide Levels Elevated in Diabetes and Correlated With Glucose Concentration in Blood: A New Test for Monitoring the Disease?* Chest, 1999. **116**(4): p. 1007-1011.
  157. Matsusaki, T., et al., *Increased exhaled carbon monoxide concentration during living donor liver transplantation*. Int J Mol Med, 2008. **21**(1): p. 75-81.
  158. Goldbaum, L., T. Orellano, and E. Dergal, *Mechanism of the toxic action of carbon monoxide*. Annals of Clinical & Laboratory Science, 1976. **6**(4): p. 372-376.
  159. Goebel, U. and J. Wollborn, *Carbon monoxide in intensive care medicine—time to start the therapeutic application?!* Intensive Care Medicine Experimental, 2020. **8**(1): p. 2.

160. Ryter, S.W., K.C. Ma, and A.M.K. Choi, *Carbon monoxide in lung cell physiology and disease*. American Journal of Physiology-Cell Physiology, 2018. **314**(2): p. C211-C227.
161. Ryter, S.W., D. Morse, and A.M. Choi, *Carbon monoxide: to boldly go where NO has gone before*. Sci STKE, 2004. **2004**(230): p. Re6.
162. Stone, J.R. and M.A. Marletta, *Soluble guanylate cyclase from bovine lung: activation with nitric oxide and carbon monoxide and spectral characterization of the ferrous and ferric states*. Biochemistry, 1994. **33**(18): p. 5636-40.
163. Furchgott, R.F. and D. Jothianandan, *Endothelium-dependent and -independent vasodilation involving cyclic GMP: relaxation induced by nitric oxide, carbon monoxide and light*. Blood Vessels, 1991. **28**(1-3): p. 52-61.
164. Chauveau, C., et al., *Heme oxygenase-1 expression inhibits dendritic cell maturation and proinflammatory function but conserves IL-10 expression*. Blood, 2005. **106**(5): p. 1694-1702.
165. Riquelme, S.A., S.M. Bueno, and A.M. Kalergis, *Carbon monoxide down-modulates Toll-like receptor 4/MD2 expression on innate immune cells and reduces endotoxic shock susceptibility*. Immunology, 2015. **144**(2): p. 321-332.
166. Otterbein, L.E., et al., *Carbon monoxide has anti-inflammatory effects involving the mitogen-activated protein kinase pathway*. Nature Medicine, 2000. **6**(4): p. 422-428.
167. Morse, D., et al., *Suppression of Inflammatory Cytokine Production by Carbon Monoxide Involves the JNK Pathway and AP-1*. Journal of Biological Chemistry, 2003. **278**(39): p. 36993-36998.
168. Ning, W., A.M.K. Choi, and C. Li, *Carbon monoxide inhibits IL-17-induced IL-6 production through the MAPK pathway in human pulmonary epithelial cells*. American Journal of Physiology-Lung Cellular and Molecular Physiology, 2005. **289**(2): p. L268-L273.
169. Bilban, M., et al., *Carbon Monoxide Orchestrates a Protective Response through PPARgamma*. Immunity, 2006. **24**(5): p. 601-610.
170. Chin, B.Y., et al., *Hypoxia-inducible factor 1 alpha stabilization by carbon monoxide results in cytoprotective preconditioning*. Proc Natl Acad Sci U S A, 2007. **104**(12): p. 5109-14.
171. Kim, H.S., et al., *Carbon monoxide activates NF-kB via ROS generation and Akt pathways to protect against cell death of hepatocytes*. American Journal of Physiology-Gastrointestinal and Liver Physiology, 2008. **295**(1): p. G146-G152.
172. Jung, S.-S., et al., *Carbon monoxide negatively regulates NLRP3 inflammasome activation in macrophages*. American Journal of Physiology-Lung Cellular and Molecular Physiology, 2015. **308**(10): p. L1058-L1067.
173. Sawle, P., et al., *Carbon monoxide-releasing molecules (CO-RMs) attenuate the inflammatory response elicited by lipopolysaccharide in RAW264.7 murine macrophages*. British Journal of Pharmacology, 2005. **145**(6): p. 800-810.
174. Chora, Á.A., et al., *Heme oxygenase-1 and carbon monoxide suppress autoimmune neuroinflammation*. The Journal of Clinical Investigation, 2007. **117**(2): p. 438-447.
175. Chung, S.W., et al., *Heme oxygenase-1-derived carbon monoxide enhances the host defense response to microbial sepsis in mice*. The Journal of Clinical Investigation, 2008. **118**(1): p. 239-247.
176. Lancel, S., et al., *Carbon Monoxide Rescues Mice from Lethal Sepsis by Supporting Mitochondrial Energetic Metabolism and Activating Mitochondrial Biogenesis*. Journal of Pharmacology and Experimental Therapeutics, 2009. **329**(2): p. 641-648.

177. Wegiel, B., et al., *Nitric Oxide-Dependent Bone Marrow Progenitor Mobilization by Carbon Monoxide Enhances Endothelial Repair After Vascular Injury*. *Circulation*, 2010. **121**(4): p. 537-548.
178. Bauer, B., et al., *Cover Feature: Methyl Fumarate-Derived Iron Carbonyl Complexes (FumET-CORMs) as Powerful Anti-inflammatory Agents (ChemMedChem 23/2017)*. *ChemMedChem*, 2017. **12**(23): p. 1907-1907.
179. Zhang, J. and C.A. Piantadosi, *Mitochondrial oxidative stress after carbon monoxide hypoxia in the rat brain*. *The Journal of clinical investigation*, 1992. **90**(4): p. 1193-1199.
180. Schieber, M. and Navdeep S. Chandel, *ROS Function in Redox Signaling and Oxidative Stress*. *Current Biology*, 2014. **24**(10): p. R453-R462.
181. Wiseman, H. and B. Halliwell, *Damage to DNA by reactive oxygen and nitrogen species: role in inflammatory disease and progression to cancer*. *Biochemical Journal*, 1996. **313**(1): p. 17-29.
182. Hansford, R.G., B.A. Hogue, and V. Mildaziene, *Dependence of H<sub>2</sub>O<sub>2</sub> formation by rat heart mitochondria on substrate availability and donor age*. *J Bioenerg Biomembr*, 1997. **29**(1): p. 89-95.
183. Tahara, E.B., F.D.T. Navarete, and A.J. Kowaltowski, *Tissue-, substrate-, and site-specific characteristics of mitochondrial reactive oxygen species generation*. *Free Radical Biology and Medicine*, 2009. **46**(9): p. 1283-1297.
184. Boveris, A., N. Oshino, and B. Chance, *The cellular production of hydrogen peroxide*. *Biochemical Journal*, 1972. **128**(3): p. 617-630.
185. Chance, B., H. Sies, and A. Boveris, *Hydroperoxide metabolism in mammalian organs*. *Physiol Rev*, 1979. **59**(3): p. 527-605.
186. Brand, M.D., *The sites and topology of mitochondrial superoxide production*. *Experimental gerontology*, 2010. **45**(7-8): p. 466-472.
187. Tavender, T.J. and N.J. Bulleid, *Molecular Mechanisms Regulating Oxidative Activity of the Ero1 Family in the Endoplasmic Reticulum*. *Antioxidants & Redox Signaling*, 2010. **13**(8): p. 1177-1187.
188. Chaube, R. and G.H. Werstuck, *Mitochondrial ROS versus ER ROS: Which Comes First in Myocardial Calcium Dysregulation?* *Frontiers in cardiovascular medicine*, 2016. **3**: p. 36-36.
189. Tu, B.P. and J.S. Weissman, *Oxidative protein folding in eukaryotes: mechanisms and consequences*. *The Journal of cell biology*, 2004. **164**(3): p. 341-346.
190. Dixon, B.M., et al., *Assessment of Endoplasmic Reticulum Glutathione Redox Status Is Confounded by Extensive Ex Vivo Oxidation*. *Antioxidants & Redox Signaling*, 2008. **10**(5): p. 963-972.
191. Tu, B.P. and J.S. Weissman, *The FAD- and O<sub>2</sub>-Dependent Reaction Cycle of Ero1-Mediated Oxidative Protein Folding in the Endoplasmic Reticulum*. *Molecular Cell*, 2002. **10**(5): p. 983-994.
192. Dingjan, I., et al., *Oxidized phagosomal NOX2 complex is replenished from lysosomes*. *Journal of cell science*, 2017. **130**(7): p. 1285-1298.
193. Ambasta, R.K., et al., *Direct interaction of the novel Nox proteins with p22phox is required for the formation of a functionally active NADPH oxidase*. *J Biol Chem*, 2004. **279**(44): p. 45935-41.
194. Block, K., Y. Gorin, and H.E. Abboud, *Subcellular localization of Nox4 and regulation in diabetes*. *Proceedings of the National Academy of Sciences of the United States of America*, 2009. **106**(34): p. 14385-14390.

195. Chamulitrat, W., et al., *Association of gp91phox homolog Nox1 with anchorage-independent growth and MAP kinase-activation of transformed human keratinocytes*. *Oncogene*, 2003. **22**(38): p. 6045-6053.
196. Kuroda, J., et al., *The superoxide-producing NAD(P)H oxidase Nox4 in the nucleus of human vascular endothelial cells*. *Genes to Cells*, 2005. **10**(12): p. 1139-1151.
197. Henderson, L.M. and R.W. Meech, *Evidence that the product of the human X-linked CGD gene, gp91-phox, is a voltage-gated H(+) pathway*. *J Gen Physiol*, 1999. **114**(6): p. 771-86.
198. Paardekooper, L.M., et al., *Human Monocyte-Derived Dendritic Cells Produce Millimolar Concentrations of ROS in Phagosomes Per Second*. *Frontiers in Immunology*, 2019. **10**(1216).
199. Chen , K., et al., *Regulation of ROS signal transduction by NADPH oxidase 4 localization*. *Journal of Cell Biology*, 2008. **181**(7): p. 1129-1139.
200. Wu, R.-F., et al., *Nox4-Derived H2O2 Mediates Endoplasmic Reticulum Signaling through Local Ras Activation*. *Molecular and Cellular Biology*, 2010. **30**(14): p. 3553-3568.
201. Tyler, D.D., *Polarographic assay and intracellular distribution of superoxide dismutase in rat liver*. *The Biochemical journal*, 1975. **147**(3): p. 493-504.
202. Sheng, Y., et al., *Superoxide dismutases and superoxide reductases*. *Chemical reviews*, 2014. **114**(7): p. 3854-3918.
203. Winterbourn, C.C., *Toxicity of iron and hydrogen peroxide: the Fenton reaction*. *Toxicol Lett*, 1995. **82-83**: p. 969-74.
204. Kehrer, J.P., *The Haber-Weiss reaction and mechanisms of toxicity*. *Toxicology*, 2000. **149**(1): p. 43-50.
205. Lim, J.B., et al., *Analysis of the lifetime and spatial localization of hydrogen peroxide generated in the cytosol using a reduced kinetic model*. *Free Radical Biology and Medicine*, 2015. **89**: p. 47-53.
206. Schreck, R., P. Rieber, and P.A. Baeuerle, *Reactive oxygen intermediates as apparently widely used messengers in the activation of the NF-kappa B transcription factor and HIV-1*. *The EMBO journal*, 1991. **10**(8): p. 2247-2258.
207. Lee, S.-R., et al., *Reversible Inactivation of Protein-tyrosine Phosphatase 1B in A431 Cells Stimulated with Epidermal Growth Factor*. *Journal of Biological Chemistry*, 1998. **273**(25): p. 15366-15372.
208. Salmeen, A., et al., *Redox regulation of protein tyrosine phosphatase 1B involves a sulphenyl-amide intermediate*. *Nature*, 2003. **423**(6941): p. 769-773.
209. Kamata, H., et al., *Reactive Oxygen Species Promote TNF $\alpha$ -Induced Death and Sustained JNK Activation by Inhibiting MAP Kinase Phosphatases*. *Cell*, 2005. **120**(5): p. 649-661.
210. Guzy, R.D., et al., *Mitochondrial complex III is required for hypoxia-induced ROS production and cellular oxygen sensing*. *Cell Metabolism*, 2005. **1**(6): p. 401-408.
211. Chandel, N.S., et al., *Mitochondrial reactive oxygen species trigger hypoxia-induced transcription*. *Proceedings of the National Academy of Sciences*, 1998. **95**(20): p. 11715-11720.
212. Bulua, A.C., et al., *Mitochondrial reactive oxygen species promote production of proinflammatory cytokines and are elevated in TNFR1-associated periodic syndrome (TRAPS)*. *The Journal of experimental medicine*, 2011. **208**(3): p. 519-533.

213. Nakahira, K., et al., *Autophagy proteins regulate innate immune responses by inhibiting the release of mitochondrial DNA mediated by the NALP3 inflammasome*. Nature immunology, 2011. **12**(3): p. 222-230.
214. Scherz-Shouval, R., et al., *Reactive oxygen species are essential for autophagy and specifically regulate the activity of Atg4*. The EMBO journal, 2007. **26**(7): p. 1749-1760.
215. Freudenthal, B.D., et al., *Uncovering the polymerase-induced cytotoxicity of an oxidized nucleotide*. Nature, 2015. **517**(7536): p. 635-639.
216. Leon, J., et al., *8-Oxoguanine accumulation in mitochondrial DNA causes mitochondrial dysfunction and impairs neuritogenesis in cultured adult mouse cortical neurons under oxidative conditions*. Scientific reports, 2016. **6**: p. 22086-22086.
217. Duan, J., et al., *Irreversible cellular senescence induced by prolonged exposure to H<sub>2</sub>O<sub>2</sub> involves DNA-damage-and-repair genes and telomere shortening*. The International Journal of Biochemistry & Cell Biology, 2005. **37**(7): p. 1407-1420.
218. Chen, Q. and B.N. Ames, *Senescence-like growth arrest induced by hydrogen peroxide in human diploid fibroblast F65 cells*. Proceedings of the National Academy of Sciences of the United States of America, 1994. **91**(10): p. 4130-4134.
219. Singh, M., H. Sharma, and N. Singh, *Hydrogen peroxide induces apoptosis in HeLa cells through mitochondrial pathway*. Mitochondrion, 2007. **7**(6): p. 367-373.
220. Xu, L., et al., *Hydrogen peroxide induces oxidative stress and the mitochondrial pathway of apoptosis in RAT intestinal epithelial cells (IEC-6)*. Molecular Biology, 2016. **50**(2): p. 270-277.
221. Giorgio, M., et al., *Hydrogen peroxide: a metabolic by-product or a common mediator of ageing signals?* Nat Rev Mol Cell Biol, 2007. **8**(9): p. 722-8.
222. Fruhwirth, G.O. and A. Hermetter, *Mediation of apoptosis by oxidized phospholipids*. Subcell Biochem, 2008. **49**: p. 351-67.
223. Rodrigues, C., et al., *Human Aquaporin-5 Facilitates Hydrogen Peroxide Permeation Affecting Adaption to Oxidative Stress and Cancer Cell Migration*. Cancers, 2019. **11**(7): p. 932.
224. Lee, S.Y., et al., *Reactive oxygen species induce epithelial-mesenchymal transition, glycolytic switch, and mitochondrial repression through the Dlx-2/Snail signaling pathways in MCF-7 cells*. Mol Med Rep, 2019. **20**(3): p. 2339-2346.
225. Zhang, B., Z. Liu, and X. Hu, *Inhibiting cancer metastasis via targeting NADPH oxidase 4*. Biochem Pharmacol, 2013. **86**(2): p. 253-66.
226. Maechler, P., L. Jornot, and C.B. Wollheim, *Hydrogen Peroxide Alters Mitochondrial Activation and Insulin Secretion in Pancreatic Beta Cells*. Journal of Biological Chemistry, 1999. **274**(39): p. 27905-27913.
227. Kaneto, H., et al., *Role of Reactive Oxygen Species in the Progression of Type 2 Diabetes and Atherosclerosis*. Mediators of Inflammation, 2010. **2010**: p. 453892.
228. Anderson, E.J., et al., *Mitochondrial H<sub>2</sub>O<sub>2</sub> emission and cellular redox state link excess fat intake to insulin resistance in both rodents and humans*. The Journal of clinical investigation, 2009. **119**(3): p. 573-581.
229. Heusch, P., et al., *The contribution of reactive oxygen species and p38 mitogen-activated protein kinase to myofilament oxidation and progression of heart failure in rabbits*. British journal of pharmacology, 2010. **160**(6): p. 1408-1416.

230. Li, J.-M., et al., *Activation of NADPH Oxidase During Progression of Cardiac Hypertrophy to Failure*. Hypertension, 2002. **40**(4): p. 477-484.
231. Marengo, B., et al., *Redox Homeostasis and Cellular Antioxidant Systems: Crucial Players in Cancer Growth and Therapy*. Oxidative Medicine and Cellular Longevity, 2016. **2016**: p. 6235641.
232. Wang, K., et al., *Redox homeostasis: the linchpin in stem cell self-renewal and differentiation*. Cell Death & Disease, 2013. **4**(3): p. e537-e537.
233. Akerboom, T.P., M. Bilzer, and H. Sies, *The relationship of biliary glutathione disulfide efflux and intracellular glutathione disulfide content in perfused rat liver*. J Biol Chem, 1982. **257**(8): p. 4248-52.
234. Lu, S.C., *Regulation of glutathione synthesis*. Molecular aspects of medicine, 2009. **30**(1-2): p. 42-59.
235. Trachootham, D., et al., *Redox regulation of cell survival*. Antioxidants & redox signaling, 2008. **10**(8): p. 1343-1374.
236. Holmgren, A. and F. Aslund, [29] *Glutaredoxin*, in *Methods in Enzymology*. 1995, Academic Press. p. 283-292.
237. Hinchman, C.A. and N. Ballatori, *Glutathione conjugation and conversion to mercapturic acids can occur as an intrahepatic process*. J Toxicol Environ Health, 1994. **41**(4): p. 387-409.
238. Suthanthiran, M., et al., *Glutathione regulates activation-dependent DNA synthesis in highly purified normal human T lymphocytes stimulated via the CD2 and CD3 antigens*. Proceedings of the National Academy of Sciences of the United States of America, 1990. **87**(9): p. 3343-3347.
239. Collet, J.-F. and J. Messens, *Structure, Function, and Mechanism of Thioredoxin Proteins*. Antioxidants & Redox Signaling, 2010. **13**(8): p. 1205-1216.
240. Netto, L.E.S. and F. Antunes, *The Roles of Peroxiredoxin and Thioredoxin in Hydrogen Peroxide Sensing and in Signal Transduction*. Molecules and cells, 2016. **39**(1): p. 65-71.
241. Jones, P. and A. Suggett, *The catalase-hydrogen peroxide system. Kinetics of catalatic action at high substrate concentrations*. The Biochemical journal, 1968. **110**(4): p. 617-620.
242. George, P., *The effect of the peroxide concentration and other factors on the decomposition of hydrogen peroxide by catalase*. The Biochemical journal, 1949. **44**(2): p. 197-205.
243. Jones, P. and H.B. Dunford, *The mechanism of Compound I formation revisited*. Journal of Inorganic Biochemistry, 2005. **99**(12): p. 2292-2298.
244. Jee, J.-P., et al., *Stabilization of all-trans retinol by loading lipophilic antioxidants in solid lipid nanoparticles*. European Journal of Pharmaceutics and Biopharmaceutics, 2006. **63**(2): p. 134-139.
245. Fan, P., et al., *Supplemental lipoic acid relieves post-weaning diarrhoea by decreasing intestinal permeability in rats*. Journal of Animal Physiology and Animal Nutrition, 2017. **101**(1): p. 136-146.
246. Barros, A.I., et al., *Effect of cooking on total vitamin C contents and antioxidant activity of sweet chestnuts (Castanea sativa Mill.)*. Food Chem, 2011. **128**(1): p. 165-72.
247. Prasad, A.S., et al., *Antioxidant effect of zinc in humans*. Free Radical Biology and Medicine, 2004. **37**(8): p. 1182-1190.
248. Bowman, G.L., et al., *Uric acid as a CNS antioxidant*. Journal of Alzheimer's disease : JAD, 2010. **19**(4): p. 1331-1336.
249. Madaan, A., et al., *A stepwise procedure for isolation of murine bone marrow and generation of dendritic cells*. Journal of Biological Methods, 2014. **1**(1).

250. Rahman, I., A. Kode, and S.K. Biswas, *Assay for quantitative determination of glutathione and glutathione disulfide levels using enzymatic recycling method*. Nat Protoc, 2006. **1**(6): p. 3159-65.
251. Sato, H., et al., *Redox Imbalance in Cystine/Glutamate Transporter-deficient Mice*. Journal of Biological Chemistry, 2005. **280**(45): p. 37423-37429.
252. Conrad, M. and H. Sato, *The oxidative stress-inducible cystine/glutamate antiporter, system x (c) (-) : cystine supplier and beyond*. Amino Acids, 2012. **42**(1): p. 231-46.
253. Kim, T.S., et al., *Inhibition of interleukin-12 production by auranofin, an anti-rheumatic gold compound, deviates CD4(+) T cells from the Th1 to the Th2 pathway*. British journal of pharmacology, 2001. **134**(3): p. 571-578.
254. Brück, J., et al., *Nutritional control of IL-23/Th17-mediated autoimmune disease through HO-1/STAT3 activation*. Scientific Reports, 2017. **7**(1): p. 44482.
255. Ghoreschi, K., C. Weigert, and M. Röcken, *Immunopathogenesis and role of T cells in psoriasis*. Clinics in Dermatology, 2007. **25**(6): p. 574-580.
256. Guenova, E., et al., *IL-4 abrogates Th17 cell-mediated inflammation by selective silencing of IL-23 in antigen-presenting cells*. Proceedings of the National Academy of Sciences, 2015: p. 201416922.
257. Hegazi , R.A.F., et al., *Carbon monoxide ameliorates chronic murine colitis through a heme oxygenase 1-dependent pathway*. Journal of Experimental Medicine, 2005. **202**(12): p. 1703-1713.
258. El Ali, Z., et al., *Therapeutic effects of CO-releaser/Nrf2 activator hybrids (HYCOs) in the treatment of skin wound, psoriasis and multiple sclerosis*. Redox Biology, 2020: p. 101521.
259. Rémy, S., et al., *Carbon Monoxide Inhibits TLR-Induced Dendritic Cell Immunogenicity*. The Journal of Immunology, 2009. **182**(4): p. 1877-1884.
260. Mayr, F.B., et al., *Effects of Carbon Monoxide Inhalation during Experimental Endotoxemia in Humans*. American Journal of Respiratory and Critical Care Medicine, 2005. **171**(4): p. 354-360.
261. Fagone, P., et al., *Prevention of clinical and histological signs of proteolipid protein (PLP)-induced experimental allergic encephalomyelitis (EAE) in mice by the water-soluble carbon monoxide-releasing molecule (CORM)-A1*. Clinical & Experimental Immunology, 2011. **163**(3): p. 368-374.
262. Piantadosi, C.A., J. Zhang, and I.T. Demchenko, *Production of hydroxyl radical in the hippocampus after CO hypoxia or hypoxic hypoxia in the rat*. Free Radic Biol Med, 1997. **22**(4): p. 725-32.
263. Zuckerbraun, B.S., et al., *Carbon monoxide signals via inhibition of cytochrome c oxidase and generation of mitochondrial reactive oxygen species*. Faseb j, 2007. **21**(4): p. 1099-106.
264. Nath, K.A., et al., *Induction of heme oxygenase is a rapid, protective response in rhabdomyolysis in the rat*. The Journal of clinical investigation, 1992. **90**(1): p. 267-270.
265. De Bundel, D., et al., *Loss of system x(c)- does not induce oxidative stress but decreases extracellular glutamate in hippocampus and influences spatial working memory and limbic seizure susceptibility*. J Neurosci, 2011. **31**(15): p. 5792-803.
266. Brennan, M.S., et al., *Dimethyl fumarate and monoethyl fumarate exhibit differential effects on KEAP1, NRF2 activation, and glutathione depletion in vitro*. PloS one, 2015. **10**(3): p. e0120254-e0120254.
267. Lin, S.X., et al., *The anti-inflammatory effects of dimethyl fumarate in astrocytes involve glutathione and haem oxygenase-1*. ASN neuro, 2011. **3**(2): p. e00055.

268. Knickelbein, R.G., et al., *Characterization of multiple cysteine and cystine transporters in rat alveolar type II cells*. *Am J Physiol*, 1997. **273**(6): p. L1147-55.
269. Lewerenz, J., et al., *The cystine/glutamate antiporter system x(c)(-) in health and disease: from molecular mechanisms to novel therapeutic opportunities*. *Antioxidants & redox signaling*, 2013. **18**(5): p. 522-555.
270. Fan, X., et al., *The LEGSKO mouse: a mouse model of age-related nuclear cataract based on genetic suppression of lens glutathione synthesis*. *PloS one*, 2012. **7**(11): p. e50832-e50832.
271. Merckx, E., et al., *Absence of system xc- on immune cells invading the central nervous system alleviates experimental autoimmune encephalitis*. *Journal of Neuroinflammation*, 2017. **14**(1): p. 9.
272. Mehling, R., et al., *Immunomodulatory role of reactive oxygen species and nitrogen species during T cell-driven neutrophil-enriched acute and chronic cutaneous delayed-type hypersensitivity reactions*. *Theranostics*, 2021. **11**(2): p. 470-490.
273. Liu, S., et al., *Oxidative stress after subarachnoid hemorrhage in gp91phox knockout mice*. *The Canadian journal of neurological sciences. Le journal canadien des sciences neurologiques*, 2007. **34**(3): p. 356-361.
274. Manuel, A.M. and N. Frizzell, *Adipocyte protein modification by Krebs cycle intermediates and fumarate ester-derived succination*. *Amino Acids*, 2013. **45**(5): p. 1243-1247.
275. Zheng, L., et al., *Fumarate induces redox-dependent senescence by modifying glutathione metabolism*. *Nature Communications*, 2015. **6**(1): p. 6001.
276. Alderson, N.L., et al., *S-(2-Succinyl)cysteine: A novel chemical modification of tissue proteins by a Krebs cycle intermediate*. *Archives of Biochemistry and Biophysics*, 2006. **450**(1): p. 1-8.
277. Balasubramanyam, M., et al., *Curcumin-induced inhibition of cellular reactive oxygen species generation: novel therapeutic implications*. *J Biosci*, 2003. **28**(6): p. 715-21.
278. Biswas, S.K., et al., *Curcumin Induces Glutathione Biosynthesis and Inhibits NF- $\kappa$ B Activation and Interleukin-8 Release in Alveolar Epithelial Cells: Mechanism of Free Radical Scavenging Activity*. *Antioxidants & Redox Signaling*, 2004. **7**(1-2): p. 32-41.
279. Larasati, Y.A., et al., *Curcumin targets multiple enzymes involved in the ROS metabolic pathway to suppress tumor cell growth*. *Scientific Reports*, 2018. **8**(1): p. 2039.
280. Lampropoulou, V., et al., *Itaconate Links Inhibition of Succinate Dehydrogenase with Macrophage Metabolic Remodeling and Regulation of Inflammation*. *Cell Metabolism*, 2016. **24**(1): p. 158-166.
281. Mills, E.L., et al., *Itaconate is an anti-inflammatory metabolite that activates Nrf2 via alkylation of KEAP1*. *Nature*, 2018. **556**(7699): p. 113-117.
282. Bambouskova, M., et al., *Electrophilic properties of itaconate and derivatives regulate the I $\kappa$ B $\zeta$ -ATF3 inflammatory axis*. *Nature*, 2018. **556**(7702): p. 501-504.
283. Zaro, B.W., et al., *Dimethyl Fumarate Disrupts Human Innate Immune Signaling by Targeting the IRAK4-MyD88 Complex*. *The Journal of Immunology*, 2019. **202**(9): p. 2737-2746.
284. Johnson, D.A., et al., *The absence of the pro-antioxidant transcription factor Nrf2 exacerbates experimental autoimmune encephalomyelitis*. *Toxicological*



- sciences : an official journal of the Society of Toxicology, 2010. **114**(2): p. 237-246.
285. Gillard, G.O., et al., *DMF, but not other fumarates, inhibits NF- $\kappa$ B activity in vitro in an Nrf2-independent manner*. Journal of Neuroimmunology, 2015. **283**: p. 74-85.
286. Nguyen, T., et al., *Nrf2 Controls Constitutive and Inducible Expression of ARE-driven Genes through a Dynamic Pathway Involving Nucleocytoplasmic Shuttling by Keap1*. Journal of Biological Chemistry, 2005. **280**(37): p. 32485-32492.
287. Hayes, J.D. and A.T. Dinkova-Kostova, *The Nrf2 regulatory network provides an interface between redox and intermediary metabolism*. Trends in Biochemical Sciences, 2014. **39**(4): p. 199-218.
288. Shin, C.-S., et al., *The glutamate/cystine xCT antiporter antagonizes glutamine metabolism and reduces nutrient flexibility*. Nature Communications, 2017. **8**(1): p. 15074.
289. Kavian, N., et al., *The Nrf2-Antioxidant Response Element Signaling Pathway Controls Fibrosis and Autoimmunity in Scleroderma*. Frontiers in immunology, 2018. **9**: p. 1896-1896.
290. Harris, Isaac S., et al., *Glutathione and Thioredoxin Antioxidant Pathways Synergize to Drive Cancer Initiation and Progression*. Cancer Cell, 2015. **27**(2): p. 211-222.
291. Frizzell, N., et al., *Succination of Thiol Groups in Adipose Tissue Proteins in Diabetes: SUCCINATION INHIBITS POLYMERIZATION AND SECRETION OF ADIPONECTIN*. Journal of Biological Chemistry, 2009. **284**(38): p. 25772-25781.
292. Ternette, N., et al., *Inhibition of Mitochondrial Aconitase by Succination in Fumarate Hydratase Deficiency*. Cell Reports, 2013. **3**(3): p. 689-700.
293. Blewett, M.M., et al., *Chemical proteomic map of dimethyl fumarate-sensitive cysteines in primary human T cells*. Science signaling, 2016. **9**(445): p. rs10-rs10.
294. Kornberg, M.D., et al., *Dimethyl fumarate targets GAPDH and aerobic glycolysis to modulate immunity*. Science, 2018. **360**(6387): p. 449-453.
295. Adam, J., et al., *Renal Cyst Formation in Fh1-Deficient Mice Is Independent of the Hif/Phd Pathway: Roles for Fumarate in KEAP1 Succination and Nrf2 Signaling*. Cancer Cell, 2011. **20**(4): p. 524-537.

## 9 PUBLICATIONS

### PEER-REVIEWED JOURNAL

Bauer B, Göderz AL, Braumüller H, Neudörfl JM, Röcken M, Wieder T, Schmalz HG. **Methyl Fumarate-Derived Iron Carbonyl Complexes (FumET-CORMs) as Powerful Anti-inflammatory Agents**. ChemMedChem, 2017. **12**(23): p. 1907-1907.

### POSTER PRESENTATIONS

Bauer B, Braumüller H, Wieder T, Röcken M (2016). **Redox-mediated modulation of immune activation through toll-like receptors (TLR)**. 43rd Annual Meeting of the Arbeitsgemeinschaft Dermatologische Forschung. Wien.

Bauer B, Göderz AL, Braumüller H, Röcken M, Wieder T, Schmalz HG (2017). **Immune modulatory effects of methyl fumarate-derived iron carbonyl complexes**. 44th Annual Meeting of the Arbeitsgemeinschaft Dermatologische Forschung. Göttingen.

Bauer B, Wieder T, Röcken M (2018). **Glutathione deficiency in cystine/glutamate antiporter knockout mice is not sufficient for induction of dimethyl fumarate-mediated immune deviation**. 45th Annual Meeting of the Arbeitsgemeinschaft Dermatologische Forschung. Zürich.

Burkhardt F, Rentschler M, Weidemann S, Braumüller H, Bauer B, Röcken M, Wieder T (2018). **Crosstalk between cytokine-induced apoptosis and cytokine-induced senescence in human cancer cells**. 45th Annual Meeting of the Arbeitsgemeinschaft Dermatologische Forschung. Zürich.

## 10 ERKLÄRUNG ZUM EIGENANTEIL

The work was performed at the University Hospital Tübingen, Department of Dermatology under the supervision of Prof. Dr. Martin Röcken.

All experiments of this thesis as well as their statistical evaluation were performed independently by me.

Parts of this dissertation from chapter 4.2 have already been published in the following publication: Bauer B, Göderz AL, Braumüller H, Neudörfl JM, Röcken M, Wieder T, Schmalz HG. *Methyl Fumarate-Derived Iron Carbonyl Complexes (FumET-CORMs) as Powerful Anti-inflammatory Agents*. ChemMedChem, 2017. **12**(23): p. 1907-1907. Synthesis, chemical characterization and supply of the compounds were performed by Anna-Lena Göderz. All experiments for the biological characterization of substances, which are part of this thesis, were conducted by myself. The conceptual design of the studies was done in collaboration with Prof. Dr. Thomas Wieder and Prof. Dr. Hans-Günther Schmalz. All co-authors contributed equally to the writing of the manuscript.

I affirm that I have written this dissertation independently and that I have not used any sources other than those indicated by me.

---

Ort, Datum

---

Unterschrift

## 11 EIDESSTATTLICHE ERKLÄRUNG

„Ich erkläre hiermit, dass ich die zur Promotion eingereichte Arbeit mit dem Titel „Anti-inflammatory effects of methyl fumarate-derived iron carbonyl complexes (FumET-CORMs) and reactive oxygen species on dendritic cell differentiation“ selbständig verfasst, nur die angegebenen Quellen und Hilfsmittel benutzt und wörtlich oder inhaltlich übernommene Stellen als solche gekennzeichnet habe. Ich erkläre, dass die Richtlinien zur Sicherung guter wissenschaftlicher Praxis der Universität Tübingen (Beschluss des Senats vom 25.5.2000) beachtet wurden. Ich versichere an Eides statt, dass diese Angaben wahr sind und dass ich nichts verschwiegen habe. Mir ist bekannt, dass die falsche Abgabe einer Versicherung an Eides statt mit Freiheitsstrafe bis zu drei Jahren oder mit Geldstrafe bestraft wird.

---

Ort, Datum

---

Unterschrift